AN ABSTRACT OF THE THESIS OF

Ian P. Madin for the degree of Master of Science in Geology presented on May 29, 1986.

Title: Structure and Neotectonics of the Northwestern Nanga Parbat-Haramosh Massif.

Abstract approved: Redacted for Privacy

Robert D. Lawrence

The Nanga Parbat-Haramosh massif (NPHM) is a unique structural and topographic high in the northwestern corner of the Himalayan convergence zone. Previously, the NPHM was thought to be bounded by the MMT, a thrust along which the Kohistan-Ladakh island arc was obducted onto the northern margin of India. This study presents field evidence for the existence of the Raikot fault, an active dextral reverse fault which has truncated the MMT and forms the western boundary of the NPHM. The Raikot fault separates medium-grade Mesozoic to mid-Cenozoic mafic metasediments and intrusive rocks of the Kohistan sequence from high-grade Proterozoic metasediments and orthogneiss of the Nanga Parbat group. The Kohistan sequence rocks have experienced one tight to isoclinal folding event probably associated with the obduction of the island arc, and a second folding event associated with movement on the Raikot fault. The Nanga Parbat group rocks were transposed by a pre-Himalayan isoclinal folding event and have subsequently been folded around east-trending axes in the early Cenozoic by

the obduction of Kohistan, then around north-trending axes in the late Cenozoic, associated with the uplift of the NPHM and the initiation of the Raikot fault. The Raikot fault consists of both mylonite zones and numerous major and minor faults. Slickensides and mylonitic lineations both indicate dextral reverse slip.

The Raikot fault and associated folding appear to have accommodated 15 to 25 km of uplift in the late Cenozoic. The concentration of the uplift and involvement of the Moho suggests that the Raikot fault follows a major crustal structure, possibly a pre-collision Indian plate boundary. If this is the case, rotational underthrusting of greater India along the MMT would require dextral slip along the Raikot fault. It is proposed that the Raikot fault is a terminal tear fault on the MCT.

Four ages of glaciation are recognized in the area, and correlated with regional glacial chronologies. Numerous Holocene offsets of glacial deposits and alluvial fans occur. A till surface attributed to the most recent major advance has been offset approximately 160 m vertically by strands of the Raikot fault. Analysis of the offsets in combination with thermoluminessence dating yield a maximum Holocene uplift rate of 3.9 $^{mm}/_{yr}$. This uplift rate is compatible with published values derived from fission-track cooling rates.

Structure and Neotectonics of the Northwestern Nanga Parbat-Haramosh Massif.

by

Ian P. Madin

A THESIS

submitted to

Oregon State University

in partial fulfillment of
the requirements for the
degree of

Master of Science

Completed May 29, 1986

Commencement June 1987

APPROVED:

Redacted for Privacy

Dr. R.D. Lawrence, Associate Professor of Geology in charge of major

Redacted for Privacy

Dr. J. G. Johnson, Chairman of the Department of Geology

Redacted for Privacy

Dean of the Graduate School

Date thesis is presented May 29, 1986.

Thesis presented by Ian P. Madin

TABLE OF CONTENTS

LIST OF FIGURES

LIST OF FIGURES

FIGURE PAGE #

LIST OF TABLES

Structure and Neotectonics of the Northwestern Nanga Parbat-Haramosh Massif.

Introduction

The Nanga Parbat-Haramosh massif (NPHM) is an unique structural and topographic high which occurs in the northwest corner of the Himalayan collision zone at a major shift in Himalayan structural trends (fig. 0-1). Because the NPHM is the northernmost exposure of Indian continental basement, it provides a deep structural section through the suture zone between India and the island arc terranes accreted to the Asian continent to the north. Because it is located in the core of the western Himalayan syntaxis, it also records the post-collisional transition from convergence along the Himalayan thrust systems to left lateral motion along the Chaman transform. Finally, the NPHM was demonstrated by Zeitler (1985) to be currently undergoing rapid uplift which began as recently as the late Miocene. All of these points make the geology and neotectonics of the massif of great interest and importance in understanding the evolution of the Himalaya and of collision orogens in general.

Despite its geologic importance, little detailed geologic data has been available from the NPHM. Early work by Wadia (1933) and Misch (1949) recognized the existence of the massif, but did not produce much tectonically applicable data. Geologic data for the northwestern part of the massif was essentially non-existent. In 1979, Tahirkheli

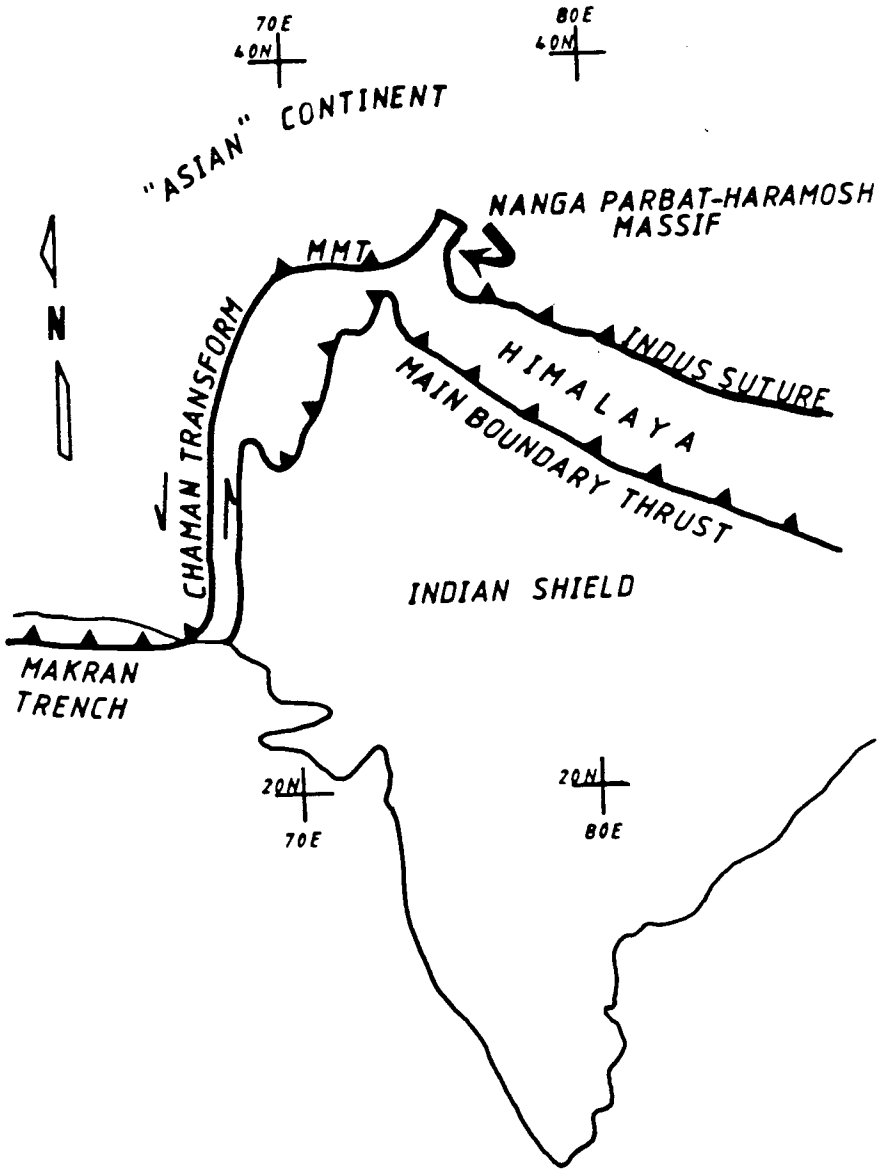

Figure 0-1. Plate Tectonic Map. Generalized map of the western part of the Himalayan collision zone. MMT = Main Mantle thrust.

et al proposed an interpretation of the large scale structure of the area based on limited reconnaissance on the NPHM itself, and substantial work in adjacent Kohistan. They proposed that the NPHM bisected the Kohistan-Ladakh island arc, which had been obducted onto India during the early stages of collision. The Main Mantle thrust (MMT), along which the island arc was obducted was thought to loop around the NPHM to join the Indus suture zone (ISZ) in the east. In 1983, Lawrence and Ghauri recognized the existence of an active reverse fault along the northwestern margin of the NPHM, with the opposite sense of motion to that proposed for the MMT. This study is based on mapping of the previously unmapped northwestern part of the massif in an attempt to characterize the Raikot fault, determine its slip direction and displacement, and evaluate its neotectonic activity. In addition, the internal structure of the massif has been studied to understand its tectonic origin.

The results of the study are presented as two manuscripts, one on the lithostratigraphy, structure and tectonic evolution of the massif, the second on the Quaternary geology and neotectonic activity on the Raikot fault. More detailed data are presented in appendices.

Geology and Structure of the Northwestern Nanga Parbat-Haramosh Massif; crustal uplift associated with a terminal tear fault on the Main Central Thrust?

Introduction

The Nanga Parbat-Haramosh massif (NPHM) in northern Pakistan (Figure I-1) is a north-trending topographic and structural high which forms part of the western Himalayan syntaxis. A part of the Indian-Asian plate boundary, the syntaxis reflects the transition from south directed convergence in the Himalaya to left lateral translation along the Chaman transform zone. The NPHM is doubly important because it is the locus of the change in trend of the India-Asia plate boundary, and because it is the northernmost exposure of Indian continental crust, and thus reflects the original collision and suturing of India and Asia.

The area of this study is located at the northwestern corner of the NPHM (Figure I-2) between the western end of the Himalaya at Nanga Parbat and the Karakoram range to the north. Inaccessibility and rugged terrain have limited the geologic data available from the area, although the structure has been discussed repeatedly in the literature. This paper presents a tectonic interpretation of the origin of the NPHM based on previous work and on new geologic data collected in the northwestern part of the massif.

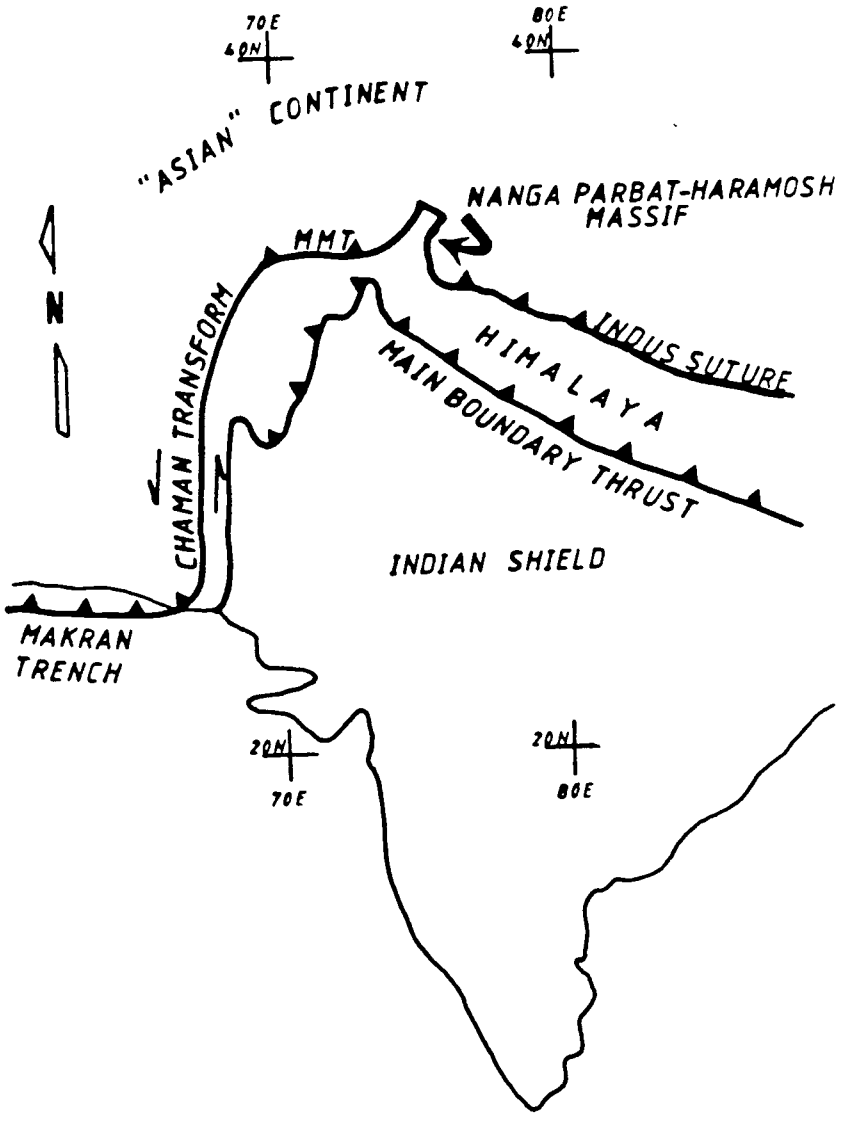

Figure I-1. Plate Tectonic Map. Generalized map of the India-Asia plate boundary in the Northwestern Himalaya.

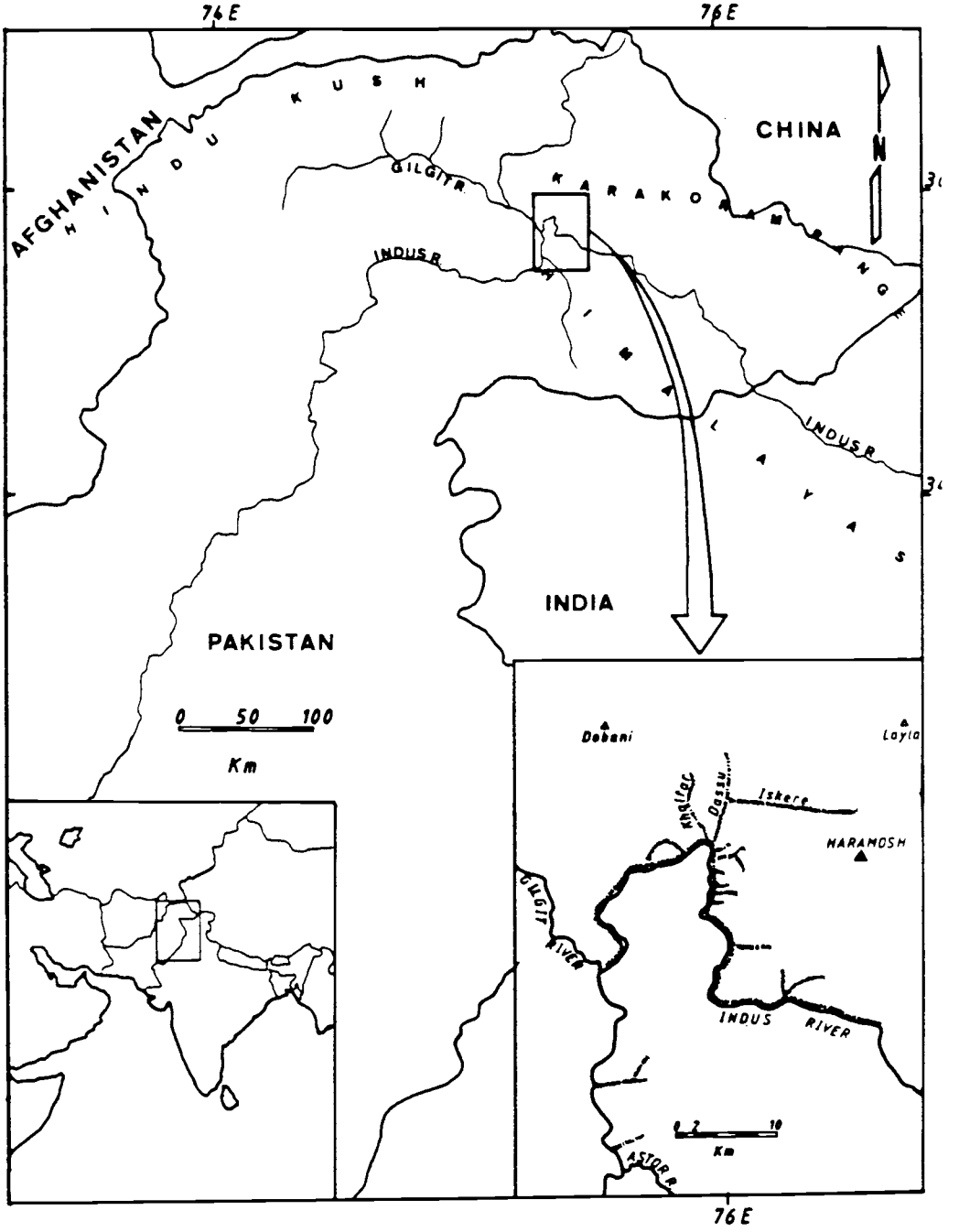

Figure I-2. Location Map. Study area indicated by box. Traverses indicated by hatched lines in inset.

Published geologic data for the area is sparse. The earliest work is that of Wadia (1933), who mapped the southern end of the NPHM, and recognized its association with the western Himalayan syntaxis. Misch (1934, 1949) made a petrographic study of the Nanga Parbat area and concluded that the NPHM was a zone of extensive metasomatic granitization and that its boundaries were steeply dipping isograds. Desio (1964) included the area in his geologic map of the Karakoram, and Gansser (1979) included some reconnaissance data from the area in a discussion of the Himalayan suture. Zulfiqar and others (1977) studied the petrology of metamorphic rocks just west of the NPHM, and Pettersen (1985) studied and dated intrusive rocks just west of the massif. Zeitler (1982, 1985) calculated cooling and uplift rates for the area on the basis of mineral fission track and $^{39}Ar/^{40}Ar$ ages from samples collected in the massif, and Coward (unpublished manuscript) has made a reconnaissance structural traverse across the massif.

With the advent of plate tectonic theory, the NPHM has been recognized as an important element in the India-Asia collision zone (Figure I-3). Wadia (1961), Gansser (1964) and Desio (1979) proposed that the massif might have been a northward directed topographic promontory of pre-collision India, or a major antiform associated with the folding of the western Himalayan syntaxis. Tahirkheli et al (1979) recognized the existence of an island arc terrane between India and Asia in the western end of the collision zone, and they proposed that the NPHM separated the western half (Kohistan island arc) from the eastern (Ladakh island arc). In Pakistan, the Kohistan island arc was obducted onto the Indian plate along the Main Mantle thrust (MMT), probably during suturing of the Indian and Asian continents which

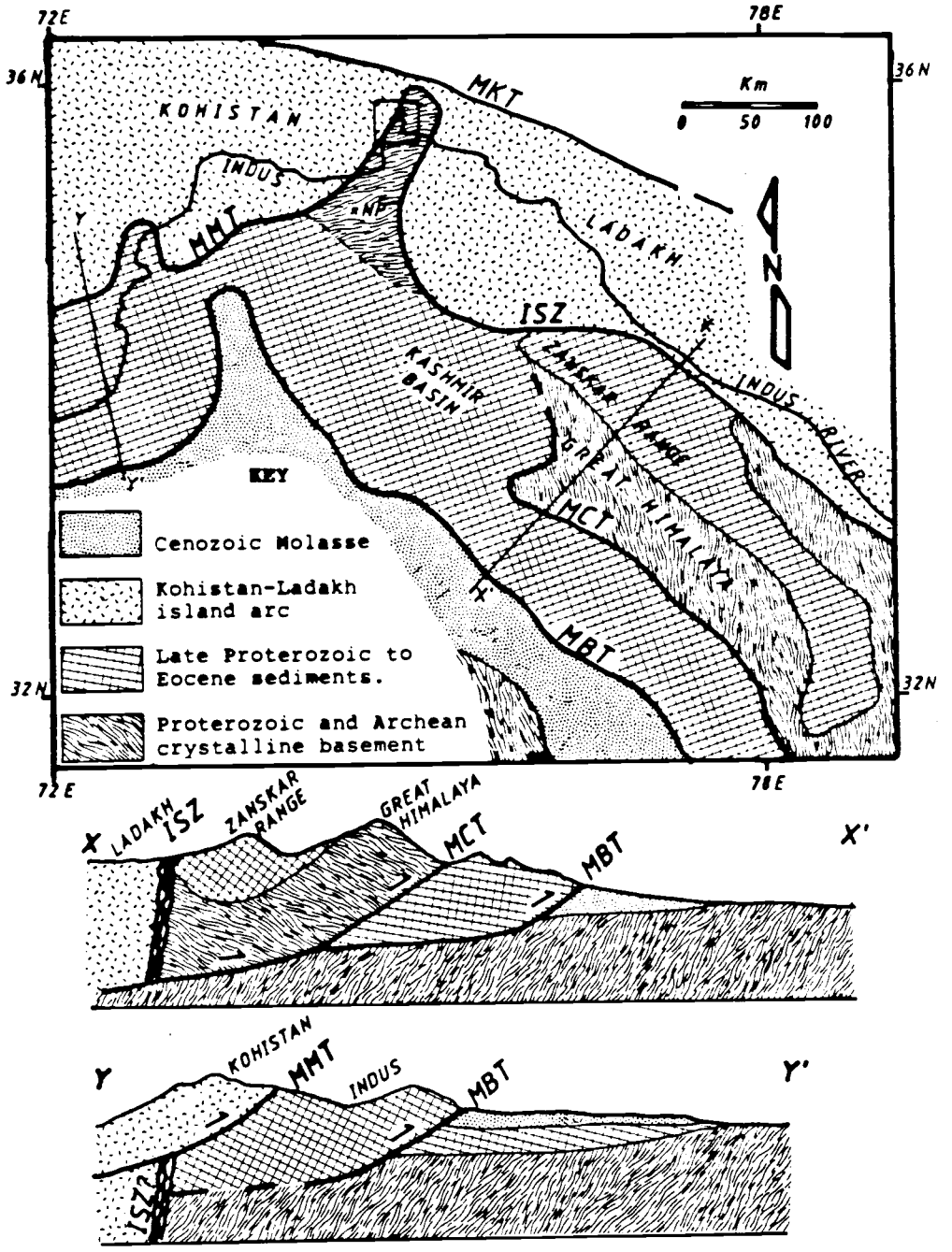

Figure I-3. Regional Geologic Map. Generalized geologic map and cross sections of the northwest Himalya, from Gansser (1964) and Yeats and Lawrence (1983). MKT = Main Karakoram Thrust, MMT = Main Mantle Thrust, ISZ = Indus Suture Zone, MBT = Main Boundary Thrust, NP = Nanga Parbat.

occurred during the Paleocene and Eocene (Klootwijk, 1985). The MMT is a broad fault zone which contains highly deformed remnants of rocks characteristic of subduction zones. Tahirkheli further proposed that the west-trending MMT along with a distinctive metamorphic stratigraphy in the Kohistan arc wraps around the NPHM to the north and connects with the Indus Suture Zone in Ladakh (Figure I-3). Gansser (1979) proposed a loop of the MMT around the NPHM which is truncated by the Main Karakoram thrust, a major fault zone between the Kohistan island arc and the Asian continent. Most recently, Lawrence and Ghauri (1983) recognized that the structure bounding the western edge of the NPHM near Nanga Parbat, which had been previously identified as the MMT, is an active fault (Raikot fault) lacking characteristic suture and subduction zone rocks.

This report is based on geologic mapping carried out during two two-month long field seasons in 1983 and 1984, and a petrographic survey of approximately 100 samples. The mapping covers a strip 30 km wide straddling the western boundary of the NPHM north of the mouth of the Astor river.

Extremely rugged terrain and a lack of Indus river crossings prevented direct observation of many features, but excellent exposure allowed for accurate telescopic observation and air photo interpretation. The actual traverse lines are indicated in Figure I-2, and the nature of geologic data, direct, telescopic or interpreted from air photo are indicated on the geologic map presented in Plate I-1.

Lithostratigraphy

Two tectonostratigraphic terranes occur in the area, separated by an active dextral reverse fault zone which is the continuation of the Raikot fault of Lawrence and Ghauri (1983) (See Plate I-1). West of the fault are medium-grade mafic metasediments and intrusives of the Kohistan island arc (Kohistan Sequence), and east of the fault are high-grade ortho- and paragneisses of the NPHM (Nanga Parbat Group).

Nomenclature

Nanga Parbat Group

Wadia (1933) originally referred to rocks of the Nanga Parbat Group as part of the Salkhala sequence. Misch (1949) used the term Nanga Parbat gneisses but did not recognize stratigraphy, instead ascribing different lithologies to varying degrees of metasomatic granitization in Salkhala sequence rocks. Zannetin (1964) mapped rocks on the eastern margin of the NPHM which he correlated with Misch's Nanga Parbat gneisses, but his units have recently been shown by P. Verplanck (personal communication) to lie outside the massif. Most other workers have continued Misch's use of the name Nanga Parbat gneisses. In this study, the various lithologies of Misch's Nanga Parbat gneisses have been divided into three distinct units; the names of which are proposed as formal metamorphic nomenclature. Possible correlations with existing nomenclature are summarized in Table I-1.

Table I-1. Tentative Nomenclature of Units. Preferred formal terms in boldface.

This Study	Previous Studies
Nanga Parbat Group	
Haramosh Schist **Iskere Gneiss** **Shengus Gneiss**	Wadia 1933, Salkhala Misch, 1949. Nanga Parbat gneiss Coward, 1982. Late Precambrian and Cambrian basement Tahirkheli, 1983. Nanga Parbat gneisses
Kohistan Sequence	
Hanuchal Amphibolite	Wadia, 1933. Salkhala Misch, 1935, 1949. Salkhala Zulfiqar, 1977. Thelichi metasediments Desio, 1964. Askore schists Coward, 1982. Kohistan Sequence metasediments Tahirkheli, 1983. Kamila amphibolite, Bahrain pyroxene granulite.
Shuta Gabbro	Wadia, 1933. Epidiorites Desio, 1964. Twar diorite Misch, 1949. Eocene Metanorites Coward, 1982. Kohistan diorite intrusive suite Tahirkheli, 1983. Ladakh intrusives

Kohistan Sequence

The rocks of the Kohistan Sequence were mapped originally by Wadia (1933) as Precambrian Salkhala metamorphics with epidiorites and basic intrusives. Desio (1964) correlated the Kohistan metamorphics and intrusives with the Askore schist and Twar diorite from the east side of the NPHM, a correlation later refuted by Zulfiqar (1977). The rocks were first recognized as a distinct group by Tahirkheli (1979) who named the entire arc complex the Kohistan Sequence. Several work-

ers have contributed mapping and nomenclature, the most recent and complete of which is by Tahirkheli, (1983). A summary of nomenclature used in the literature and in this study is presented in Table I-1. The names used in this study are proposed as formal local names, but are not correlated to any other units within the Kohistan Sequence.

Description of Units

Nanga Parbat Group

The Nanga Parbat Group is divided into three distinct units, which are tabular bodies separated by fairly sharp contacts conformable with foliation and lithologic layering. All the units have experienced amphibolite facies metamorphism accompanied by intense deformation which has transposed original structures and modified original thicknesses, and the present relative positions of the units do not necessarily reflect relative ages. From structurally lowest to highest the units are Shengus Gneiss, Iskere Gneiss and Haramosh Schist.

The metamorphic rocks of the Nanga Parbat Group bear a descriptive similarity to Proterozoic to Archean Indian crystalline basement at Zanskar (Srikantia et al, 1978). A U/Pb date of 1.8 b.y. has been obtained by Zartman (personal communication) on orthogneiss from the Iskere Gneiss. This date correlates well with U/Pb dates of 1.9 and 1.87 b.y. obtained by Choudhary et al (1984) for granite and orthogneiss intrusive into Aravalli Supergroup rocks in Rajasthan.

The Shengus Gneiss is a unit of fine-grained, finely laminated amphibolite-grade pelitic and psammitic gneisses with subordinate amphibolites and calc-silicate gneisses. Typical mineral assemblages in the Shengus Gneiss are tabulated in Table I-2. The present minimum

thickness of the unit is 5 km. The protolith of the Shengus Gneiss was probably shale, marl, arkosic sandstone and limestone.

The Iskere Gneiss is predominantly coarse-grained, coarsely layered amphibolite-grade biotite gneiss, with subordinate biotite schist, amphibolite and calc-silicate gneiss. Typical mineral assemblages of the Iskere Gneiss are given in Table I-2. The present thickness is at least 8 km, but no complete section exists. The protolith of the Iskere Gneiss is interpreted as intermediate composition plutonic rocks intruded into a sequence of arkosic and greywacke sandstones with minor marl and limestone.

The Haramosh Schist is a unit of medium- to coarse-grained amphibolite grade biotite schist and gneiss, with marble, calc-silicate gneiss and subordinate amphibolite. The various lithologies occur in layers which range from 1.0 cm to 1.0 m thick. Although the range of lithologies and mineralogy is the same as that of the Iskere Gneiss (Table I-2) the two units can be distinguished by the relative lack of coarse biotite orthogneiss in the Haramosh Schist. The minimum measured thickness of the unit is 2.5 km, but at least 10 km of may be exposed on the inaccessible north face of Haramosh. The protolith of the Haramosh Schist is interpreted as a sequence of sediments similar to the sedimentary component of the Iskere Gneiss.

Young intrusive rocks occur commonly as dikes in the Nanga Parbat Group metamorphics. The dikes are dominantly coarse-grained biotite muscovite granite pegmatites, locally mined for green tourmaline, aquamarine, topaz and garnet. Medium- to fine- grained tourmaline granite occurs as selvages to pegmatites and as independent dikes. The intrusive rocks are undeformed except within the Raikot fault zone.

Table I-2. Characteristic Mineralogy of Metamorphic Rocks.

P = Psammitic, M = Mafic, Pe = Pelitic, C = Calcic. X = major component, x = minor component, t = trace.

Mineral	Haramosh Schist				Iskere Gneiss				Shengus Gneiss				Hanuchal Amphibolite			
	P	M	C	C	C	P	P	M	C	Pe	Pe	C	M	P	M	M	C
Plagioclase	X	X				X	X	X		X	X	x	X		X	X	x
Albite														X			
Labradorite			x		X				X								
K Feldspar	X					X		t		x	X						
Microcline					x				x								t
Quartz	X	x	x	x	X	X	X	x	x	X	X	x	x	X	x		x
Biotite	x	x	t	t		x	x	x	x	x	x		x	x	x	x	t
Muscovite	x		x			x	x	t		x	x		t	x	t	t	x
Almandine	x	x				x		x		x	x		x	x	t		
Sillimanite										x	x						
Kyanite	t									x	x						
Tourmaline							t			t	t		t				
Hornblende		X	x		X			X	x				X		X	X	
Epidote														x	x	x	t
Clinozoisite					t											x	
Calcite	t	t	X	x	t			x	x			X			t		X
Dolomite			X	x													
Grossular			x						X								X
Diopside			x	X	x				X			X					
Forsterite			x														
Tremolite				x													
Scapolite			x									x					t
Margarite			x														t
Idocrase																	t
Wollastonite									x								
Zoisite	t	t			x	t	t	t	x	t							t
Sphene	t	t	t		x			t	c			t	t			t	t
Zircon	t	t	t			t	t	t	t	t	t	t	t		t	t	
Apatite	t	t		t	t	t	t	t	t	t	t	t	t	t	t	t	
Rutile						t			t	t			t				
Pyrite																	t
Opaques	t	t			t	t	t	t		t	t	t	t	t	t	t	
Graphite										t	t						

Minor amounts of Chlorite, sericite and epidote occur as retrograde minerals in most samples.

Kohistan Sequence

The Kohistan Sequence rocks adjacent to the NPHM occur in three distinct units. The Hanuchal Amphibolite is a unit of medium-grade mafic metasediments intruded extensively by matic plutons and sills of Shuta gabbro. Both of these units are intruded by at least two phases of leucocratic dikes, the Kohistan granites.

Coward et al (in press) presents $^{39}Ar/^{40}Ar$ hornblende dates for part of the Kohistan batholith directly adjacent to the study area, and some of his dates are almost certainly from plutons of the Shuta Gabbro. The ages range from 25-35 m.y. for hornblende to 17-25 m.y. for biotite, and are probably cooling ages. The Shuta Gabbro is probably Early to Middle Cenozoic. No direct dating has been done on the Hanuchal Amphibolite, but it is clearly older than the Shuta Gabbro. According to Coward et al (in press) the Hanuchal Amphibolite is less deformed than and therefore younger than the Chilas Complex. The Chilas Complex has been reported by Jan (1984) as 64 to 79 m.y. old and by Coward et al (in press) as up to 100-150 m.y. old, and so the Hanuchal Amphibolite is probably Late Mesozoic to Early Cenozoic in age.

The Hanuchal Amphibolite comprises strongly foliated, interlayered, medium-grained ortho- and para-amphibolite, biotite and hornblende schist and gneiss, granitic orthogneiss, marble and calc-silicate gneiss. Typical mineral assemblages are given in Table I-2, but the dominant rock is hornblende epidote gneiss. The common occurrence of epidote and albite places the unit in the albite epidote amphibolite facies. The unit is at least 2 km thick, but the true thickness is obscured by fault and intrusive contacts and may have

been modified by folding. The protolith of the Hanuchal Amphibolite is interpreted as a sequence of volcaniclastic sediments with some interlayered limestones and lavas.

The Shuta Gabbro is a group of sills and plutons of gabbro, norite and diorite which are intrusive into the Hanuchal Amphibolite. Intrusive contacts are locally parallel to foliation in the Hanuchal Amphibolite, but crosscut foliation on a large scale. Inclusions of Hanuchal Amphibolite are common in the Shuta gabbro, ranging from centimeters across to 100s of meters on a side. The Shuta Gabbro is locally weakly foliated, subparallel to the foliation in the Hanuchal Amphibolite. Primary igneous layering is fairly commonly observed. Typical modal mineral compositions for the Shuta Gabbro are tabulated in Table I-3. The Shuta Gabbro, because it is only weakly deformed is interpreted as part of the post-collisional intrusive complex of the Kohistan island arc, and is correlated with Cowards (1982) Kohistan Diorite intrusive suite rather than the gabbros of the Chilas Complex which Coward (1982) reports to be isoclinally folded.

Both the Shuta Gabbro and Hanuchal Amphibolite are extensively intruded by at least three phases of leucocratic dikes, locally named Kohistan granites. The dikes range up to 15 m in thickness and locally make up as much as 20% of the volume of an exposure. The modal mineralogy of the Kohistan granites is given in Table I-3. Two ages of muscovite-biotite leucogranite dikes occur, the older exhibiting considerable deformation, the younger undeformed. Both ages of granite dikes are locally cut by biotite muscovite pegmatites, some of which contain hornblende.

Table I-3. Modal mineralogy of intrusive rocks.

	Shuta Gabbro					Kohistan Granites	
Sample #	42	70	73	89	134	134B	134C
Mineral							
Plagioclase	40	45	30	48	30	55	40
K Feldspar		6		9		20	19
Quartz	1					25	35
Clinopyroxene		25		25			
Orthopyroxene				10			
Hornblende	50	10	68		35		
Epidote	5		tr		9	tr	
Biotite	2	10	tr	9	8	4	
Muscovite						tr	tr
Apatite	tr				tr		
Sphene	1				tr		tr
Calcite	tr						
Zircon	tr		tr		tr		tr
Rutile							tr
Opaques			tr	3	tr		

Structure

Extreme relief and rugged topography prevent direct access to and measurement of many structures in the area. However, the combination of relief and exposure provides observable cross sections through parts of each major structure, allowing the large-scale form to be resolved by a combination of field measurement, telescopic observation and air photo interpretation.

The most important structure in the area is the Raikot fault, which is a major dextral reverse fault trending roughly north through the area and dipping steeply to the east. In the Kohistan-sequence rocks west of the Raikot fault, the dominant structures are large-scale tight to isoclinal folds (Kohistan generation 1 folds = Kf1), with an axial plane foliation which dips steeply to moderately northwest. These folds are refolded adjacent to the Raikot fault (Kohistan generation 2 folds = Kf2). In the Nanga Parbat group rocks east of the fault, the dominant structures are two north trending antiforms (Nanga Parbat generation 3 folds = Nf3). These antiforms refold an east trending megakink on a north dipping homocline (Nanga Parbat generation 2 folds = Nf2) and early rootless isoclinal intrafolial folds (Nanga Parbat generation 1 folds = Nf1). The general relations of the large-scale structures are presented in Figure I-4.

Raikot Fault

The Raikot Fault trends roughly north from the mouth of Ramghat canyon to the head of Khaltar canyon (Plate I-1) where it bends to the northwest. The fault varies in width from .5 to 3 km and its trace is marked by hydrothermal alteration, a discontinuous band of mylonite and numerous reverse faults, some of which are active.

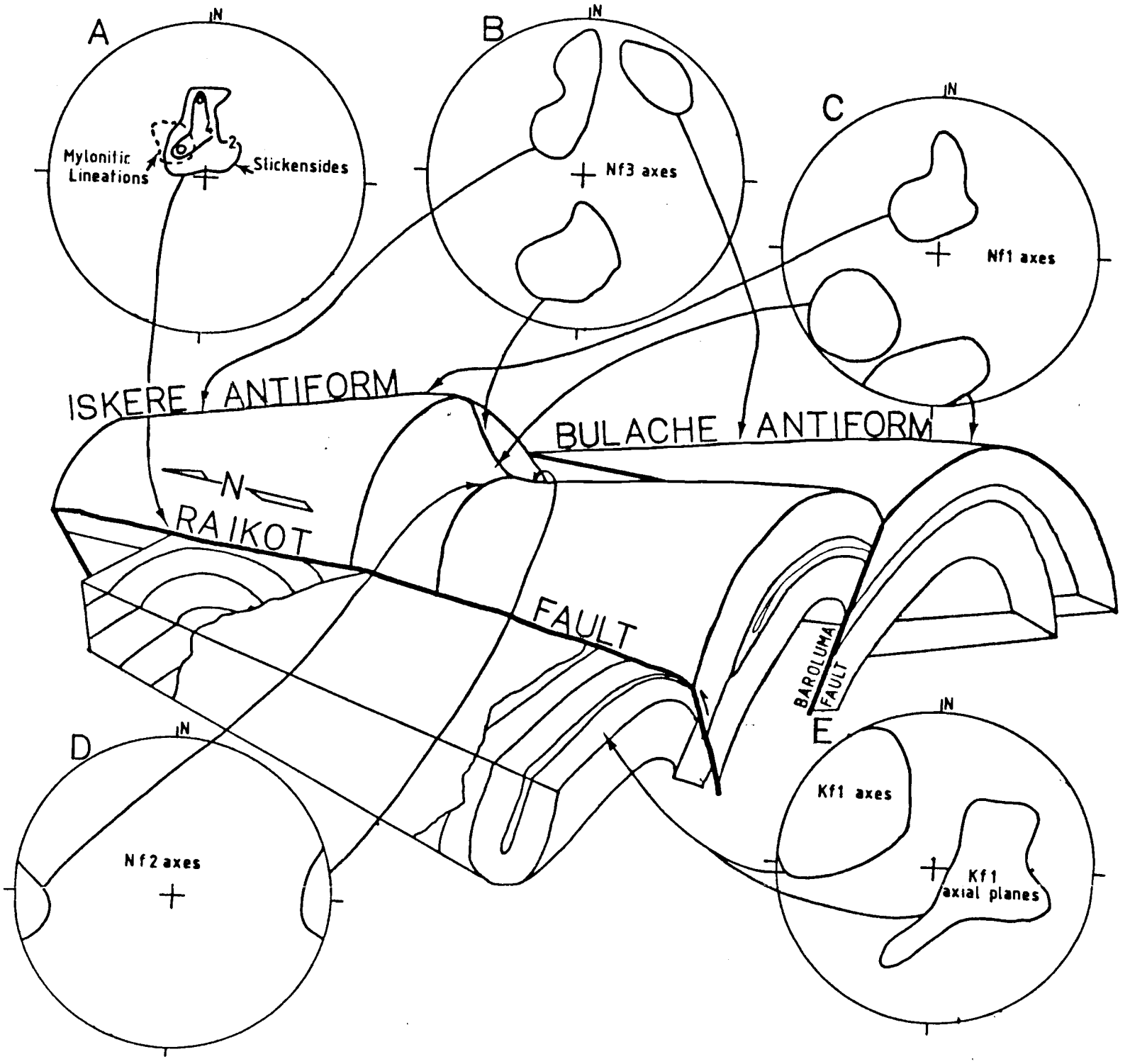

Figure I-4. Structural Summary Diagram. Major structures are schematically presented along with detailed structural data presented as lower hemisphere Wulff net projections. A. Dashed field includes all mylonitic lineations measured in both the Sassi-Khalola and Bunji mylonite sections. The contoured field includes all slickensides from the Raikot fault. B. Solid lines enclose the fields of all Nf3 axes from the domains indicated by the arrows. C. Solid lines enclose fields of all Nfl axes from domains indicated by the arrows. D. Solid lines enclose the field of Nf2 axes from the domains indicated by the arrows. E. The solid lines enclose fields of Kfl axes, and poles to Kfl axial planes from the area indicated by the arrow.

Ductile Features

The mylonite zone was studied at two accessible sections, one along the Indus River between Sassi village and Khalola canyon, and the second in Bunji canyon. At both locations the zone separates Kohistan and Nanga Parbat rocks, but the Sassi-Khalola section is west of the major brittle fault and the Bunji section is east of the brittle fault.

In the Sassi-Khalola section, mylonitic foliation and foliation in directly adjacent Kohistan and Nanga Parbat rocks are parallel and oriented 00°, 70-90° E. The core of the mylonite zone is at least 300m thick, but partially mylonitized rock occurs on either side of the core in a band 1-1.5 km wide. The borders of the mylonite zone are not sharp and within the border zone more susceptible lithologies may be strongly mylonitized while surrounding competent rocks are little deformed. Complex and locally chaotic mesoscale folding occurs locally within and adjacent to the mylonite zone. Despite locally extreme mylonitization, protoliths are generally identifiable and a fairly sharp transition from Nanga Parbat group protoliths to Kohistan sequence protoliths is recognizable. No exotic rocks are found within the mylonite zone.

The mylonite zone is well exposed on the divide between Dassu and Khaltar canyons, (Figure I-5) where Nanga Parbat group rocks clearly override the Kohistan sequence rocks.

The Bunji canyon section is a zone at least 200m thick which is truncated on the west by a major fault. Foliation in the rocks adjacent to the zone, mylonitic foliation within the zone, and the major fault are all parallel and oriented 030°, 90°. As at the Sassi-Shatot

section, a transition occurs within the zone from Kohistan sequence to Nanga Parbat group protoliths, and no exotic lithologies occur.

A strong mylonitic lineation is commonly developed in both sections, with an average orientation of 335° 55° (Figure I-4, A). Sense of shear in the mylonites was determined in oriented sections cut parallel to the lineation. Consistently reverse dextral shear was indicated by a variety of features (Simpson and Schmidt, 1983) such as microfaults in garnets, offset micas, s/c surfaces, inclined neocrystallized quartz and asymmetric debris trains on porphyroclasts.

Brittle Features

Brittle deformation is common throughout the Raikot fault zone, as north-trending, steeply east-dipping reverse faults and as foliation-plane faults where foliation is suitably oriented. Most of the faults occur east of the mylonite zone, but a major strand occurs west of the fault at Bunji canyon, and locally the fault strands truncate the mylonite zone.

Minor reverse faults are commonly oriented 330-030°, 50-90° east and occur sparsely up to 1.5 km away from the mylonite zone, increasing in density towards the zone, where they may occur 0.5 to 1.0 m apart. Slickensides on steeply-dipping north-striking foliation planes are common as a result of slip along numerous foliation-plane faults and minor ramp faults are commonly observed connecting foliation plane faults. Considerable slip probably occurs along these faults without producing significant evidence of offset. Slickensides associated with foliation plane faults and minor reverse faults generally plunge 360°-010°, 40-60° (Figure I-4, A), which combined with evidence of east side up diplacement indicates reverse dextral slip.

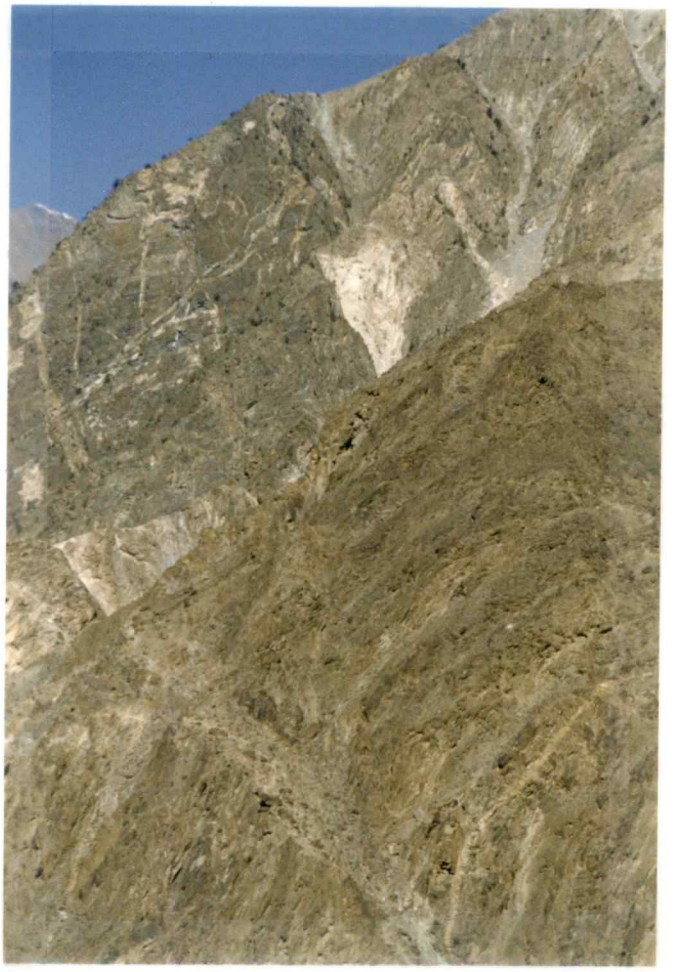

Figure I-5. Sassi-Khalola Mylonite Zone. View to the north of the divide between Dassu and Khaltar canyons. Haramosn Schist (Nanga Parbat Group) on the east overrides Shuta Gabbro (Kohistan Sequence) to the west along the Sassi-Khalola mylonite zone of the Raikot fault. Relief in the photograph is approximately 1500m.

The dominant fault strand can be traced continuously on the ground and on air photos from Bunji canyon to the head of Khaltar canyon (Plate I-1). At Bunji canyon, the fault occurs west of the mylonite zone as a northeast-trending vertical gouge zone at least 35 m thick, and north of Bunji canyon, the trace is marked by Quaternary offsets and intense hydrothermal alteration zones. Just south of Ishkapal canyon, the fault intersects the mylonite zone (Figure I-6), and in Ishkapal canyon the fault is spectacularly exposed in a cliff 1000 m high (Figure I-7).

Near Sassi, a sliver of Kohistan group rocks approximately .5 km wide and 2.5 km long is incorporated along the fault (Figure I-8, A-A'), and late Pleistocene glacial deposits overlying the sliver are significantly tilted and offset by Quaternary faulting (Madin, 1986). At Sassi, in Dassu canyon and in the headwaters of Khaltar canyon, the trace of the fault is marked by discontinuous scarps in late Pleistocene glacial deposits.

Fault displacement

The total displacement of the Raikot fault cannot be determined without correlative units on either side, but a minimum of 15 km of horizontal slip is indicated by the Quaternary offset of the course of the Indus across the fault (Madin, 1986). The sense of slip is dextral reverse, based on mylonitic lineations and shear sense indicators, slickensides, Quaternary offsets and the shape of Kf_2 folds.

The onset or motion along the fault postdates the young granitic dikes on both sides of the fault, but neither group is reliably dated. Currently the best constraint is Zeitler's (1985) data, which suggests that uplift began 7 m.y. ago, and accelerated exponentially.

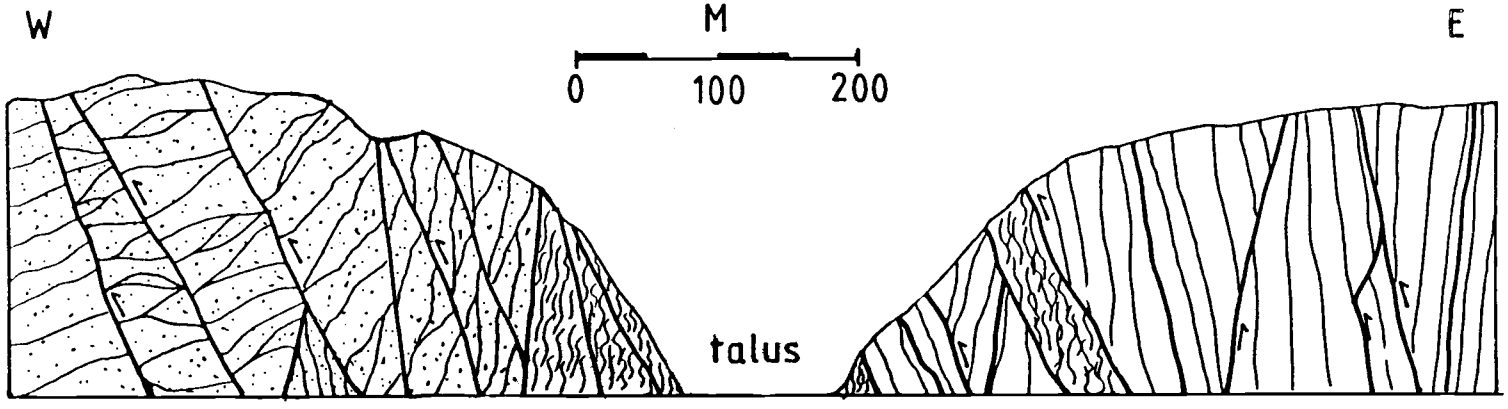

Figure I-6. Cross Section of Raikot Fault. Cross section of Raikot fault exposed on the east bank of the Indus between Khalola Canyon and Ishkapal Canyon. Kohistan Sequence rocks shown with stipple, Nanga Parbat Group rocks without pattern. Mylonite shown with fine wavy line pattern, faults with heavy line and foliation with fine lines.

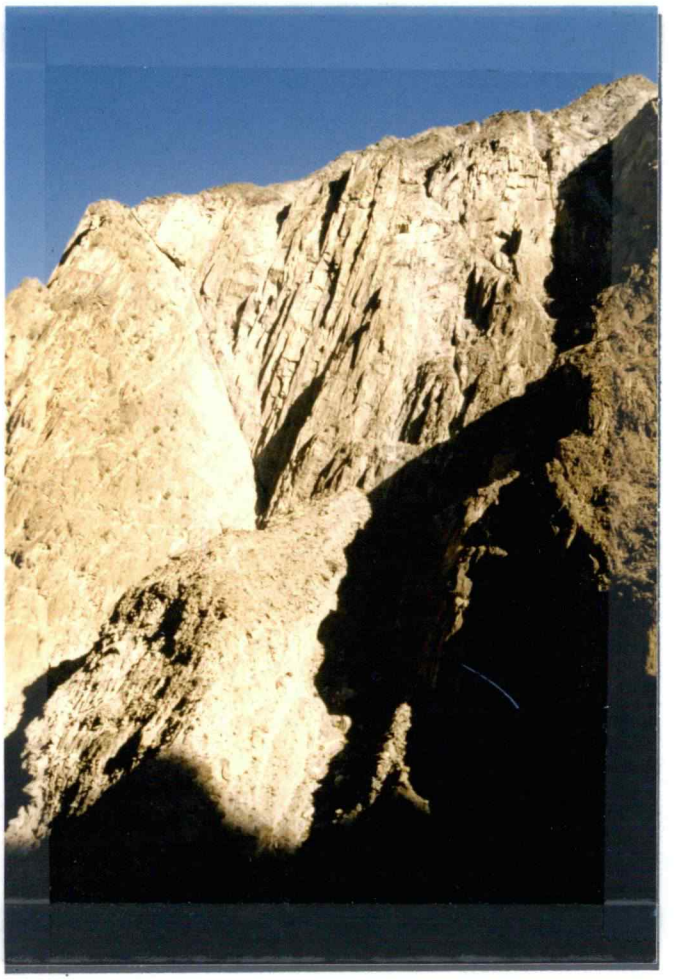

Figure I-7. Major Strand of the Raikot Fault. View to the north of the north wall of Ishkapal Canyon showing major strand of Raikot fault. Relief in the photograph is approximately 1000m.

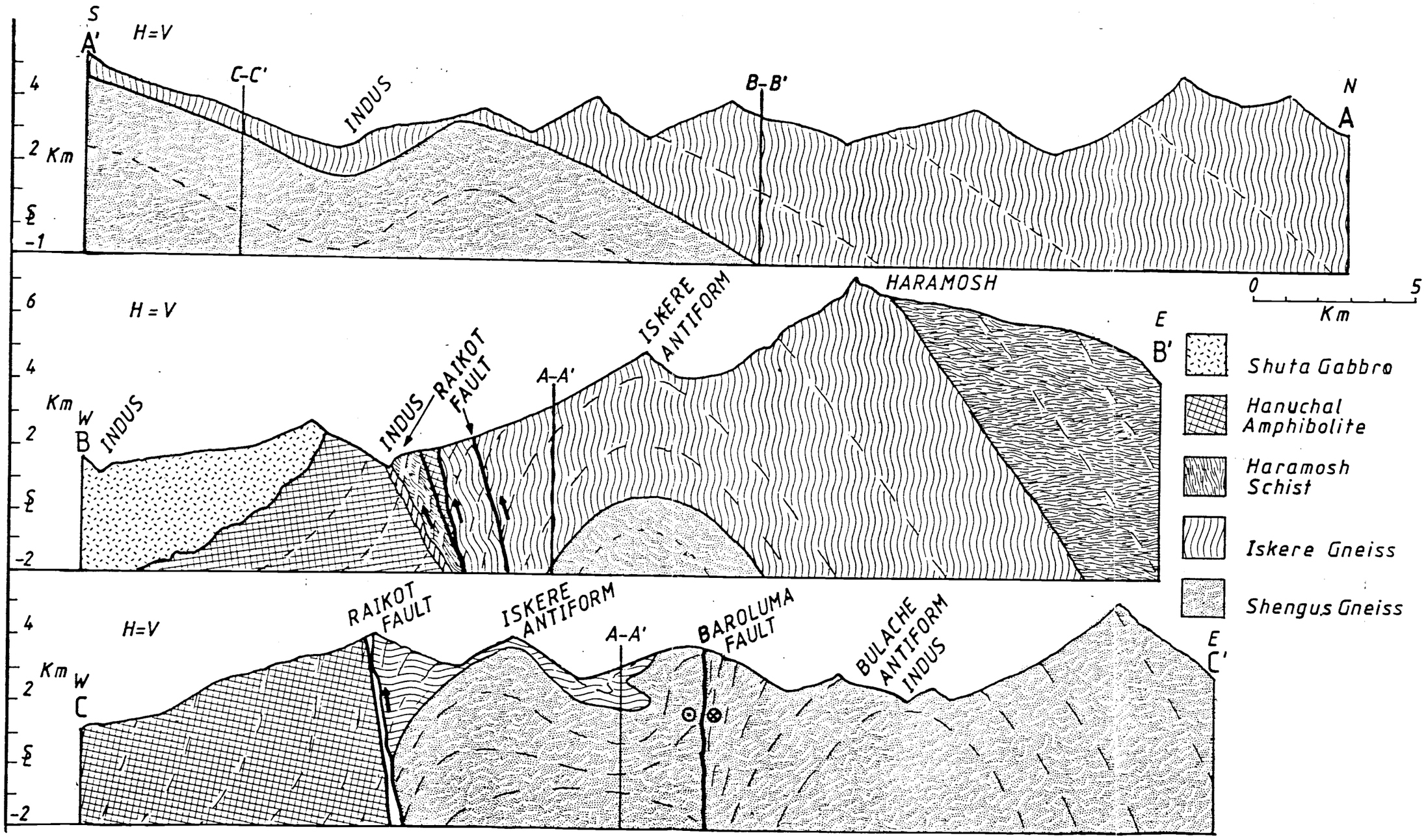

Figure I-8. Geologic Cross Sections. Geologic cross sections drawn with no vertical exaggeration. Location of section lines indicated on map in Plate I-1.

Kohistan Structures

Structure in the Kohistan sequence adjacent to the NPHM is defined by foliation in the metasediments and weakly developed subparallel foliation and igneous layering in the intrusive rocks. Intrusive contacts tend to be parallel to foliation in outcrop, but crosscut foliation at map scale. Two main ages of deformation are recognized in the Kohistan rocks. The first, Kf1 is responsible for the regional northwest strike and north dip with associated mesoscale isoclinal folds, fold boudins and penetrative S1 foliation. Kf2 folds are large scale asymmetric folds and mesoscale open folds which occur adjacent to the Raikot fault, and are clearly related to motion along the fault.

Kf1 structures

Large scale folds of the Kf1 generation were not recognized in the area, but upright isoclinal macrofolds with northwest trending axes occur in similar rocks on the west bank of the Indus opposite Bunji (Misch, 1935, Desio 1964, Coward 1982a) and probably continue onto the east bank at Bunji.

Mesoscale Kf1 folds are commonly tight to isoclinal or intraorlial. A strong axial mineral lineation is commonly observed, and axial planes are commonly subparallel to local S1 foliation. Fold axes and lineations trend approximately 315°, 40°, (Figure I-4 E) and axial planes are rather scattered, possibly because most measurements were taken near the Raikot fault and reflect refolding associated with the fault. The S1 foliation is probably an axial planar fabric developed in association with the Kf1 folds, as the minerals defining the folia-

tion are unstrained away from the Raikot fault.

Kf1 deformation probably predated the intrusion of the essentially unstrained Shuta Gabbro which weakly constrains the deformation to the early to middle Cenozoic. These folds have been related by Coward (1982a) to the Jaglot syncline, a proposed crustal scale upright syncline with horizontal east-west trending axes. However, the Jaglot syncline has not been confirmed in the field and the northwest orientation of Kf1 folds (Desio 1964) is not consistent with the structure proposed by Coward. The general orientation and intensity of Kf1 folding suggests that it developed in associated with the obduction of the Kohistan island arc onto India along the MMT.

Kf2 Structures

Large scale steeply plunging Kf2 folds occur adjacent to the Raikot fault. In the Indus gorge between Shuta and Sassi (Plate I-1, Figure I-4), the foliation is folded from approximately 310° 45° N distant from the Raikot fault, to 010° 60° W adjacent to the fault, but the shape and continuity of the fold is obscured by intrusions. In the south at Bunji canyon the foliation is folded progressively from 090° 75° N 2.5 km west of the fault to 030° 85° E at the fault. The shape of both folds implies dextral slip along the Raikot fault.

Mesoscale open Kf2 folds are common near the Raikot fault, with axes which plunge moderately to the southeast and which lie roughly in the plane of the Raikot fault. A weak to moderate crenulation is also associated with Kf2 folds, and is oriented approximately 030° 50° N. The crenulation is not parallel to the fault, but is roughly axial planar to the large scale Kf2 folds.

Nanga Parbat Group Structures

As indicated in Figure I-4 the dominant structures in the Nanga Parbat Group are two upright north-trending Nf3 folds, the Iskere and Bulache antiforms. The two folds are separated by or possibly offset along the northeast-trending Baroluma fault (Plate I-1, Figure I-4). The Nf3 antiforms refold a relatively simple Nf2 fold, and both Nf2 and Nf3 refold Nf1 folds and their associated axial planar foliation.

Nf1 Structures

The earliest and most fundamental structure is a sequence of three distinct metamorphic units layered parallel to a dominant S1 fabric which is defined by lithologic layering and segregation banding, and by a penetrative mineral fabric. The formation of the lithologic banding and foliation reflects the earliest and strongest penetrative deformation which folded and transposed some earlier structure, leaving only highly attenuated isoclinal folds and fold boudins of the Nf1 generation.

Nf1 folds occur at all scales (Figure I-9) with axial planes consistently parallel to foliation, and axes variously oriented due to refolding by Nf2 and Nf3 folds. Evidence of this generation of fold occurs only where hinges are preserved. The majority of the rock consists of transposed fold limbs, causing a marked lack of lateral continuity of lithologic layering in most Nanga Parbat Group rocks. Locally, a strong mineral lineation is associated with the axes of Nf1 folds. In view of the Proterozoic age of the Nanga Parbat Group rocks, the Nf1 folds almost certainly reflect Proterozoic or early Paleozoic tectonics, and are not related to Himalayan tectonics.

A

B

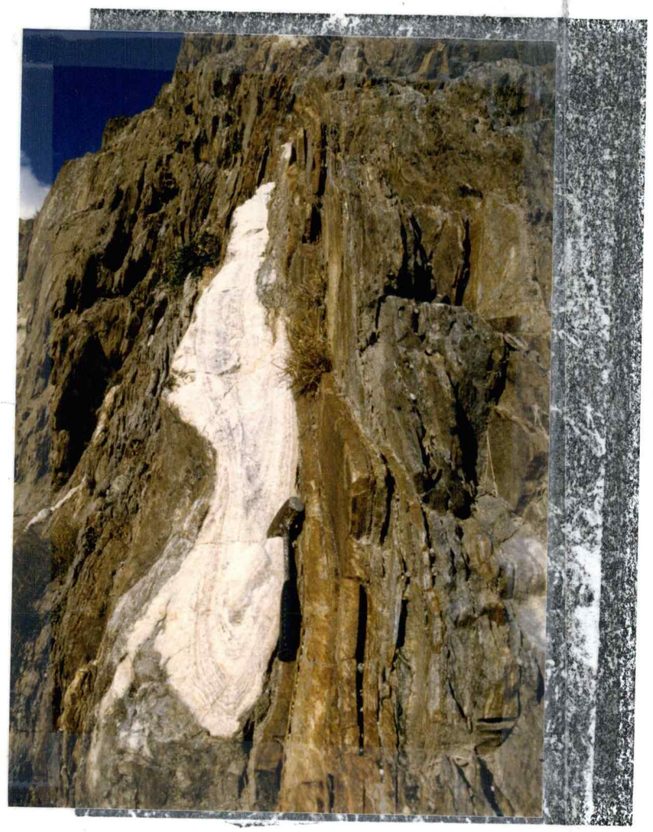

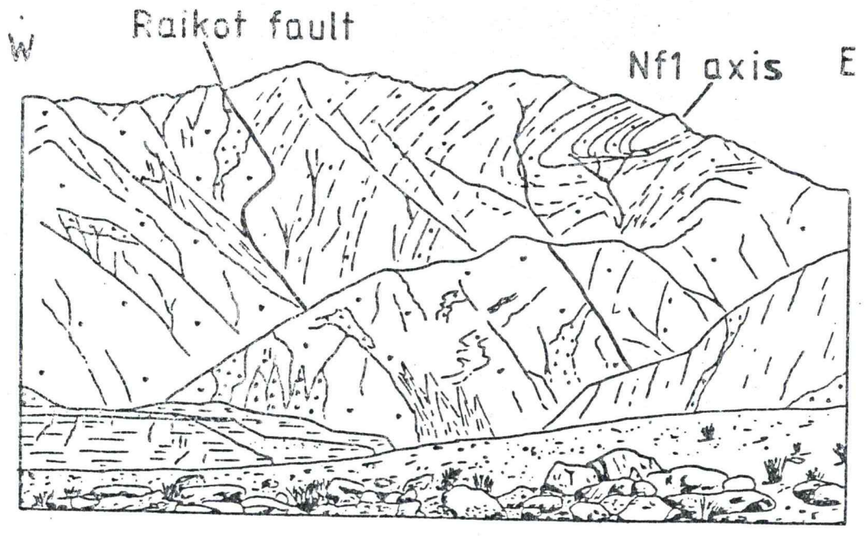

C

Figure I-9. Nf1 Folds. A. Photomicrograph of Nf1 isoclinal fold in para-amphibolite layer from Iskere gneiss. Photo is approximately 4 cm by 2 cm, and the Nf1 fold is refolded by either Nf2 or Nf3 folds. B. Photograph of rootless isoclinal intrafolial fold hinge in marble layer surrounded by Haramosn biotite schist. C. Sketch of megascale isoclinal intrafolial Nf1 fold in the north wall of Ramghat canyon. Fold is truncated by Raikot fault and refolded by Iskere Antiform. Sketch contains approximately 2500 m of relief. (Sketch courtesy of Dr. R.D. Lawrence, see also Misch, 1949).

Nf2 Structures

The second generation of folds occurs along the Indus gorge at Shengus, as an abrupt antiform-synform pair with roughly horizontal east-west axes. The simplest unfolding of the later Nf3 structures resolves the Nf2 structure into a north-dipping homocline which may have extended as far as 40 km north of Bunji canyon. The homocline is folded by the antiform-synform pair, with the form of a large scale kink (Figure I-8, A-A'). The hinges of the kink are 4 km apart, and the amplitude is approximately 2 km. The axes of the kink are recognizable near Shengus in the broad hinge of the Iskere Antiform but are indistinguisable on the steep limbs of the Iskere antiform. Where recognizable, Nf2 axes are clearly folded by Nf3 folds (Figure I-4 D) and hence Nf3 postdates Nf2. Locally a weak crenulation or mineral lineation is associated with the Nf2 axes.

The north-dipping Nf2 homocline and east-west trending kink may have been formed during the obduction of the Kohistan arc onto the margin of the Indian plate. The northward dip of the homocline is consistent with downwarping of the Indian plate beneath the island arc, and the sense of vergence and orientation of the kink are consistent with southward transport of the arc along the MMT. If correct, this correlation constrains the age of Nf2 structures to sometime during the suturing of India and Asia, in the early Cenozoic (Klootwijk, 1985).

Nf3 Structures

The major Nf3 folds are both upright, tight, asymmetric antiforms, with thin steeply dipping western limbs and thick, more gently

dipping eastern limbs (Figure I-8, B-B', C-C'and Figure I-10, A,B).

The axis of the Bulache antiform trends 030° and plunges 50 °N north of the Indus, and was not studied south of the Indus. The eastern limb of the antiform is approximately 10 km thick, and is truncated to the east by the Stak fault zone (Verplanck, personal communication).

The axis of the Iskere antiform trends generally 350° and plunges 50° except where it intersects the Nf2 kink (Figure I-4). At the intersection a large scale "egg carton" interference pattern occurs, exposing structural domes of Shengus Gneiss, structurally the lowest unit (Figure I-8, C-C'). The hinge of the Iskere antiform is generally sharp except at the intersection with the kink, where it is gentle with numerous large open parasitic folds. The difference in style is probably due to the resistance of the kink to refolding. At Shengus, the Iskere antiform is truncated just east of the hinge by the Baroluma fault, but to the north at Haramosh the eastern limb dips consistently 50 degrees east, and is at least 10 km thick.

Mesoscale parasitic Nf3 folds are common on both antiforms, with axes generally parallel to the local megafold axis (Figure I-4, B) except on the western limb of the Iskere antiform near the Raikot fault where all minor fold axes are dragged into the mylonitic lineation direction. A weak to moderately strong axial crenulation occurs throughout the fold, and the lineation formed by the intersection of foliation and crenulation parallels the local orientation of Nf3 axes.

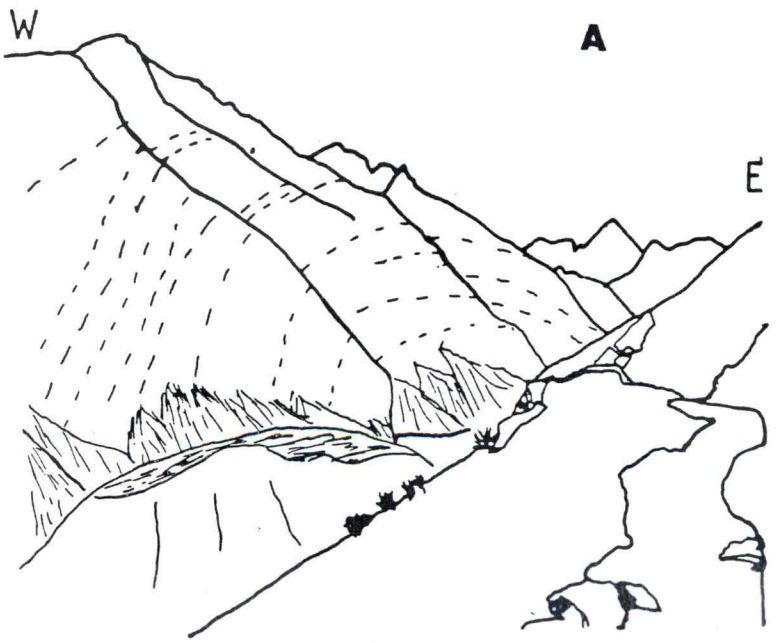

Figure I-10. Nf3 Folds. A. Sketch looking north of the north wall of Iskere canyon, showing a cross section across tne hinge of the north plunging Iskere Antiform. Foliation planes indicated by dashed lines. Sketch includes 3500 m of relief. B. Photograph looking to the east. The hinge of the Bulache antiform is visible east of the Baroluma fault which is in the drainage in the foreground.

The two Nf3 folds are separated by the Baroluma fault (Figure I-3, cross section C-C' and figure I-4), which is vertical and trends 030-050. Exposure of the Baroluma fault is poor, but tight folding and some incipient mylonitization are seen in rocks immediately adjacent to the fault. No structural data are available to determine the sense or amount of motion. The Iskere and Bulache antiforms may have originally been a single fold which has simply been offset and repeated by 20 to 25 km of left lateral slip along the Baroluma fault.

The north-south trending Nf3 folds are perpendicular to the main Himalayan trend of south or southwestern convergence along west- to northwest-trending structures. The Nf3 folds are clearly related to the Raikot fault, which has been active since the Miocene and so the age of Nf3 folding must be mid to late Cenozoic.

Petrofabrics and Metamorphism

Raikot Fault

Dynamic metamorphism occurs in rocks of both the Kohistan Sequence and Nanga Parbat Group in association with the Raikot fault. Deformation begins 1.0 to 1.5 km away from the fault zone with incipient bending of mica and hornblende, subgrain formation in quartz and feldspar and the development of a protomylonitc foliation defined by grain size reduction in parallel shear bands. Deformation progresses through protomylonites with hornblende, garnet and plagioclase porphyroclasts in a fine polygonized/neocrystallized matrix of quartz, mica and feldspar and culminates as strongly foliated mylonites and ultramylonites. The degree of mylonitization is a function both of position relative to the rault and mineralogy, so that strongly mylonitized incompetent rocks may be interlayered with weakly deformed competent rocks. The most incompetent mineral is quartz, followed by kyanite, calcite, mica, plagioclase, epidote, hornblende and garnet, in order of increasing competence.

Kohistan sequence

Hanuchal amphibolite

The dominant fabric in the Hanuchal amphibolite is a strong (S1) foliation defined primarily by segregation bands and preferred orientation of mica, hornblende, and epidote. Quartz and feldspar fabrics tend towards equigranular-polygonal, with generally straight to gently curved grain boundaries, and all phases are generally unstrained. The metamorphic minerals and the foliation appear to have crystallized during a single prograde metamorphism, which occurred

during and after Kf1 folding. The lack of contact aureoles in Hanuchal Amphibolite surrounding the Shuta Gabbro implies that the main metamorphism occurred before the intrusion.

Minor retrograde metamorphism has caused replacement of garnet and hornblende by quartz, feldspar and epidote, and minor sericitic alteration of plagioclase and chloritization of biotite. Hydrothermal alteration in some rocks results in widespread growth of chlorite and epidote on hornblende, alteration of plagioclase, and in some cases, growth of biotite and tourmaline.

All the Hanuchal Amphibolite studied contained chlorite only as a retrograde phase. Zulfiqar (1977), however reports chlorite schists and phyllites from the Thelichi area opposite Bunji. This suggests a moderate regional metamorphic gradient, with grade increasing towards the east, possibly reflecting uplift of the easternmost Kohistan rocks by drag along the Raikot fault.

Shuta Gabbro

Metamorphism in the gabbros is essentially limited to weak retrograde metamorphism or alteration of primary ferromagnesian minerals to biotite, epidote and chlorite. Deformation of the gabbros has produced a weak foliation defined by flattening of all phases, with weak strain evident in most quartz and some plagioclase. The deformation of the gabbros may be autodeformation associated with intrusion, or may be due to the latest phases of Kf1 folding. Primary igneous fabric is locally observed, defined by strong alignment of coarse elongate plagioclase grains. In many gabbros, equigranular pyroxene with hornblende or biotite rims and equant subhedral plagioclase are surrounded by interstitial or poikilitic K feldspar. The abundance of late K

feldspar and hornblende in orthopyroxene bearing rocks suggests late hydrous contamination, possibly from the Hanuchal amphibolite country rock.

Nanga Parbat Group

Nanga Parbat Group rocks reveal a more complex metamorphic and deformational history. The dominant fabric is a strong foliation (S1) which is strongly defined by segregation bands and elongate clots of minerals, but only moderately defined by preferred orientation of micas. S1 is commonly bent around porphyroblasts, and commonly contains isoclinal intrafolial fold hinges. In both instances the minerals defining the deformed foliation have been coarsely recrystallized in weakly aligned unstrained aggregates. The dominant fabric in quartzofeldspatnic layers and calc-silicate gneisses is strongly equigranular-polygonal. All of these features suggest that the deformation which produced S1 was followed by a static metamorphism, and that no significant penetrative ductile deformation occurred after the final metamorphism.

The Shengus gneiss presents an unique overall texture which is polygonal-equigranular but unusually fine grained. The texture, which developed at sillimanite grade, may have been due to rapid neomineralization due to rapid heating, or neomineralization following extensive tectonic grain size reduction. In either case, the final static metamorphism was fairly short, in order to prevent the growth of coarse-grained crystals.

Although the petrographic data alone are not sufficient to determine maximum P/T conditions of metamorphism, they are consistent with

conditions close to anatexis. Muscovite was commonly observed being replaced by sillimanite and K feldspar in the presence of quartz in pelitic gneisses. This suggests the reaction: muscovite + quartz = aluminosilicate + K feldspar which implies a minimum temperature of 600 to 725° C, depending on the choice of triple point for the aluminosilicates (Winkler, 1976).

Field evidence of anatexis includes migmatitic granite gneisses in Iskere gneiss and thin conformable pegmatitic layers in Shengus gneiss. Petrographic evidence is observed in the form of fine selvages of quartz or feldspar occurring along grain boundaries in polygonal-equigranular quartz feldspar aggregates. The films may be remnants of an interstitial melt.

The petrographic evidence for the path of metamorphism is ambiguous. In pelitic gneisses, kyanite commonly occurs as prismatic crystals strongly aligned with S1 but sillimanite occurs as randomly oriented needles or fibrolite masses and is clearly later. However, the growth of sillimanite instead of kyanite could result either from isobaric heating or isothermal decompression. Determination of P/T paths by mineral chemistry is currently underway (Chamberlain, P., work in progress).

Minor retrograde alteration of plagioclase to sericite and biotite to chlorite are common.

Two tectonic scenarios may account for the observed metamorphism. In the first scenario a kyanite grade metamorphic terrain of Proterozoic or Paleozoic age was overridden by the Kohistan island arc, initiating a dynamothermal metamorphism. As overthrusting ceased, the rapidly buried terrain experienced a static sillimanite grade culmina-

tion before the onset of Himalayan age uplift. In the second and preferred scenario, the dynamothermal metamorphism associated with the obduction of the Kohistan island arc was followed by rapid uplift, and rapid decompression of very hot metamorphic rocks resulting in a static recrystallization and down pressure retrograde metamorphism.

The Nanga Parbat Group certainly experienced extensive Precambrian metamorphism, and only the very latest metamorphic events are related to Himalayan tectonics. Regardless of path, the final static high grade metamorphism probably occurred after all three folding events. The age of the Himalayan metamorphism is crudely constrained between the early Cenozoic estimates for the age of suturing of India to Asia, and a biotite $^{39}Ar/^{40}Ar$ date of 4.04 m.y. reported by Zeitler (1985).

Conclusions

The most fundamental conclusion of this study is that the MMT does not, as previously supposed, wrap around the NPHM to connect with the ISZ in Ladakh. Instead, the Raikot fault has completely removed the MMT along the western border of the NPHM and reversed the original sense of motion of the MMT by thrusting Indian continental basement over the Kohistan island arc. The uplift associated with the Raikot fault has removed the overlying MMT and Kohistan arc rocks completely. the Raikot fault may extend to the north in the Hunza valley where it may be responsible for high uplift rates recorded by Zeitler (1985) To the south, the fault probably passes west of Nanga Parbat into the unmapped region north of Kashmir.

The information collected in this study on the nature and activity of the Raikot fault and the structure of the NPHM leads to a model for the uplift of the massif. The important features are the amount, timing, mechanism and localization of uplift. This uplift model also suggests a a plate scale model for the origin of the NPHM.

Uplift of the NPHM

Estimation of the amount of uplift of the NPMH can be accomplished by three indirect methods. The first is to integrate the uplift rate/age curve published by Zeitler (1985) which yields a total of approximately 16 km of uplift in the last 6-8 million years. The second approach combines the 15 km lateral offset of the Indus river across the Raikot fault (Madin 1986) with the slip vector of approxi-

mately 45° plunge to the north measured along the fault. This data implies approximately 15 km or uplift since the initiation of the Raikot fault.

The final approach is to reconstruct the original stratigraphy of the area and determine how much material has been eroded away. Before the onset or uplift, the basement gneisses of the NPHM were probably overlain by Phanerozoic sediments and the Kohistan island arc (Figure 11). The Phanerozoic sediments have not beeen studied at the NPHM, but are known from two nearby sections. In Zanskar, Srikantia (1978) finds over 10 km or Precambrian to Eocene sediments lying on top or the crystalline basement. In Kashmir, Gansser (1964) reports over 12 km of "Tethyan" sedimentary rocks. It is reasonable to assume that the Nanga Parbat Group rocks in the NPHM were overlain by at least 11 km of sedimentary cover before collision and the obduction of the Kohistan island arc. During the obduction of the Kohistan island arc, this sedimentary cover would have been strongly deformed, into nappes and thrust sheets as suggested by Coward (1982a) and documented by Rosenberg (1985) in the sediments just beneath the MMT at Karakar Pass. In the NPHM, the structures associated with the obduction of the Kohistan island arc are limited to the large but simple Nf2 kink fold, which implies that the Nanga Parbat Group rocks were insulated from more intense deformation by the sedimentary cover. Malinconico (1986) has recently modeled the Kohistan island arc using gravity data, and suggests that it is approximately 8 km thick. Finally there is 6 km of relief between the highest exposure of Nanga Parbat group rocks and the lowest exposure of Kohistan Sequence rocks. The total uplift implied by this stratigraphy is approximately 25 km.

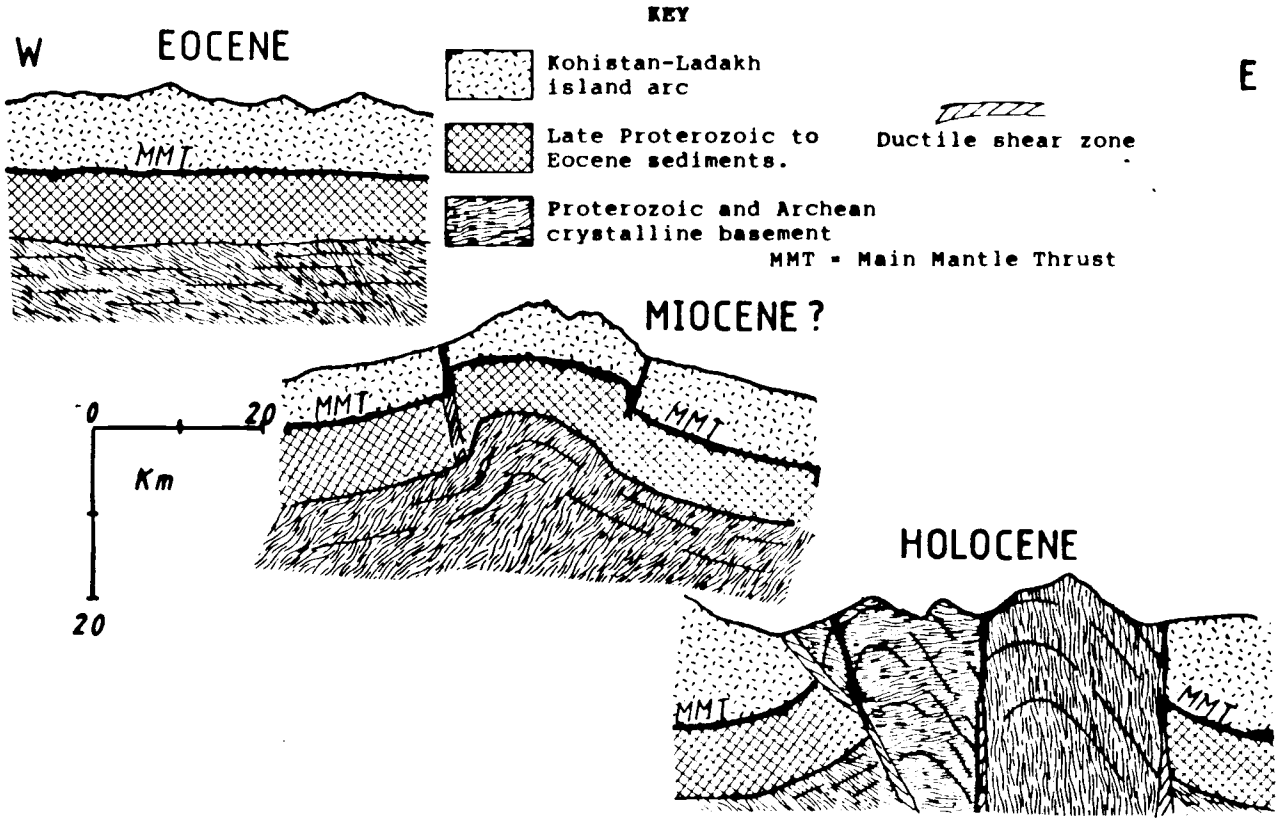

Figure I-10. Evolution of the NPHM. In the Eocene, Indian crystalline basement and sedimentary cover are overridden by the Kohistan island arc. East-west compression begins in the latest Miocene, and causes folding at depth, formation of a ductile shear zone above the fold in intermediate depths, and faulting at the surface above the ductile shear zone. At present, 15-25 km of uplift have completely removed the Kohistan island arc rocks, the MMT and the sedimentary cover, and have juxtaposed folds, mylonite zones and faults at the surface.

Zeitler's (1985) data suggests that much of this uplift has probably taken place in the last 6-8 million years and continues today at 5 mm/yr. This is supported by Madin (1986) who finds abundant evidence of Quaternary movement along the Raikot fault, with maximum Holocene uplift rates of 4.0 mm/yr.

This extreme uplift appears to have resulted from east-west compression, and has been accommodated by a combination of anticlinal folding at great depth, concentrated ductile shear at intermediate depth and faulting in near surface rocks (Figure I-11). The uplift has juxtaposed all three types of structures at the surface, and all three types of deformation probably continue beneath the NPHM today.

One of the most striking things about the extreme uplift of the NPHM is the strong localization of deformation. Over 25 km of uplift has been accomodated across a zone which averages 20-40 km wide and is locally as narrow as 10 km. Zeitlers (1985) uplift data shows that the uplift rates drops off sharply adjacent to the NPHM, and no significant late Cenozoic faulting or folding is known in the adjacent Kohistan or Ladakh island arcs. Such a concentration of deformation suggests the presence of a major pre-existing structure in the Indian continental crust. Finally, Kaila (1981) reports a 12 km upwarp of the Moho beneath the NPHM, which suggests that the structure which localizes the deformation involves the entire crust.

Regional Tectonics

The most persistent model for the origin of the NPHM has been that originally proposed by Wadia (1964) in which a northward promontory of the Indian plate makes first contact with Asia and is preser-

ved as a basement high. Zeitler (1985) amplified this model with the suggestion that the rapid uplift of the massif is the result of a feedback mechanism involving decompressive conversion of eclogite to granulites and amphibolites. It is unlikely that such a promontory would have persisted, as it would have experienced even more convergence and crustal shortening than the rest of the Indian plate, and its structure should be dominated by north-south shortening. In addition, such an origin would require the NPHM to be older than the MMT which it clearly is not.

The rigid indenter model of Molnar and Tapponnier (1975) also involves bending of the collision zone around the point of first contact. This model does not adequately explain the origin of the NPHM because it requires that uplift begin in the early Cenozoic.

The most plausible model for the tectonic origin of the NPHM combines Klootwijk's (1985) model of rotational underthrusting of and the proposal of Yeats and Lawrence (1983) and Coward (in preparation) that the Raikot fault is the terminal tear fault of the MCT. On the basis of paleomagnetic evidence, Klootwijk proposes that a significant amount of Indian continental crust has underthrust the Himalaya along the MCT, with a greater amount of underthrusting at the eastern end of the range. This requires the crustal slab above the MCT to rotate clockwise with respect to the slab below the MCT. The rotation and underthrusting result in south to southwest slip along the MCT. As shown in Figure I-12, this southwest thrusting must translate into southwest directed strike slip where the MCT encounters the western edge of the slab, and should cause east-west compression against the Asian plate material to the west.

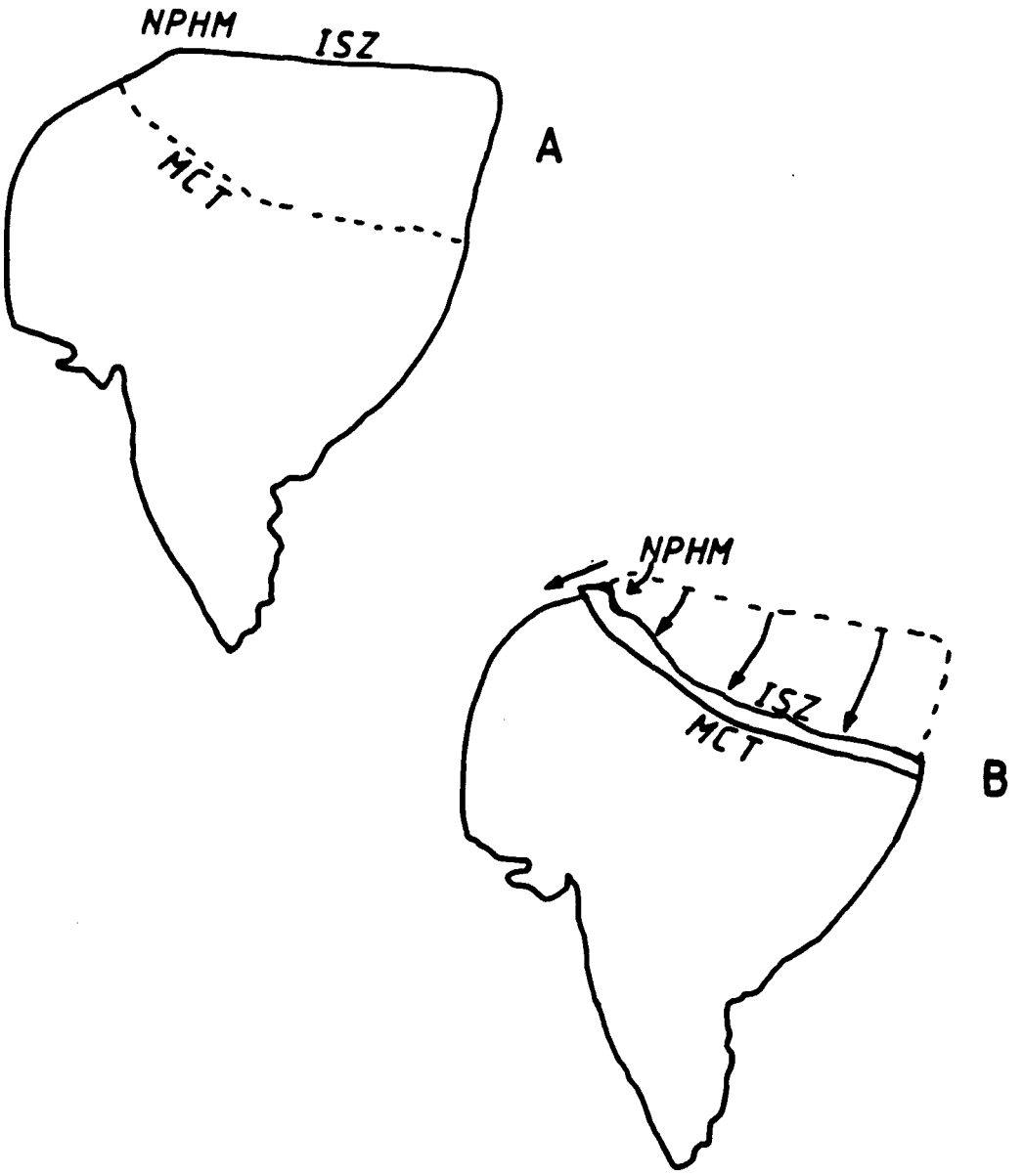

Figure I-12. Rotational Underthrusting Model. A. Greater India sutures to Asia along ISZ in early Cenozoic. Continued convergence initiates underthrusting along MCT (dashed). In the Late Cenozoic greater underthrusting in the east results in rotation, which translates into west-southwest slip at the western end of the MCT (NPHM). MCT = Main Central thrust, ISZ = Indus Suture Zone, NPHM = Nanga Parbat-Haramosh massif. After Klootwijk, 1985.

Several lines of evidence are consistent with the suggestion that the western margin of the overthrust slab occurs at the NPHM, and that the Raikot fault is in fact a strike slip tear fault terminating the MCT. No connection has been demonstrated between the MCT and the Raikot fault, but recent mapping by Thakur (1981) suggests that the MCT passes north of the Kashmir Basin (Figure I-3) into unmapped terrain instead of south to intersect the MBT as depicted by Gansser (1964). No Indian crustal rocks are recorded northwest of the NPHM, although such rocks may extend well beneath Kohistan. The involvement of the entire lithosphere in the uplift of the NPHM suggests that the structural discontinuity which localizes the uplift may in fact be the northwestern margin of overthrust slab. If this is so, then motion along the MCT must translate to strike slip at the NPHM along the Raikot fault.

The proposed connection of the MCT and Raikot fault are depicted in a revised regional geologic map (Figure I-13). South of Nanga Parbat, the Raikot fault swings east to connect with the MCT in northern Kashmir. Beneath the NPHM, the Raikot fault flattens to join the MCT. the Raikot fault truncates the MMT beneath Kohistan, and brings crystalline basement west over Kohistan.

In summary, it is proposed that the Raikot fault is the terminal tear fault of the MCT and the NPHM is the northwestern margin of the overthrust Indian plate. The rapid and localized uplift of the NPHM is the result of oblique compression across the plate margin as a result of large scale underthrusting and rotation along the MCT. The present high rate of uplift and activity along the Raikot fault suggests that similar activity may occur along other parts of the MCT.

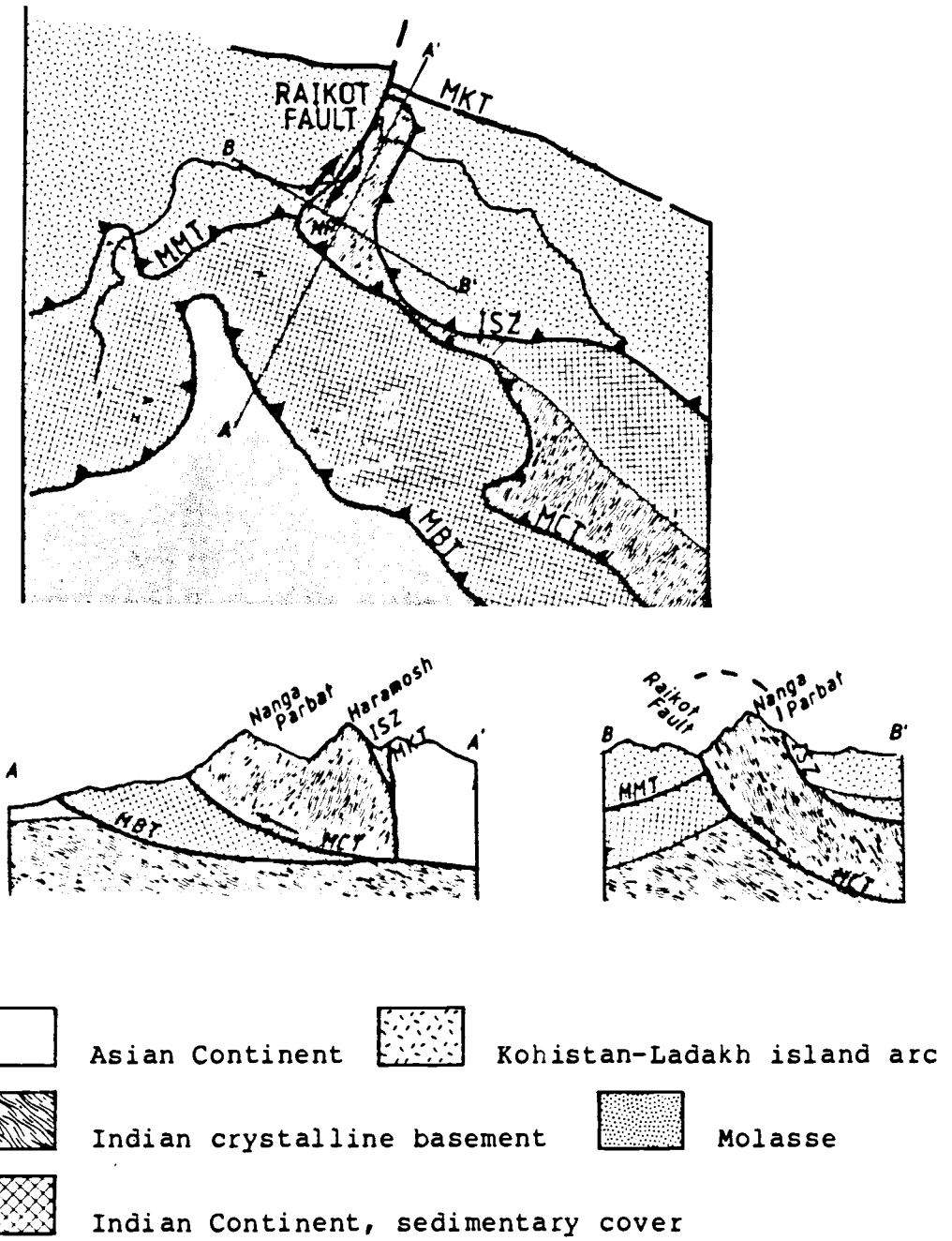

Figure 13. Revised Regional Geologic map. Regional geologic map depicting the proposed connection between the Raikot fault and the MCT. MKT = Main Karakoram thrust, MMT = Main Mantle thrust, ISZ = Indus Suture zone, NP = Nanga Parbat, MCT = Main Central Thrust, MBT = Main Boundary thrust.

Neotectonics of the Northwestern Nanga Parbat-Haramosh Massif

Introduction

The Nanga Parbat-Haramosh massif (NPHM) is a unique structure in the Himalayan collision zone both because it is the northernmost exposure of continental India, and because it occurs in the western Himalyan syntaxis where southwestward convergence along the great Himalayan thrust systems is translated into left-lateral motion along the Chaman transform. The recent tectonic history of the NPHM is therefore of great interest in understanding the geodynamics of the collision. Zeitler (1985) made the first attempt to date and quantify the uplift of the massif with cooling dates derived largely from fission-track dating. Lawrence and Ghauri (1983) identified the Raikot fault, which is active and bounds the western margin of the NPHM, and suggested that the uplift might be localized along the fault. Evidence of Quaternary faulting along the Raikot fault would confirm its importance in the uplift of the NPHM, and refine estimates of uplift rates.

Although high uplift and erosion rates have removed most Quaternary deposits from the NPHM, enough remain to be correlated with Quaternary deposits located on the downthrown side of the Raikot fault. Shroder (in review) has recently documented the presence of an unusually complete Pleistocene section in the middle Indus and Gilgit valleys, and has obtained some absolute (thermoluminessence) ages for some stages. This study focuses on the identification of Quaternary tectonic features along the Raikot fault, and includes a local glacial stratigraphy which correlates well with that of Shroder, allowing

estimates of Quaternary uplift rates for the NPHM.

The NPHM is located in northern Pakistan (Figure II-1) at the junction of the Great Himalaya, Karakorum and Hindu Kush ranges and extends from the western end of the high Himalaya at Nanga Parbat to the southern edge of the Karakoram at Rakaposhi. East of the NPHM, the Indus river leaves the broad valley of Skardu at the western edge of the Haramosh range and cuts a tremendous gorge between Nanga Parbat (8132 m) and Haramosh (7400 m) to reach the broad middle Indus valley below the confluence with the Gilgit river. Topographically the NPHM stands 3 to 4 km above the surrounding countryside.

The NPHM was mapped originally by Wadia (1933) as a northward projection of Precambrian rocks of the Indian continent, and by Misch (1949) as a zone of Himalayan-age metasomatic granitization. The western boundary of the NPHM was interpreted (Tahirkheli, 1979, 1982; Gansser, 1980, Coward, 1982) as the northeastward continuation of the Main Mantle thrust, along which the Kohistan island arc was obducted onto the Indian plate in the early Cenozoic. However, Lawrence and Ghauri (1983) and Madin (1986) have shown the boundary to be an active fault, named the Raikot fault.

The earliest observations of Quaternary features in the area were made by Misch (1939) and Wadia (1933) and consist largely of mapping of undifferentiated Quaternary cover, in the Nanga Parbat region and up the Indus as far as the Gilgit river. Wiche (1959) studied some glacial deposits in several of the tributary valleys in the study area, and Derbyshire and others (1983) completed an extensive study of the Quaternary history of the Hunza valley northwest of the Haramosh range.

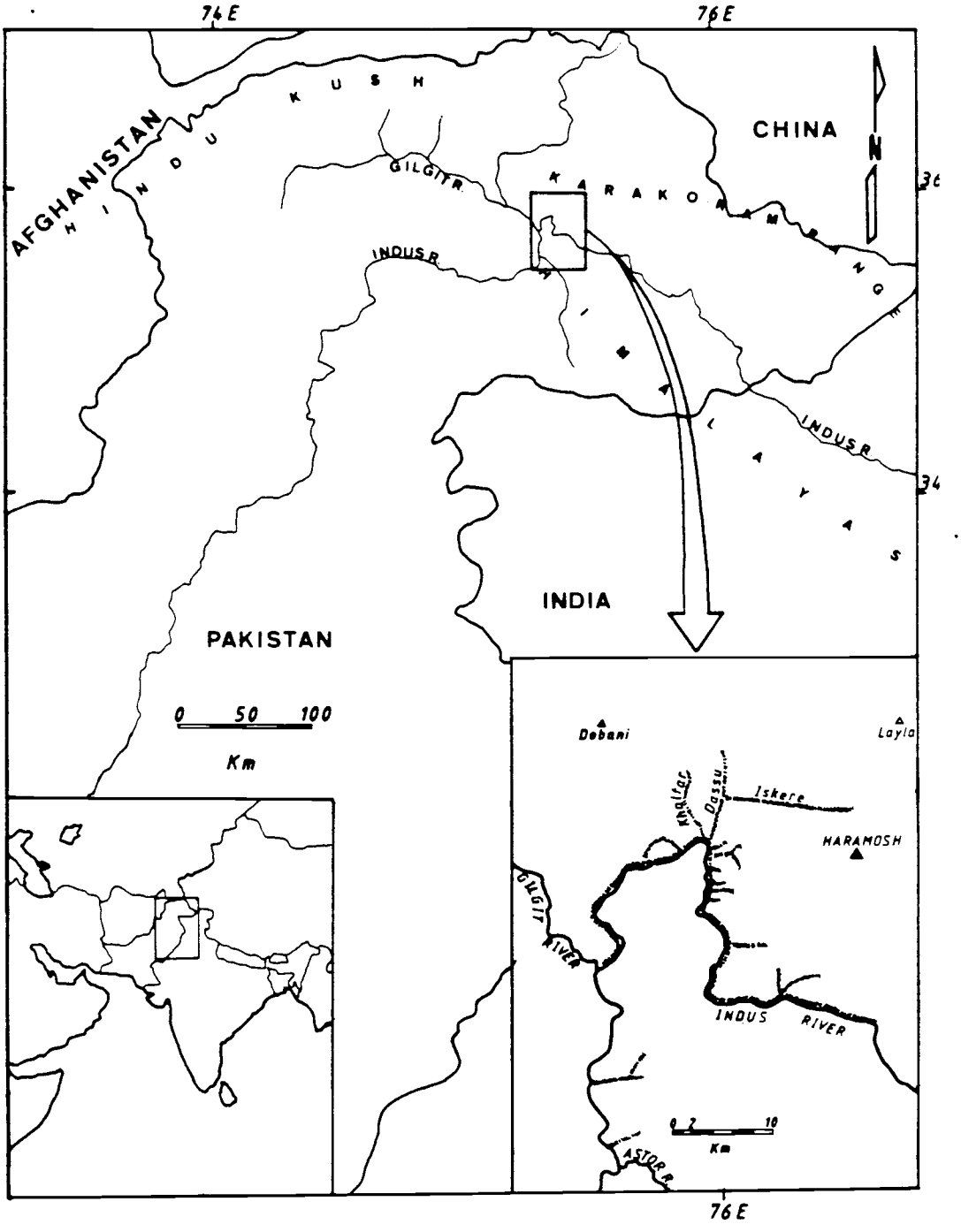

Figure II-1. Location and Traverse Map. Location of the study area indicated by box in large diagram. Actual traverses are indicated with hatched lines in the inset.

The most complete work in the area is that of Shroder (in review) who has done considerable mapping of the of the Hunza, Gilgit and middle Indus valley and has made a reconaissance traverse across the NPHM to Skardu. Shroder's work includes several new thermoluminessence dates on glacial deposits and a summary of glacial deposits and chronologies in the Karakoram, but does not extend upstream of the Gilgit river in detail.

The current climate of the area is that of a mountain desert. High ranges of the Himalaya to the south intercept monsoon borne moisture, and annual precipitation is minimal and falls largely as snow. Minor streams are either fed year round directly from icemelt, or are dry gullies which run only during severe storms. Natural vegetation in the Indus gorge is very sparse below 3,000 m, above which scrub, meadows and forest extend to 5,000 m. Extreme relief and uplift rates severely limit the preservation of Quaternary deposits, and more than 75% of the study area is exposed bedrock. Temperature at the bottom of the gorge ranges from approximately 0° C to 50°C.

This paper presents the results of 4 months of field work carried out in the fall of 1983 and 1984, covering a 30 km wide swath along the western margin of the NPHM range as indicated on the traverse map in Figure II-1. Quaternary geology and active fault traces mapped on a 1:50,000 topographic base maps are presented in Plate II-1. Supplemental observations were made telescopically and with stereo air photos. A local Quaternary stratigraphy was developed based on relative position of deposits and degree of preservation of original landforms. The study includes one thermoluminescence date collected by Dr. J. Shroder and processed by Alpha Analytical Labs.

Bedrock Geology

The Raikot fault, which bounds the western NPHM, is a zone up to 3 km wide of mylonite, cataclastite, and minor faults which separates Kohistan-sequence matic metasediments and intrusives from Nanga Parbat-group granitic and psammitic gneisses and schists. (Figure II-2). The faults in the zone generally strike 350° to 010°, and dip 60° to 90° east. Offsets are consistently east side up, and numerous parallel strands are commonly observed. Slickensides and mylonitic lineations are oriented 010°, 50° and indicate dextral reverse slip.

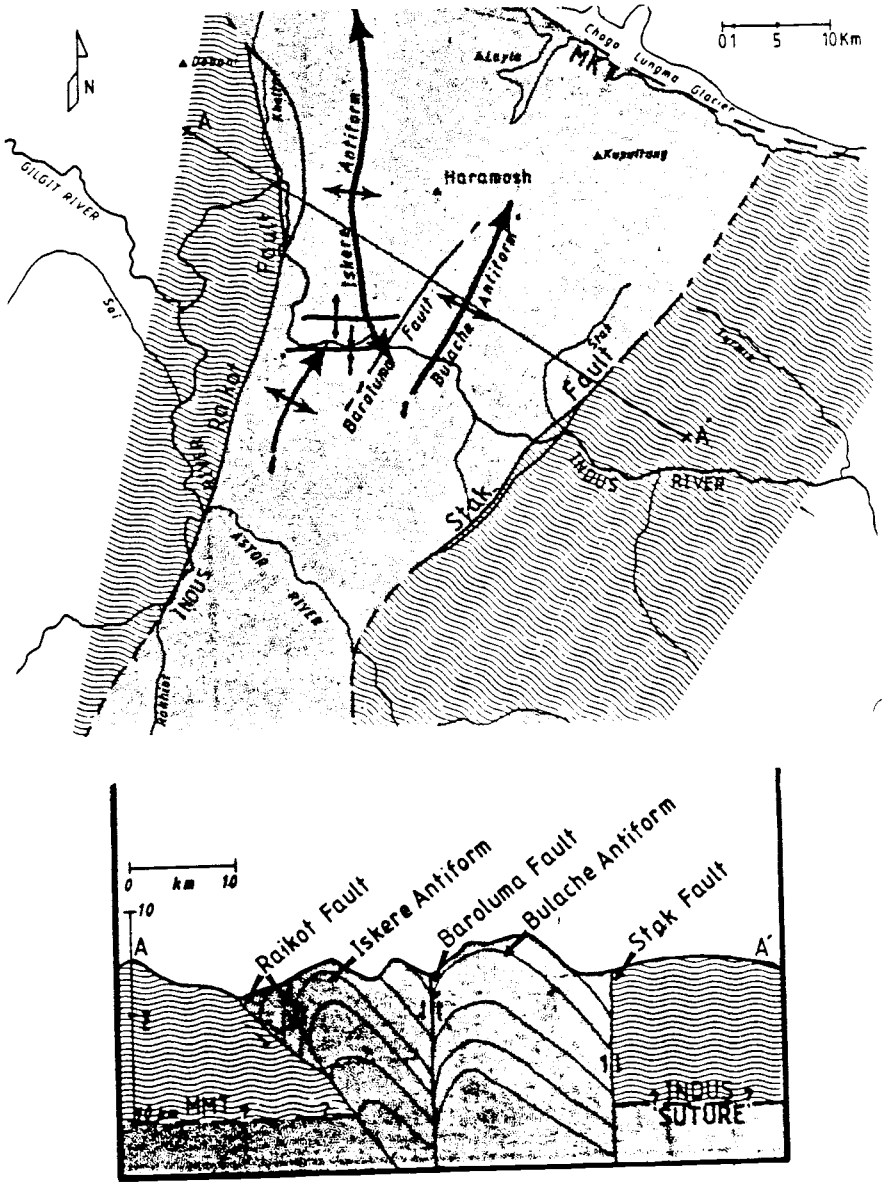

Figure II-2. Geologic Map and Cross Section. Geologic map and cross section of the NPHM, from Madin (1986) and Verplanck (personal communication). Nanga Parbat group rocks shown in fine dot pattern, Kohistan-Ladakh island arc rocks in wavy line pattern.

Quaternary Stratigraphy

Four ages of glaciation are suggested by deposits and topography in the area; an early event represented by high planation surfaces, two middle events represented by tills, fluvial and lacustrine sediments, and a neoglacial event, indicated by moraines and trimlines. One absolute age was obtained by thermoluminescence dating, but the rest of the deposits are dated by indirect correlation with the chronology of Shroder (in review). A summary of published glacial chronologies prepared by Schroder with correlations of glaciations of this study is presented in Table II-1.

Dobani Glaciation

The oldest glaciation is suggested by a conspicuous high elevation plateau locally preserved on the downthrown side of the Raikot fault. A strongly dissected plateau surrounds Dobani, and a remarkably flat broad plateau caps the divide between Dassu and Khaltar canyons (Figure II-3) and is visible on Landsat image in Figure II-4. These upland planations are 1200 to 1500m above the adjacent modern valley floors, and are similar to those described in the adjacent Hunza valley by Derbyshire, and are tentatively correlated with the early Pleistocene Shanoz and Jalipur glaciations of Derbyshire et al (1984) and Shroder (in review).

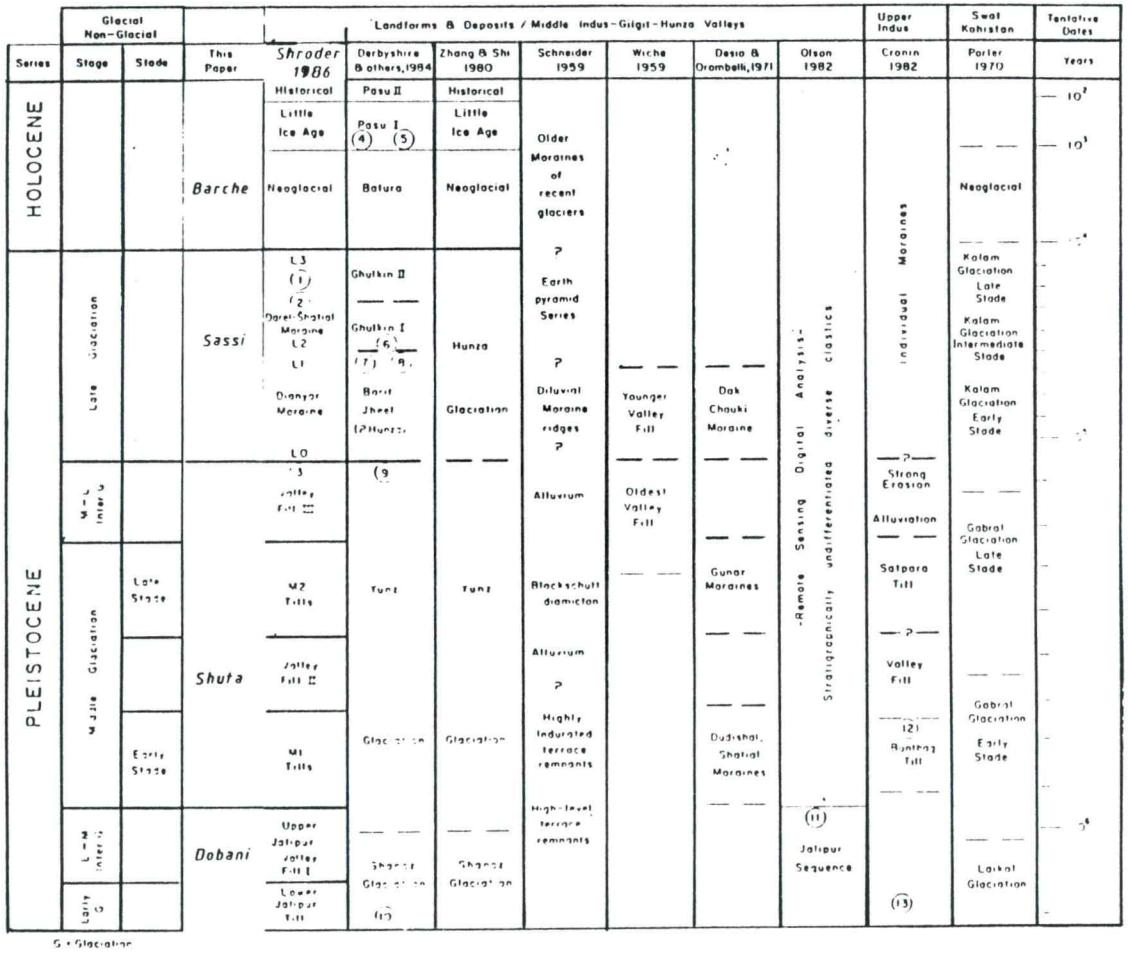

Table II-1. Regional Glacial Chronology. Summary of stratigraphic units and associated glacial events in the Karakoram range. After Shroder (in review)

Figure II-3. Dobani and Barche Glacial Features. View to the west down Iskere canyon to Dassu canyon and the Khaltar-Dassu divide. The plateau on the top of the divide is a Dobani age planation. A Barche age terminal moraine is visible in Iskere canyon.

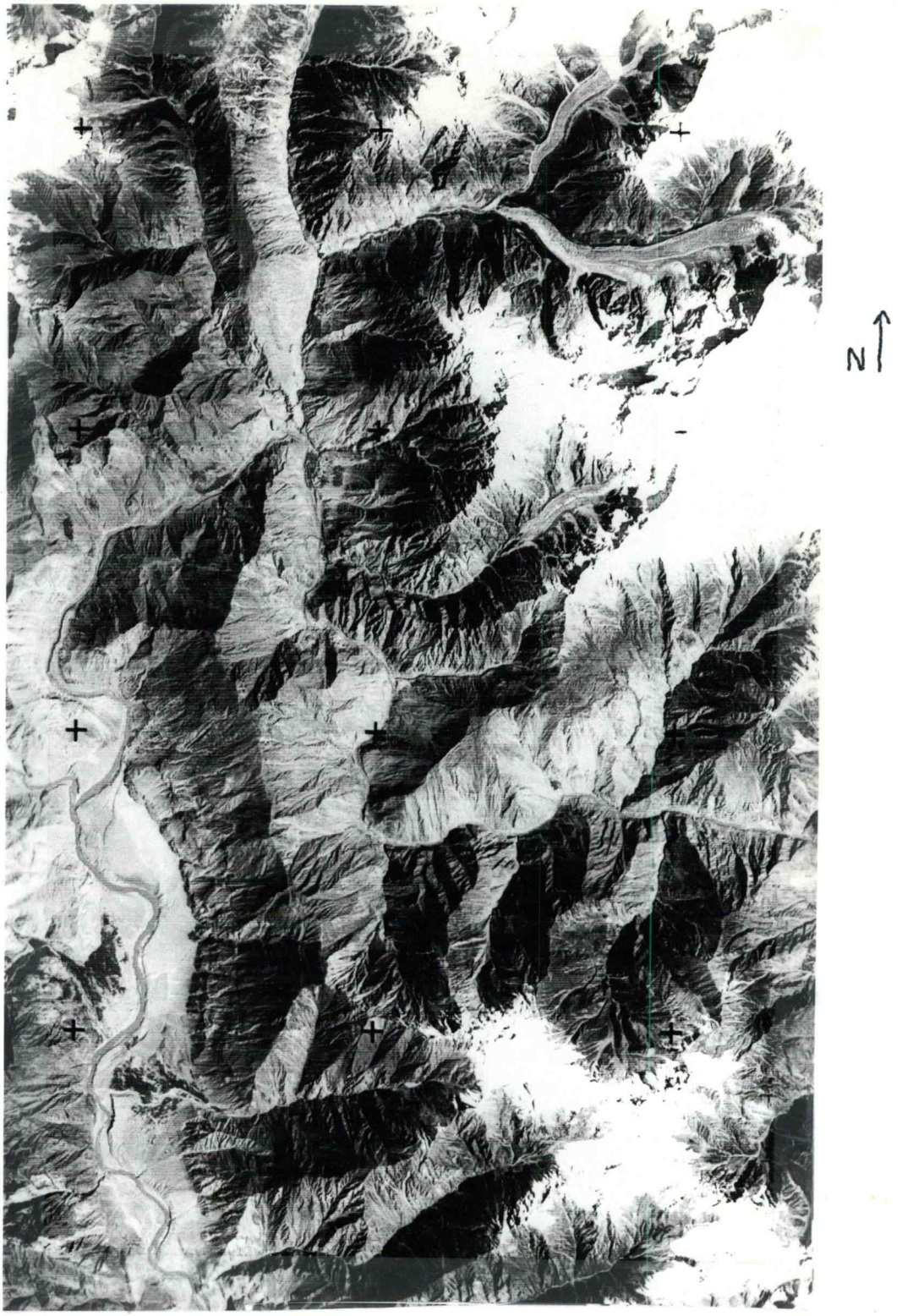

Figure II-4. RBV Landsat Image of the northwestern NPHM.

Shuta Glaciation (t3)

Shuta age glaciation is represented by strongly dissected, indurated till banked against the steep walls of the Indus gorge up to 1000 m above the present river level. The surface of the only accessible deposit is too strongly dissected for surficial weathering to have a reliable relation to the age of the till. The till as a whole is moderately weathered, and strongly cemented by clays derived from the abundant micas of the Nanga Parbat gneisses. From the general color of the tills, the clasts appear to be dominantly derived from local gneiss or gabbro bedrock.

Original morphology is not clearly recognizable, but a major flat topped body of till on the inaccessible south bank of the Indus opposite Shuta may be a terminal moraine although telescopic observation suggests that the till may be veneer banked against deeply weathered bedrock. This deposit is the downstream most Shuta till that is derived solely from the upper Indus but it is not known at present whether the glacier that deposited the till originated in the Skardu area, or more locally from Haramosh. The majority of the rest of the Shuta till is probably lodgement and lateral moraine.

Remnants of till occur along the east bank of the Indus between Bunji and the mouth of the Gilgit river. The deposits, observed only telescopically and on airphotos, are between 150 and 600 m above the modern valley floor and appear to be derived from ice filling the Indus, not local valleys. This till was probably deposited during the extensive middle Pleistocene Indus valley filling glaciation of Shroder, by ice from the Gilgit valley and possibly from the upper Indus.

Lake sediments associated with the Shuta till can be observed

telescopically on top of the till deposit opposite Shuta as an area of rolling topography cut in horizontally laminated light colored sediment. Opposite Hanuchal a patch of layered silts is preserved against the south wall of the Indus gorge approximately 500 m above river level. This lone deposit is the either result of a post Shuta age ice dam in the Indus downstream or damming of streams along the edge of the glacier. Fluvial gravels of Shuta age are deposited on bedrock beneath the Shuta till at Shuta village.

At Sassi, the Indus gorge is quite broad, and a prominent bedrock planation occurs at 150 to 200 m above the modern Indus. The bedrock planation appears to have been cut by the Shuta age glacier, as the surface is incised locally by abandoned Indus channels packed with tills of the next youngest age.

The moraines of Shuta age represent deposits from a glacier which filled the Indus gorge with ice 800 m thick above a valley floor approximately 150 m above the modern river level. This thickness of ice is consistent with that present in the Gilgit and middle Indus valleys at the same time (Shroder, personal comunication). The Shuta ice may have been the dowstream end of an extensive valley glacier originating in the Skardu basin, or may have been caused by the coalescence of the Khalola, Ishkapal, Sassi, Dassu and Khaltar canyon glaciers. In the latter case, the upper Indus gorge should have been filled with fluvial and lacustrine deposits behind an 800 m high glacial dam. No such sediments are preserved in the upper gorge.

The Shuta glaciation is tentatively considered middle Pleistocene, and correlated with the M1 and M2 glaciations of Shroder, and Yunz glaciation of Derbyshire et al, and hence is probably older than

139,000 years. Only this one till has been recognized, in contrast to two tills from this stage noted in many locations by Shroder (in review) but very little till of this age is preserved at all in the Indus gorge. It is also possible that the Shuta glaciation was an early stade of the late Pleistocene glaciation, and would then correlate with the Dianyor stage of Shroder.

Sassi Glaciation (t2)

The Sassi glaciation is represented by extensive till, fluvial and lacustrine deposits in the main Indus valley and moraines associated with modern glaciers in tributary valleys. Sassi tills are moderately dissected and locally forested, but many original surfaces persist. Weathering of clasts on the surfaces is moderate, with pitting, spalling and extensive cover by desert varnish commonly observed. Sassi tills are commonly indurated by clays derived from Nanga Parbat gneiss micas and possibly carbonates derived from marbles. Local hot springs activity has strongly altered the clasts, and cemented the till with silica, iron oxides and clay.

Nanga Parbat group gneisses are the dominant clasts in the main Indus valley, but Sassi tills associated with minor valley glaciers originating in the Kohistan basic terrain are composed of Kohistan sequence clasts. Original depositional morphology is commonly recognized in Sassi tills; lateral moraines are beautifully preserved in some minor hanging valleys and adjacent to existing glaciers (Figure II-5) and a well preserved lateral and terminal moraine occurs at Bunji. Dissected remnants of Sassi age till occur commonly in tributary valleys of all sizes and more rarely along the Indus gorge upstream of Sassi.

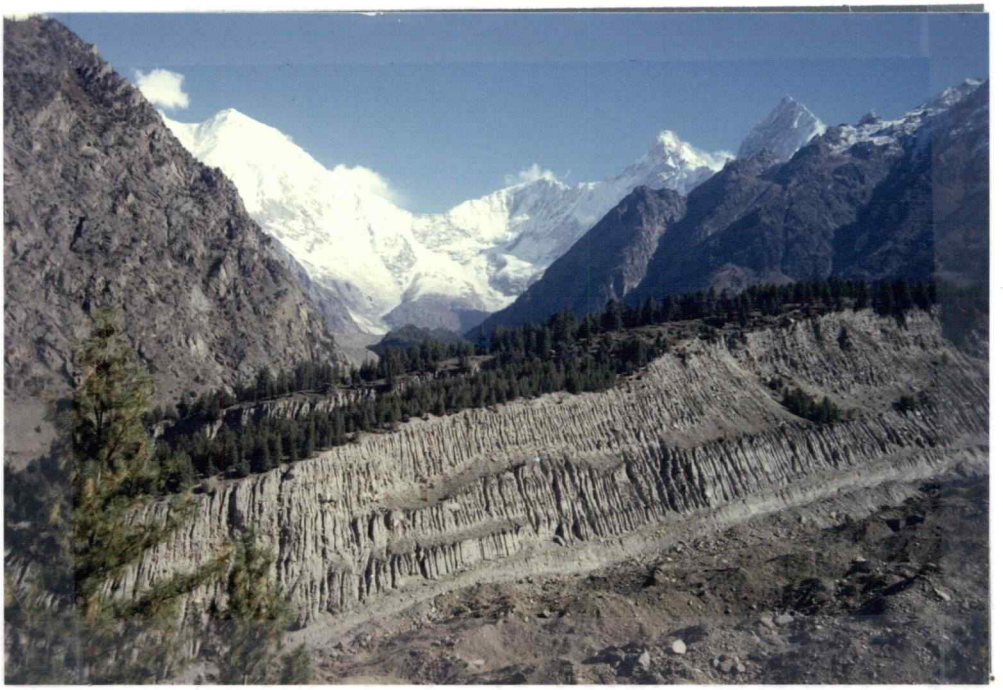

Figure II-5. Sassi Age Moraines. View to the north of a Sassi age lateral moraine on the north side of the Mani glacier. The top of the moraine stands 100 to 150 m above the modern ice surface.

Sassi till was deposited as a continuous sheet of lodgement till 150 to 200 m thick extending down the Indus gorge from Sassi village Khaltar canyon, and up Dassu canyon to the mouth of Iskere canyon (Figure II-6). Striae on bedrock beneath Sassi till in Sassi canyon trend west, down Sassi canyon and indicate some contribution from tributary valleys. Figure II-7 details the stratigraphy of glaciofluvial sediments and tills beneath the till plateau. Till and gravels derived from a fault sliver of Kohistan sequence gabbros wedges out to the north, indicating a considerable component of downvalley ice movement.

The glaciofluvial gravels depicted in Figure II-7 are crudely bedded boulder gravels which are at least 40 m thick at Sassi canyon and thin to the south. The gravels occur on both sides of the Sassi-Dassu fault and are offset approximately 100 m up to the east across the fault.

The lacustrine sediments in Figure II-7 are sands, pebbly sands and silts, poorly consolidated and well bedded in continuous layers 0.5 to 10.0 cm thick. Cross bedding or channel and fill structures are rare, but "flame" structures and intralayer soft sediment folding are common, suggesting syndepositional earthquake activity. The unit is at least 40 m thick , and thins to 2 to 5 m thickness south of Sumari canyon. The lacustrine sediments do not occur on the upthrown side of the Sassi-Dassu fault, and may have been deposited against a rising fault scarp.

Minor deposits of lacustrine sediment associated with Sassi glaciation occur upstream of Sassi village. The largest occurs at the small westward bend of the Indus just upstream of Shatot. The deposit,

Figure II-6. Sassi Till Plateau. View to the south down Dassu canyon, showing Sassi age till plateau.

Figure II-7. Quaternary Relations at Sassi. A. Schematic diagram showing stratigraphy of tills and glaciofluvial deposits and location of faults, scarps and the Sumari landslide. B. Detailed section across the Sassi-Dassu and Hurban fault scarps, showing the true offset.

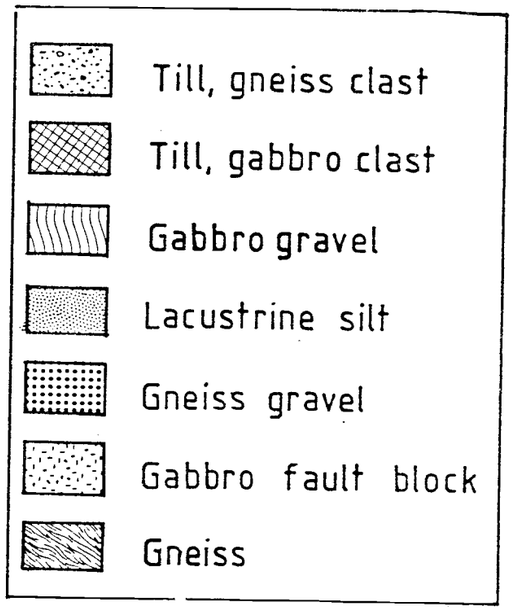

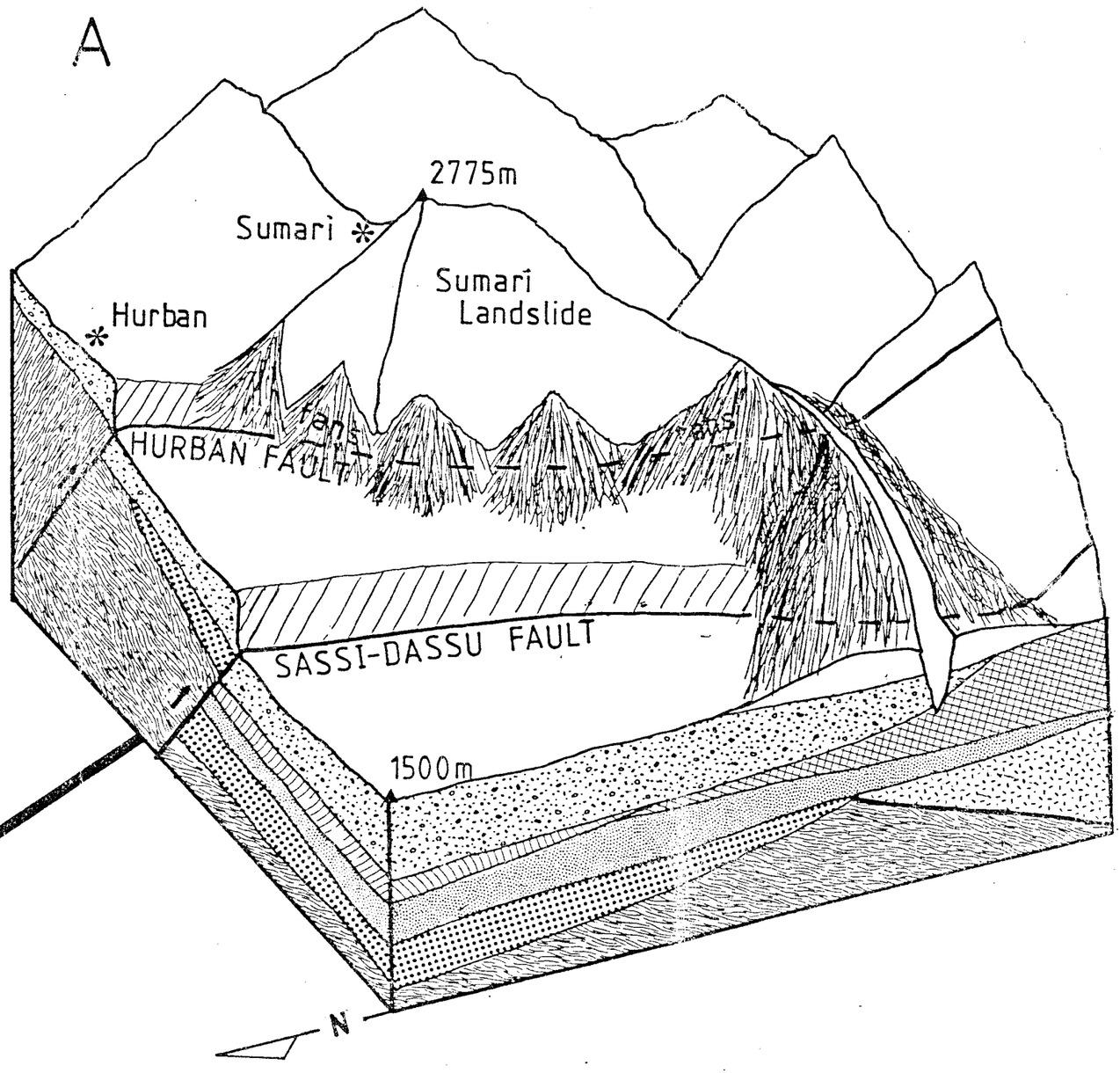

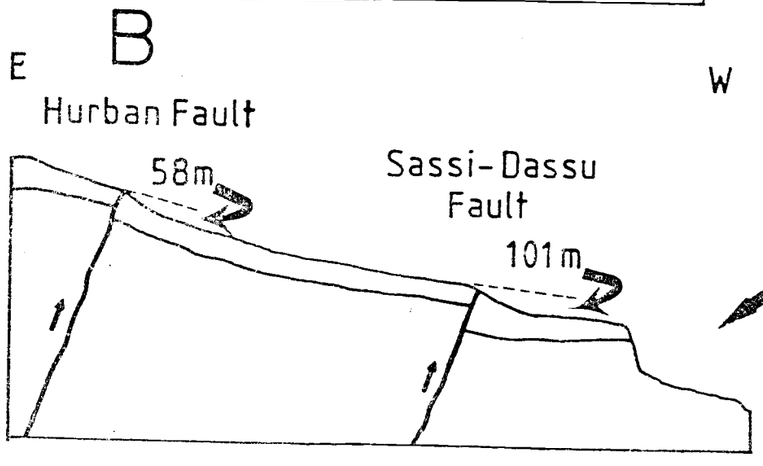

which is 80 m above the modern river, and is a sequence of laminated pebbly sand and silt at least 30 m thick may be related to a late glacial ice dam from Ishkapal canyon. All of the minor Sassi age lacustrine deposits have been tilted up to 4° by Quaternary tectonics.

Extent of Glaciation

Because the Sassi glaciation was the youngest major event in the area, it has left a more complete record of the extent and geometry of the ice which deposited the tills. A good measure of the extent of side valley glaciers is found in a minor drainage just north of the mouth of Khaltar canyon. This drainage has a catchment of approximately 5 km^2, and a maximum elevation of 4000 m, yet it contained a significant glacier which left well formed lateral moraines over 50 m high. Figure II-8, based on the distribution of till and extrapolation from the example cited above shows nearly every tributary valley in the area filled with a Sassi age glacier. The Indus gorge may have been locally filled with a considerable glacier produced by the coalescence of tributary glaciers, even in the absence of a major valley filling glacier originating in the upper Indus or Skardu basin. The combination of evidence for extensive glaciation in minor tributaries and the general lack of glacial deposits imply extremely high post glacial erosion rates, which may have obliterated evidence for a major Indus trunk glacier upstream of Sassi.

The stratigraphy of Sassi age deposits at Sassi village (Figure II-7) suggests that at the beginning of deposition, a valley-filling glacier, possibly locally derived, was flowing north with fluvial reworking of till at a snout near Sassi. Subsequently, the gorge was dammed downstream by ice from Dassu and Khaltar canyons, causing

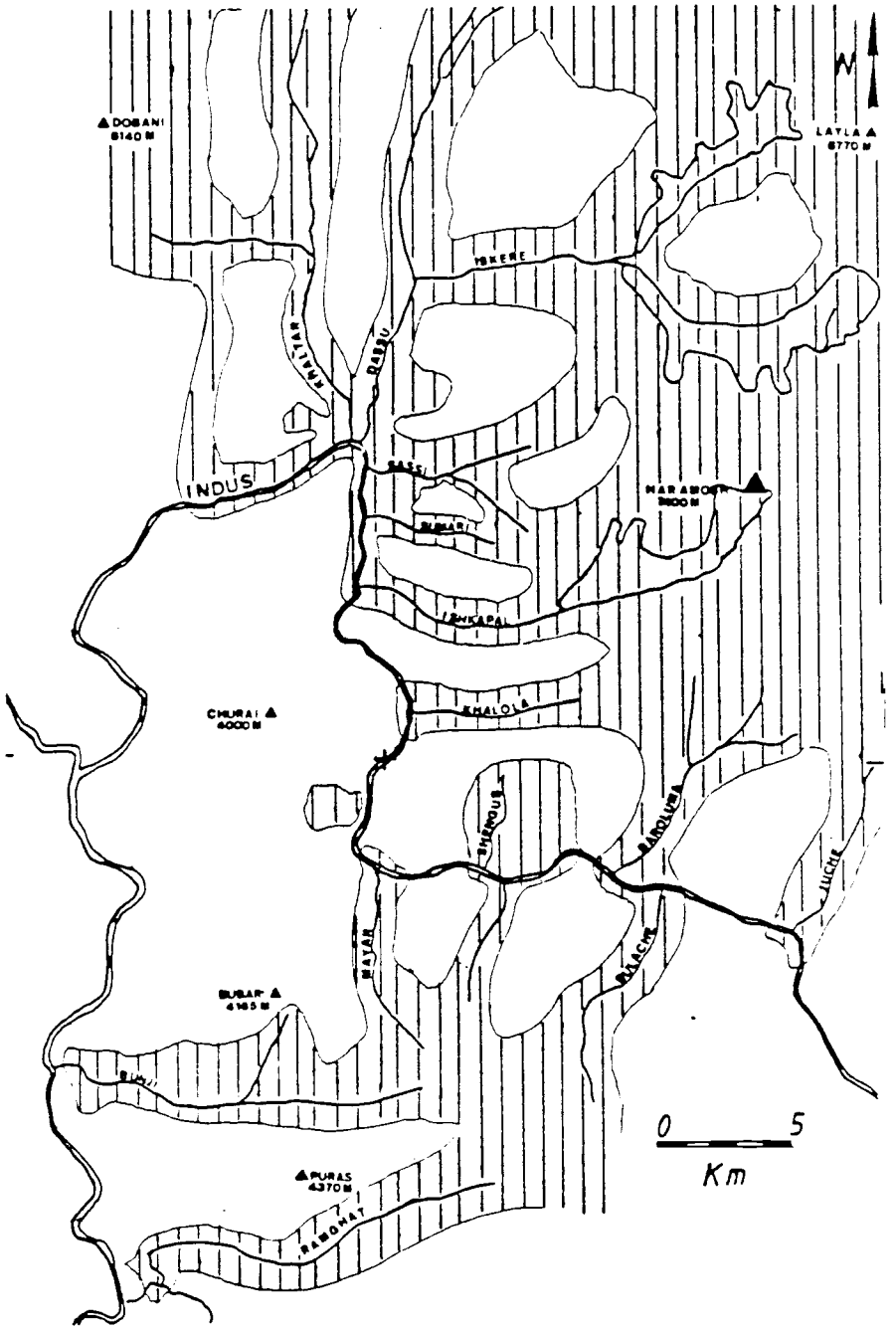

Figure II-8. Extent of Sassi Age Ice. The patterned areas indicate the assumed extent of ice at the peak of Sassi age glaciation.

deposition of lake sediments over the fluvial sediments. The advancing ice then deposited the sheet of lodgment till, and the continuity of the sheet up Dassu canyon suggests that the Indus valley filling glacier was controlling the depositional base level of the Dassu and Khaltar canyon glaciers. The absence of lateral moraines associated with the valley filling glacier is puzzling, but may have been due to the fact that the Indus must still have flowed in the gorge, presumably between the ice and the bedrock walls.

In upper Iskere canyon, the Mani glacier flows along the foot of the north wall of Haramosh. The Mani, and the Baskal glacier which flows off the south slopes of Layla are the remnants of the major Iskere-Dassu valley glacier. The Mani glacier has well-developed Sassi age lateral moraines which were studied by Wiche (1959). He concluded that the moraines were of Würm age, but incorrectly assumed that the Würm ice did not extend past the confluence of the Mani and Baskal glaciers. The Sassi laterals on the Mani glacier stand 150 to 200 m above the present ice surface. They do not however abut against the north wall of the canyon, which suggests that the canyon was cut by a more extensive previous glaciation, probably the Shuta.

An interesting feature of Sassi age glaciation at Mani glacier is Kutwai lake, a small lake on the northern Mani lateral which is encircled by terminal moraines. On airphotos, the terminal moraines clearly open to the south, and are directly in line with a hanging glacier on the face of Haramosh. This feature, originally noted by Wiche (1959) is probably due to surging of the hanging glacier across the Mani glacier some time late in the Sassi glaciation. The lake and its encircling moraines are visible on the Landsat image in Figure II-4.

On the basis of position and preservation of original morphology, the Sassi age glacial deposits are considered to have been deposited by the most recent major advance, and are therefore late Pleistocene. They are tentatively correlated with the Dianyor moraine of Shroder (in review) and the Borit Jheel or Ghulkin moraines of Derbyshire et al (1984). If the Sassi till is correlated with the Dianyor till then the age is is approximately 31,000 to 38,000 years based on thermoluminescence dating by Shroder (in review).

A sample of lacustrine silts from beneath the till plateau at Sassi (Figure II-7) was processed by Alpha Analytic Labs (Coral Gables Fl.), but unfortunately the sample showed anomalous fading during processing. The calculated age of 41, 000 years is therefore a minimum age.

Barche Glaciation

The Barche glaciation is a major neoglacial advance represented by small terminal moraines a few km downstream of modern glacial terminii, and trim lines on Sassi moraines adjacent to modern glaciers.

Two Barche moraines were visited, both composed of poorly consolidated, moderately weathered till derived from local lithologies. The moraines occur in upper Dassu and Iskere canyons (Figure II-3) and both retain original rounded morphology. Both moraines have dammed their respective streams, producing gently graded reaches upstream of the moraine, and cascades directly at the moraine. Sharp terraces on the inner walls of Sassi age lateral moraines of the Nani glacier suggest a neoglacial advance which increased the level of the ice approximately 50 to 70 m above the modern level (Figure II-5). In

Ishkapal canyon a poorly preserved Barche terminal occurs at the mouth of the canyon. The absence of a Barche moraine in Khaltar canyon is attributed to the lack of a modern glacier in the canyon. Both the Dassu and Iskere canyon moraines are clearly visible on the Landsat image in Figure II-4.

The Barche moraines are correlated with the Batura or possibly Pasu stages of Derbyshire et al (1984) and the neoglacial moraines of Shroder (in review) As such their age is constrained to be between 31,000 and 350 years.

Other Quaternary Deposits

Young fluvial deposits occur along the inner Indus gorge and are probably related to aggradation associated with neoglacial glacial advances. It is also possible that the young sediments are associated with landslide or tributary glacial damming of the Indus. Such deposits are widespread along the east bank of the Indus from Bunji to the mouth of the Gilgit river where they overlie a complex valley fill series derived from several earlier glaciations. Discontinuous patches of fluvial sediments occur along the modern Indus upstream of the mouth of the Gilgit river as far as Khalola. The sediments represent one and possibly several aggradation events which filled the post Sassi gorge to a depth of approximately 50 m, following which most of the deposit was removed and the modern river entrenched in bedrock.

Young alluvial deposits also occur in gentle reaches of Dassu and Iskere canyon.

Young, steep fan deposits occur commonly along the inner walls of the Indus gorge. The fans range from true alluvial fans to talus

cones, with most being intermediate. Rainfall is rare in the area, but often occurs as heavy summer storms which cause debris avalanches and mudflows. Mudflows deposits 3 months old were observed in 1983 which were so well indurated at that time that they stood in vertical faces which could be climbed. Most fans appear to be crudely interlayered mudflow and talus and can have steep surfaces slopes, up to 40°.

Older fans, notably at Sumari canyon and Hanuchal, do not grade to the Indus, but instead probably grade to the Indus level that prevailed immediately after the retreat of Sassi age ice. These fans are deeply incised by the streams which deposited them.

In general, the sparse occurrence of fan and talus deposits in the Indus gorge points to unusually high uplift and erosion rates.

Numerous landslides occur in the area, one of the most important of which is the Sumari slide (Figure II-7) which overrides the Hurban fault. The village of Sumari is located in the graben at the head of the slide, which is filled with Sassi age till, indicating that the slide predated the Sassi glaciation.

The other gravity feature of importance is the common occurrence of toppling and possibly sackung on steep slopes underlain by rocks with strong vertical foliation. The clear susceptibility of the steeply-dipping gneiss to toppling involving the upper 100 m raise the possibility that considerable sackung (essentially large scale toppling) may occur, which may produce scarps that could be confused with active fault scarps.

Neotectonics

Direct evidence of neotectonic activity is common along several strands of the Raikot fault in the form of ground rupture or tilted Quaternary deposits. Indirect evidence of neotectonic activity includes the distribution of Quaternary deposits, subtle tilting of lacustrine deposits, and knickpoints and lateral offsets of streams.

The clearest examples of Quaternary deformation occur along the Sassi-Dassu and Hurban strands of the Raikot fault at Sassi (Plate II-1, Figure II-7A), and to the north at Dassu and Hanumal.

Just south of Sumari canyon the fluvial, lacustrine, and till deposits of Sassi age overlie a fault sliver of Kohistan basic rocks along the Sassi-Dassu fault. The sediments are tilted 20-30° to the east (Figure II-9) and along the base of the fault sliver bedrock is thrust horizontally over till.

North of Sumari canyon, the Sassi-Dassu fault passes across the broad Sassi age till plateau, and offsets it along a major east side up scarp that extends 1.5 km south and 0.5 km north of Sassi canyon (Figure II-10, II-8A). The southern end of the scarp is buried beneath fan material, and the northern end passes out of Quaternary material. The scarp is 123 m high with a scarp face slope of 22-28°, and the till plateau slopes 5° west on either side of the scarp. This (Figure II-7B) resolves into an offset of 101 m of the till plateau surface.

East of the Sassi-Dassu fault, the Hurban fault also crosses part of the Sassi age till sheet and offsets the surface along an east side up scarp (Figure II-7A). The scarp is 92 m high with a face slope of 35°, and is cut across a till surface which slopes 16° west. The total offset of the till surface is approximately 58 m (Figure II-7B).

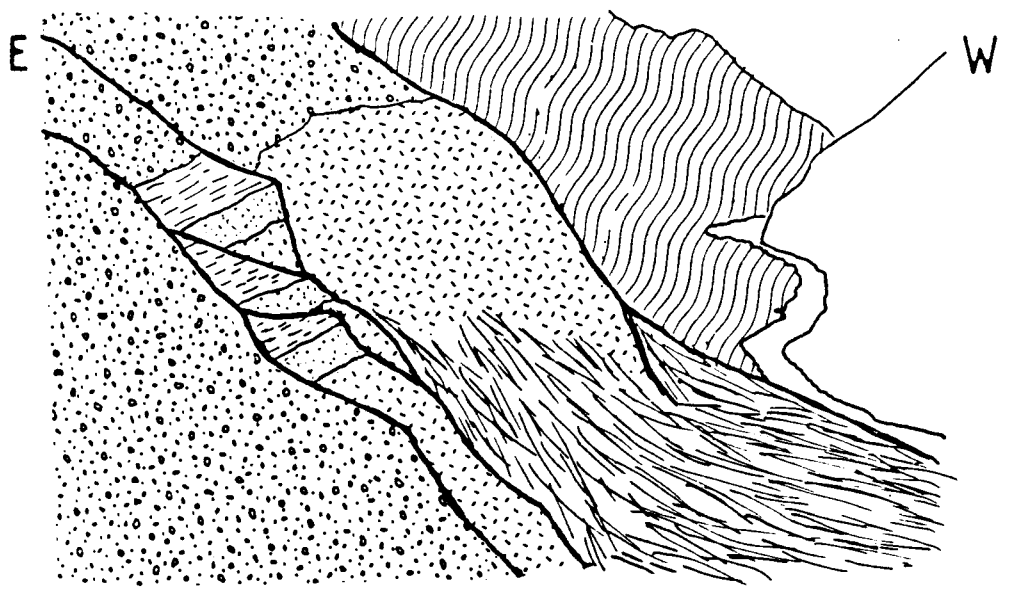

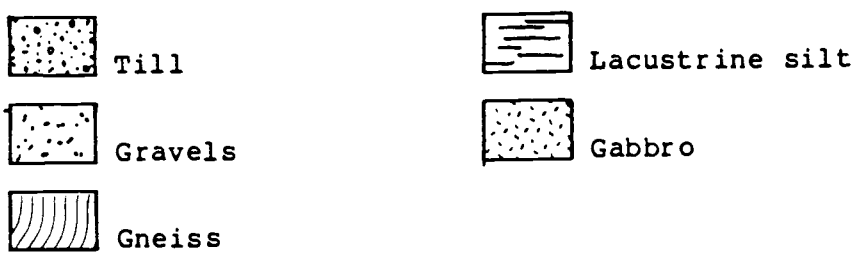

Figure II-9. Tilted Sediments. Sketch looking south along the Indus gorge from the mouth of Sumari canyon. Sassi age till, lacustrine and fluvial sediments on top of fault sliver of gabbro are tilted east along the Sassi-Dassu fault. Silt beds are approximately 4 m thick.

Figure II-10. Scarp at Sassi. View to the southeast of the Sassi-Dassu fault scarp east of Sassi.

The scarp on the Hurban fault occurs at the point where Sassi canyon opens out of a narrow bedrock gorge, and it is possible that the scarp observed is a terminal moraine produced late in the Sassi glaciation. However, bedrock traces of the Hurban fault are observed directly beneath the scarp, strongly suggesting that it is tectonic.

North of Sassi canyon, the Hurban fault extends across a slope of undifferentiated till and exposed bedrock, producing a composite scarp on the till and clear traces on the bedrock. The scarp is inaccessible but has five steps, with an estimated total height of 50 to 75 m. South of Sassi canyon, the scarp is dissected by minor gullies and fans, and the Hurban fault probably passes beneath the Sumari landslide.

Between Sassi and Dassu villages both the Sassi-Dassu and Hurban fault pass across a bedrock slope with sparse fan deposits. Discontinuous scarps occur on older inactive fan sections, and on active fans scarps are suggested by sets of minor gullies on the fan surface which all head along the same horizontal line. These features are not accessible, but appear fairly clearly on air photographs.

At Dassu village, Dassu canyon is partly filled with the Sassi age till plateau, and the eastern contact between till and bedrock is covered by fans built onto the till. The Sassi-Dassu fault roughly parallels the eastern edge of the till plateau, and offsets the toes of the alluvial fans in a series of discontinuous scarps 10 to 30 m high, one of which is depicted in Figure II-11. The scarps are preserved only on older fans which have been detached from their sources, In one fan, a steeply east-dipping fault is visible beneath the scarp, offsetting crude bedding in the fan material. The Hurban fault passes

on the bedrock slope east of Dassu village and cuts the heads of the inactive alluvial fans. Activity on the Hurban fault has separated the fans from their sources, and consequently allowed preservation of Sassi-Dassu fault scarps at the fan toes. Both fault traces are clear and fairly continuous on air photos, and the Sassi-Dassu trace and the beheaded fans are faintly visible on the Landsat image in Figure II-4.

North of Dassu village, the Hurban fault dies out or intersects the Sassi-Dassu fault, which continues north across Dassu canyon at the mouth of Iskere canyon and crosses the divide between Dassu and Khaltar canyons. At the confluence of Iskere and Dassu canyons, the village of Hanumal sits on a small remnant of glaciofluvial terrace which is definitely younger than the main Sassi till in the area, and is probably related to the Barche age terminal moraine in Iskere canyon, less than 1 km away. The Sassi-Dassu fault passes beneath the terrace and offsets the terrace surface along the east side up scarp visible in Figure II-12. The scarp was not visited, but its height is estimated to be approximately 15 m with a scarp face slope of approximately 30°. In a sheer cliff cut across the southern side of the terrace and scarp, a fault dipping 70-75° east is clearly visible directly beneath the scarp.

North of Hanumal, the Sassi-Dassu fault was not visited, but clear scarps are visible on air photos in the upper reaches of Khaltar canyon, both on colluvial slope cover and Sassi age moraine. Where the fault crosses the Khaltar-Dassu divide, the Dobani age glacial planation surface is truncated, and the fault is marked by an abrupt change in slope.

Figure II-11. Scarps at Dassu. View to the northeast of an alluvial fan built onto the Sassi till plateau at Dassu village. The toe of the fan is truncated by a scarp along the Sassi-Dassu fault.

In the southern part of the area, the Raikot fault crosses the Indus river, and passes along the inaccesible west bank, then over the divide to the head of Bunji canyon. Evidence for Quaternary deformation exists along this stretch of the fault, but could not be confirmed.

No evidence of Quaternary offset is visible in upper Bunji canyon, where Quaternary deposits are limited to active fans. High on the eastern side of the divide between Bunji canyon and the Indus, a series of up to seven linear scarps cross moderately steep grassy slopes (Figure II-13). The scarps face upslope and may be due to motion on the Raikot fault, but may also be due to sackung or other gravity processes.

Just north of the main eastward bend of the Indus, a small basin occurs on the west bank of the river. The Raikot fault clearly traverses this basin as a zone of hydrothermal alteration separating Kohistan gabbros from Nanga Parbat gneisses. Coincident with this zone is a marked linear feature, which stands out on bedrock, and across one major active fan. The feature may be a goat track, but it appears to behead a well preserved pair of Sassi age lateral moraines.

Further north along the Indus, at the small westward loop in the riverjust south of Shatot, a body of fluvial gravels and lacustrine sands deposited behind a landslide dam is offset by 0.5-1.0 m. with east side up displacement (Figure II-14). The offset directly overlies an east dipping bedrock trace of the Raikot fault. The offset lake sediments are covered by thin fan materials which are not offset.

Figure II-12. Scarp at Hanumal. View to the north of a glaciofluvial terrace astride the Sassi-Dassu fault at Hanumal. A scarp approximately 15 m high cuts the terrace.

Figure II-13. Scarps on Bunji-Indus Divide. Telephoto view the west of minor tectonic or gravity scarps on the crest of the Bunji-Indus divide, just east of Sarkun lake. Some right lateral displacement of minor gullies appears possible across the scarps.

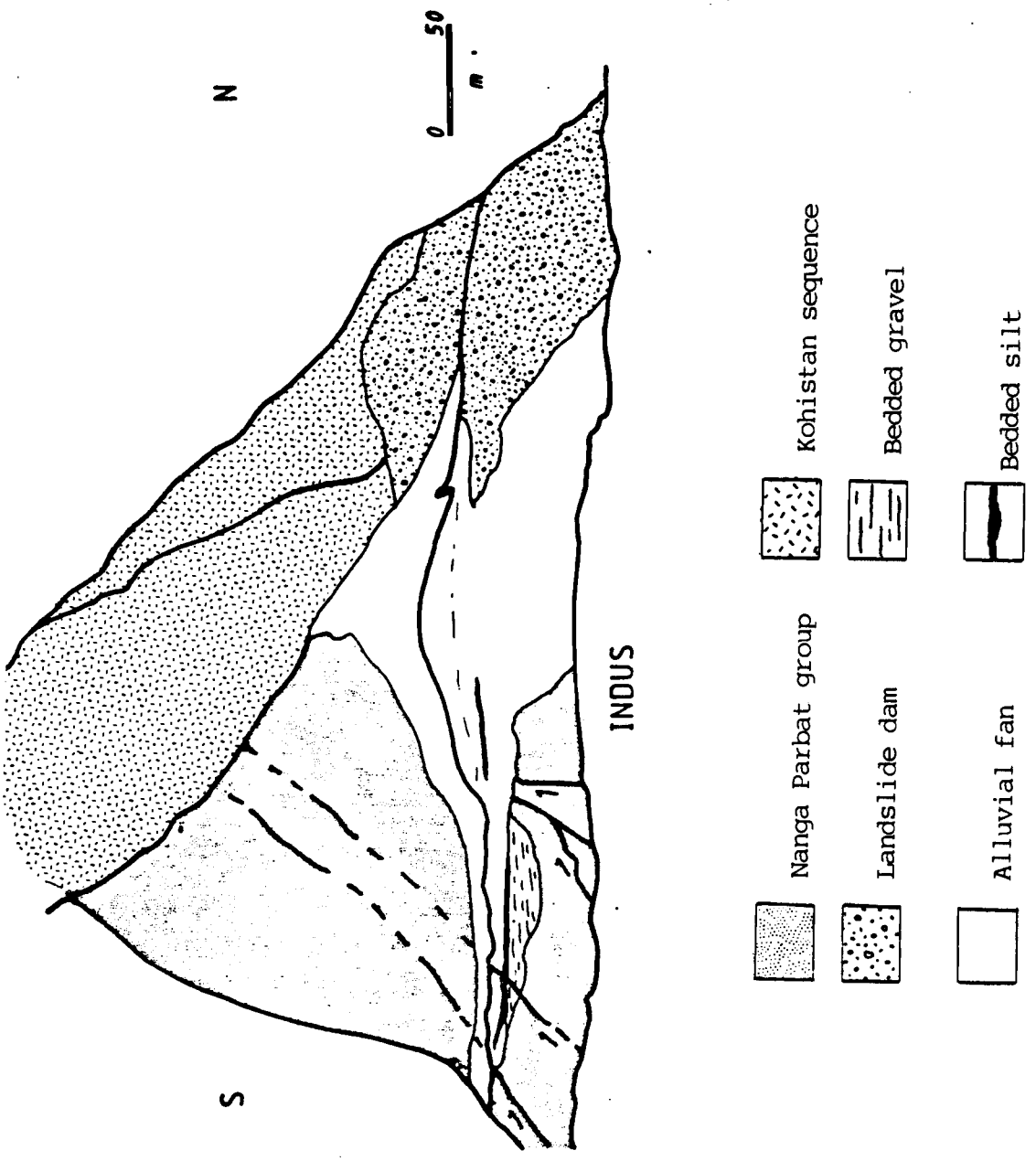

Figure II-14. Landslide dam on the Indus. Sketch looking west of the west bank of the Indus. Numerous strands of the Raikot fault are visible near the river, one of which cuts silt and gravel layers deposited behind a landslide dam. The alluvial fan material above the silts is undeformed.

Indirect Neotectonic Evidence

Small remnants of lacustrine sediments deposited behind glacial or landslide dams occur on both sides of the Raikot fault. Those on the western side dip 3-5° to the west, and those on the east block dip 3-15° to the east, indicating tilting of all blocks by Quaternary fault activity.

Active uplift along the Raikot fault is reflected indirectly in the regional distribution of Quaternary deposits. The NPHM in general has minimal Quaternary deposits, whereas on the downthrown side of the Raikot fault, the middle Indus valley contains a nearly complete Pleistocene section (Shroder, in review). In the Indus gorge upstream of the point where the Raikot fault crosses the river, Quaternary deposits other than landslides are rare, and the canyon slopes are generally steep bare rock, as indicated on the geologic map in Plate II-1.

Abrupt changes in gradient are common on streams which cross the fault. These knickpoints cannot be rigorously depicted with stream profiles because of the poor quality of the available topographic bases, but all can be clearly observed in the field. The most prominent knickpoint is a broad increase in gradient of the Indus where it crosses the fault. Figure II-15 shows a profile of the Indus which reveals steep gradients at the Raikot and Stak faults.

Streams which show marked knickpoints are Ramghat, Bunji, Ishkapal, Sassi, Khaltar and Dassu creeks. In the case of the first four, the downstream reaches are generally floored in gravel or slightly incised into bedrock. The reaches upstream of the fault are deeply incised in bedrock, with numerous cascades and waterfalls. In Dassu

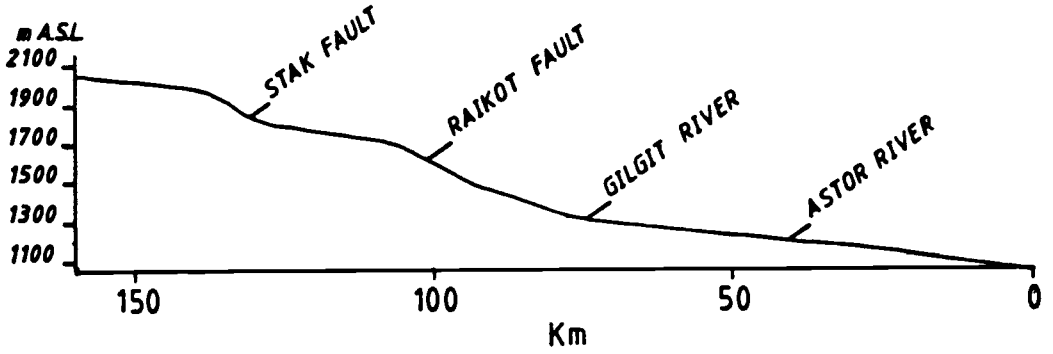

Figure II-15. Indus River Longitudinal Profile. Longitudinal profile of the Indus river across the NPHM. Data from AMS 1:250,000 sheet NI-43-1 and NI-43-3.

creek, the knickpoint is a bedrock cascade which drops 150 m. at a gradient of 1km/km and separates upstream and downstream reaches which are gently graded and entirely floored in gravels.

Lateral offsets in streams across the fault are common, and generally are on the order of 1-2 km, and with the exception of Dassu and Khaltar canyons are right lateral. The offsets are not sharp, but are distributed over 1-2 km which reflects high erosion rates that allow streams to partly straighten their course between ruptures. The sense of offset of Dassu and Khaltar canyons is left lateral, which is still geometrically consistent. The fault trends N 30-50 W across the two canyons, which trend due north. The slip direction along the fault is to the southwest, which results in the left lateral offsets in these two canyons.

The most significant lateral offset across the fault is that of the Indus itself. The river flows generally west from Skardu, then bends abruptly 90° north just downstream of Shengus and flows north along the Raikot fault to Sassi, where it bends 140° to the west, and flows generally south as far as Nanga Parbat. This abrupt step in the course of the Indus is approximately 15 km long, and is closely coincident with the Raikot fault.

Conclusions

The main aim of this study is to demonstrate that the uplift of the NPHM is localized along the Raikot fault, and to attempt to quantify Quaternary uplift rates. To this end, a glacial stratigraphy based on poorly preserved glacial deposits straddling the Raikot fault has been correlated with the more complete section in the middle Indus and Gilgit valleys in order to establish ages for surfaces offset by the Raikot fault.

Data concerning rates of slip and recurrence intervals along the Raikot fault come from the scarps produced by the Sassi-Dassu and Hurban faults in the Sassi age till plateau depicted in Figure II-7. The net offsets of the till surface across the two faults were calculated by subtracting the difference in vertical drop between the plateau slope and the scarp face slope from the total scarp height as measured with an altimeter (Figure II-7B). The faults responsible for the offset are assumed to be steeply dipping, so that the net offset roughly equals the net fault slip. The age of the Sassi till in the plateau is weakly constrained by a Thermoluminescence date of 41,000 years as a minimum age. Since the date comes from lacustrine sediments beneath the till, an age of approximately 41,000 years is assumed for the till. This is in fair agreement with an age of 31,000 years (Schroder, TL date on late Pleistocene lake sediments). No evidence was observed to indicate the size of a single event, so the calculation of a recurrence interval is based on an estimate of 2.5 m vertical movement per event. The scarp height, net slips, slip rate, recurrence interval and overall uplift rate derived from these data are summarized in Table II-2.

Table II-2. Neotectonic Summary Slip rate and recurrence intervals for the Sassi-Dassu and Hurban faults.

	Sassi-Dassu	Hurban	Total
Net slip	101 m	58 m	159 m
Age of surface	> 41,000 years		
Uplift rate (slip rate)	2.46 mm/yr	1.4 mm/yr	3.8 mm/yr
Recurrence interval	1000 yr	1782 yr	650 yr

The scarps at Dassu, Khaltar, and Hanumal were not measured, and a careful study of these features combined with further dating would certainly increase the resolution of the Quaternary fault history.

Quaternary faulting has not been previously reported from this area, nor is there any record of historical earthquakes centered in the area. A microearthquake study was conducted in 1980 by Yielding and others (1984), and Figure II-16 shows 1 month of data accumulation. A north trending band of events ranging from 0 to over 45 km in depth coincides closely with the Raikot fault.

Zeitler's data (1985) for the NPHM are consistent with the results of this study both in terms of rate and geometry of the uplift. In Figure II-17A, a histogram of uplift rate vs. time shows an exponential increase culminating at approximatley 5 mm/yr at present, consistent with the maximum uplift rate of 3.8 mm/yr for the active Raikot fault. In Figure II-17B, the cooling age profile drops sharply across the western boundary of the NPHM, consistent with localized uplift along the Raikot fault.

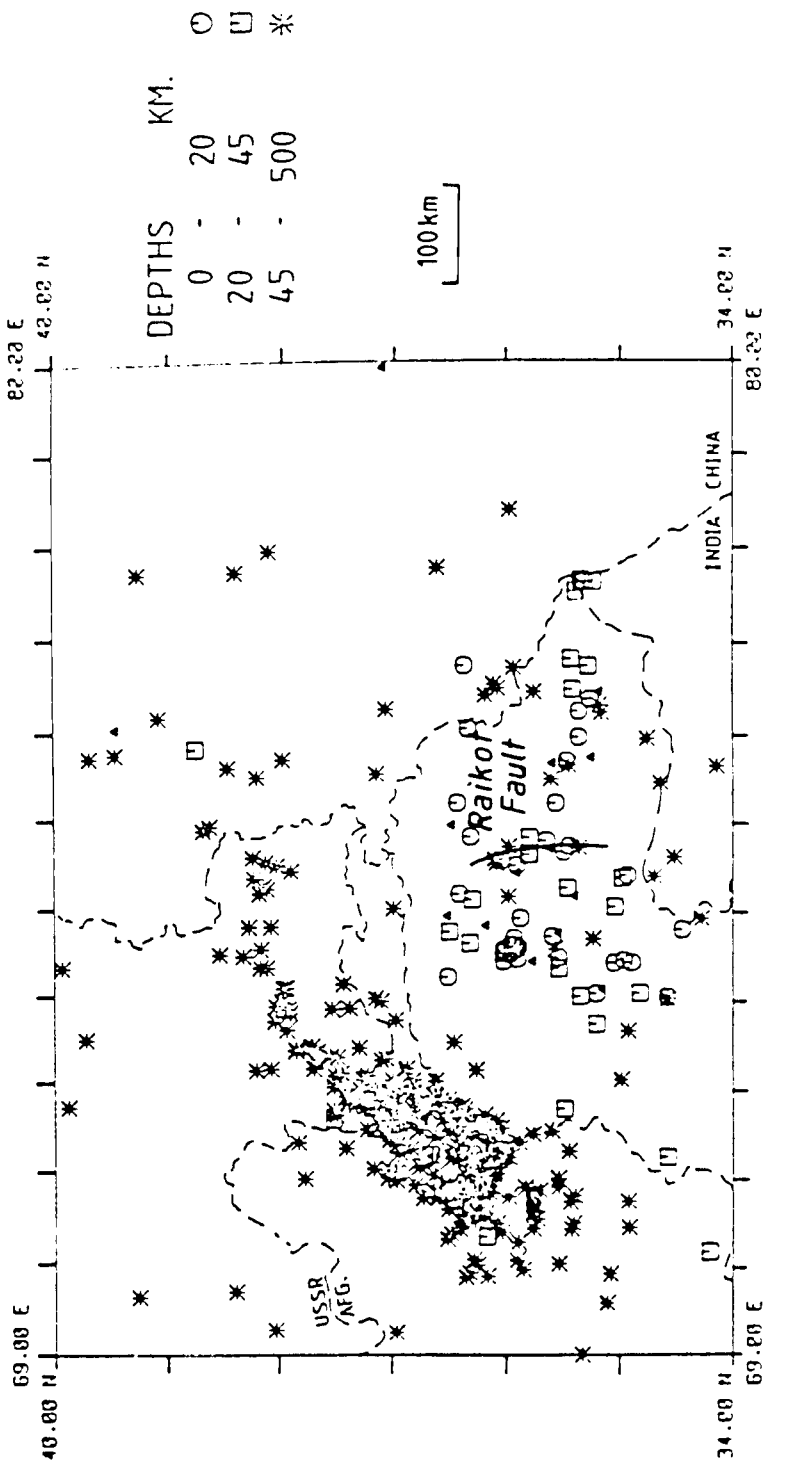

Figure II-16. Microearthquake Distribution. Intensity and distribution of all locatable events from 08/17/80 to 09/14/80. From Yielding et al, 1984.

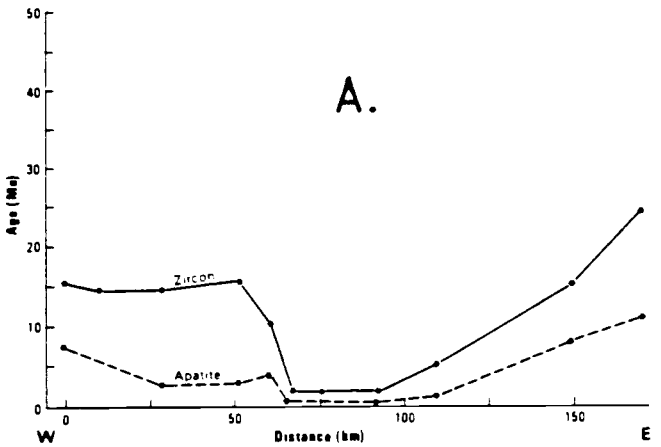

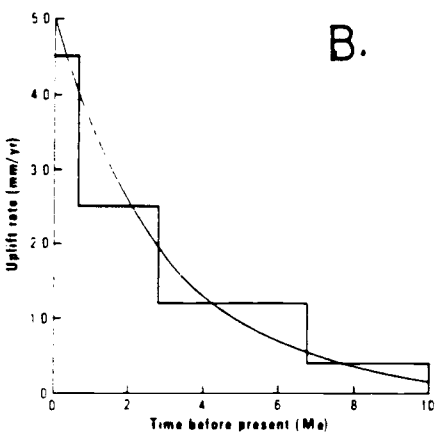

Figure II-17. Cooling Derived Uplift Data. A. Cooling age profiles across the NPHM, sharp drop coincides roughly with the Raikot fault. From Zeitler (1985). B. Histogram of uplift rate vs age for the NPHM. From Zeitler (1985).

Clearly, on the basis of this study and the work of Zeitler, the NPHM is experiencing rapid uplift along the Raikot fault which began in latest Cenozoic time. Lawrence (personal communication 1982) has proposed that the Raikot fault is in fact a terminal tear fault along the MCT, a model supported by Madin (1986). If this is so, the high rates of Quaternary activity along the Raikot fault suggest that similar activity may be taking place as yet unnoticed along the MCT as well as along the more clearly active MBT and frontal Himalayan thrusts.

Bibliography

Choudhary, A.K., Gopalan, K., and C. Anjaneya Sastry, 1984. Present status of the geochronology of the Precambrian rocks of Rajasthan. Tectonophysics, v. 105, p. 131-140.

Coward, M.P., Jan, M.Q., Rex, D., Tarney, J., Thirlwall, M., and Windley, B.F., 1982a. Geo-tectonic framework of the Himalaya of N Pakistan. J. Geol. Soc. London, V. 139 pp 299-308.

Coward, M.P., Jan, M.Q., Rex, D., Tarney, J., Thirlwall, M., and Windley, B.F., 1982. Structural evolution of a crustal section in the western Himalaya. Nature, Vo.295, No. 5844, pp 22-24.

Coward, M.P., Windley, B.F., Broughton, R., Luff, I.W., Petterson, M., Pudsey, C., Rex, D., Khan, M.A., in press. Collision Tectonics in the NW HImalayas.

Derbyshire, E., Jijun, L., Perrot, F.A., Shuying, X., and Waters, R.S., 1984, Quaternary glacial history of the Hunza valley, Karakoram mountains, Pakistan. in The International Karakoram project, K.J. Miller, Ed. Cambridge Univ. Press, 1984 v.2, p. 456-490.

Desio, A., 1964, A geological tentative map of the Western Karakorum, 1:500,000. Institute di Geoligia, Univ. Milano.

_____, 1979, Geologic evolution of the Karakorum, in Geodynamics of Pakistan:(A. Farah, and K.A. De Jong, eds.) Geol. Surv. of Pakistan, Quetta, p. 111-124.

Gansser, A., 1964, Geology of the Himalayas. Wiley Interscience, New York, 289 p.

_____, 1979 The Division between Himalaya and Karakorum. In, Proc. Intern. Commit. Geodynamics, Grp 6. Mtg Peshawar, Nov 23-29; Special Issue, Geol. Bull. Univ. Peshawar, Vol 13, 1980

Jan, M. Q., 1984. Some K/Ar dates from the Chilas complex in Swat. Geol. Bull. Univ. Peshawar, 1984, Vol. 17, pp. 171-173.

Kaila, K.L., 1981, Structure and seismotectonics of the Himalaya-Pamir-Hindu Kush region and the Indian plate boundary: In Zagros-Hindu Kush-Himalaya Geodynamic Evolution (H. Gupta and F. Delany, eds.) Am. Geophys. Union Geodynamics Series, v. 3, p. 272-293.

Klootwijk, C.T., Conaghan, P.J. and Powell, C. McA., 1985. The Himalayan Arc: large scale continental subduction, orocline bending and back arc spreading. Earth and Planetary Sciences Letters, 75

(1985) 167-183.

Lawrence, R.D., and Ghauri, A.A.K., 1983, Evidence of active faulting in Chilas District, northern Pakistan: Geol. Bull. Univ. of Peshawar, v. 16, p. 185-186.

Madin, I.P., 1986, Neotectonics of the northwestern Nanga Parbat-Haramosh massif. unpublished manuscript.

_____, 1986, Geology and structure of the northwestern Nanga-Parbat-Haramosh massif: Crustal uplift along a terminal tear fault on the MCT?, unpublished manuscript.

Misch, P., 1935, Arbeit und vorlaufige Ergebnisse des Geologen. In Finsterwalder: Forschung am Nanga Parbat: Sonderveroff. Geogr. Ges. Hannover.

_____ 1949, Metasomatic granitization of batholithic dimensions: Amer. Journ. of Sci. 247, 209-249.

Molnar, P. and Tappnier, P., 1975. Cenozoic Tectonics of Asia: Effects of a Continental Collision. Science, v. 189 # 4201, p. 419-426.

Simpson, C. and Schmidt, S.M., 1983. An evaluation of criteria to deduce the sense of movement in sheared rocks. Geol. Soc. Amer. Bull., v. 94, p.1281-1288.

Shroder, J.F., 1986, Quaternary Chronology in Himalaya of Northern Pakistan, in review.

Srikantia, S.V., Ganeshan, T.M., Rao, P.N., Sinha, P.K., and Tirkey, B., 1978. Geology of the Zanskar area. Himalayan Geology v. 8, p. 1009-1033.

Tahirkheli, R.A.K., Mattauer, M., Proust, F., and Tapponier, P., 1979, The India-Eurasia suture zone in northern Pakistan: synthesis and interpretation of recent data at plate scale: In Geodynamics of Pakistan (A. Farah, and K.A. De Jong, eds.) Geol. Surv. of Pakistan, Quetta, p. 125-130.

Tahirkheli, R.A.K., 1979, Geology of Kohistan and adjoining Eurasian and Indo-Pakistan continents, Pakistan, Geol. Bull. Univ. Peshawar Spec. Iss., 11, no. 1., p. 1-30.

_____, 1983. Geological Evolution of Kohistan Island Arc on the southern flank of the Karakoram-Hindu Kush in Pakistan. Bolletina di Geofisica Teorica ed Applicata, Vol. 25, No. 99-100 1983.

Thakur, V.C., 1981. An overview of the thrusts and nappes of the western Himalaya: In Thrust and Nappe Tectonics (K.R. McClay and N.J. price, Eds.) Geol. Soc. London Spec. Publ. 9, p 381-392.

_____, V.C., 1983. Deformation and Metamorphism of the Tso Morari crystalline complex. In Geology of the Indus Suture Zone in

Ladakh, (V.C. Thakur and K.K. Sharma, Eds)

Wiche, K. 1959a, Das Osterreichische Karakorum-Expedition 1958. Mitt. Geogr. Ges. Wien, v. 100, p 286-294.

_____, 1959b, Klimamorphologisches untersuchungen im westlichen Karakorum, Verhandl. Deutschen geographentages 32, p. 190-203.

Winkler, H.G.F., 1976. Petrogenesis of Metamorphic Rocks. 4th edition, Springer-Verlag, New York.

Wadia, D.N. 1931, The syntaxis of the northwest Himalaya: its rocks, tectonics and orogeny. Rec. Geol. Surv. India, 65, pt. 2.

_____, 1933, Note on the geology of Nanga Parbat, Mt. Diamir, and adjoining parts of Chilas, Gilgit district, Kashmir: Rec. Geol. Surv. India, 72, 2, 151-161.

_____, 1961, Geology of India 536 pp, 3rd. ed., Mac Millan, New York, 1961.

Yeats, R.S., and Lawrence, R.D., 1983, Tectonics of the Himalayan thrust belt in northern Pakistan, In Marine geology and oceanography of the Arabian sea and Coastal Pakistan. B.U. Haq, J.D. Milliman, Eds. Van Nostrand Reinhold, 1984. p. 177-198.

Yielding,, G., Ahmad, S. , Davison, I., Jackson, J.A., Khattak, R., Khurshid, A., King, G.C.P., and Lin Ban Zuo, 1984, A microearthquake study in the Karakoram, in The International Karakoram project, K.J. Miller, Ed. Cambridge Univ. Press, 1984 v. 1, p. 150-169.

Zanettin, B., 1964, Geology of the Haramosh-Mango Gusor area: Desio's Ital. Exp. to the Karakorum and Hindu Kush: Scient. Rep. v. 3 Brill, Leiden. 305 p.

Zeitler, P.K., Johnson, N.M., Waeser, G.W., and Tahirkheli, R.A.K., 1982, Fission-track evidence for Quaternary uplift of the Nanga Parbat region, Pakistan: Nature, v. 298, pp. 255-257.

_____ ,1985. Cooling History of the NW HImalaya, Pakistan. Tectonics, v. 4, no. 1, pp. 127-151.

Zulfiqar, A., Shabbir, H., Awan, A.. 1977 Petrology of the Thelichi area, Gilgit Agency. Geol. Bull. Punjab. Univ., No. 14. 1977 pp.27-38.

APPENDICES

Appendix 1, Traverse summaries

A summary of bedrock geology is presented for each traverse and the data collected on each traverse is presented by traverse, in tabular form. Select field sketches are included, referenced in the traverse summaries. Station numbers starting in 3- are 1983 field season, those starting in 4- are 1984 field season. Station locations are presented in Plate A-1. Abbreviations used for unit names are; Kh, Hanuchal amphibolite; Ks, Shuta gabbro; Ns, Shengus gneiss; Ni, Iskere gneiss, Nh, Haramosh schist.

The following conventions are used in all the data tables. Oriented samples give attitude of oriented face. Folds are designated according to generation if known (f1, f2, f3). A is trend and plunge of fold axis, AP is strike and dip of axial plane, axis always given first. Strike and dip of faults given, followed by trend and plunge of slickensides if present. Trend and plunge is given for c, crenulation lineation, or m, mineral lineation. Note that headings may change from page to page, and special data is inserted at station in question.

Traverse 3-A. Stations 3-17 to 3-22. Skardu road from Sassi north to Dassu creek bridge.

The entire traverse is in Nh, biotite and muscovite schist are dominant rocks, with gneiss, augen gneiss, garnet bearing schist and gneiss, amphibolite, calc silicate gneiss and marble. Pegmatitic material occurs both concordant with and crosscutting foliation. Various lithologies occur in laterally discontinuous layers of varying thickness, parallel to foliation. Minor chloritic alteration occurs, as well as hydrothermal bleaching and alteration, with deposition of sulfides, and crusts of sulfosalts. Much of the rock is mylonitized.

Structure is dominated by S1 foliation parallel to lithologic banding, and by a sub parallel shear foliation (S2). S2 ranges from a closely spaced cleavage or mylonitic foliation to sets of minor faults which cut S1 into phacoidal packets. Several minor faults also occur which cut shear foliation and s1 at moderately steep angles, with consistent east side up displacement. Minor faults which cut foliation commonly become parallel with foliation up or down dip and become foliation plane faults (Fig. A-1a). Two types of fold occur, one set are nf1 isoclinal intrafolial folds, the others are open undulations in foliation around generally north dipping axes, or are psuedofolds in incompetent layers adjacent to boudinaged competent layers. The nf1 intrafolial folds in some cases appear to have been isoclinally folded twice (Fig.A-1b).

Slickensides are common on S1 and S2 and a weak mineral lineation occurs parallel to slickensides.

Traverse 3-B. Stations 3-33 to 3-47. On Skardu Road from Dassu creek bridge to Hanuchal.

The traverse cuts across S1 in Nh to Khaltar creek, just west of which the main Raikot mylonite zone passes. A block of Nh a few hundred meters wide occurs west of the mylonite zone, and is in fault contact with Kh and Ks further west.

Nh consists precominantly of bio-muscovite-garnet schist and gneiss, with some amphibolite, calc, marble and pegmatitic dikes and layers. Lithologic layers are variable in thickness, and laterally discontinuous.

Kh consists of bio and garnet gneiss, epidote amphibolite, augen gneiss, gneissic granite and abundant granitic dikes which are sub concordant with lithologic layering and are moderately foliate. Lithologic layering in fairly

continuous. Ks in this section is a fine grained diorite, with incipient to moderate foliation. Minor crosscutting granite and pegmatite dikes occur. Contacts between Kh and Ks are covered in this traverse.

The Raikot mylonite zone is not exposed along the road, but the fault separating Kh from Nh is visible in the cliff north of station 3-39, as a sharp boundary parallel to foliation.

Both Kh and Nh have a strong S1 parallel to lithologic layering and an S2 mylonitic/shear foliation occurs subparallel to S1. Minor faults east side up faults are common, as well as foliation plane faults, both commonly with slickensides.

Tight f1 folds occur in the Nh, but none occur in Kh. Open folds in S1 appear to be undulations associated with lensoid structure produced by intersection of S1 and S2. A crenulation lineation and mylonitic lineation are both variably developed mostly in Nh.

Traverse 3-C. Stations 3-48 to 3-63. Up Sassi creek to Hurban village.

Bedrock at the mouth of Sassi creek is Nh, in fairly planar fine lithologic layers, schist> gneiss> amphibolite> marble. Rocks become less mylonitized proceeding east up creek. Several hundred meters upstream from the Skardu road the creek enters a narrow vertical walled gorge > 100 m deep, cut into bedrock plateau which is covered with glaciofluvial sediments. The sediments are cut by a major scarp on the Sassi Dassu fault, but bedrock is not exposed along the fault trace. At the eastern edge of the Quaternary deposits bedrock is Ni, but is part of the Sumari landslide, with inconsistent foliation attitudes. In Sassi creek east of Hurban, the Ni is well exposed as coarsely layered coarse grained granitic gneiss and amphibolite bands. The gneiss is almost massive, with weakly developed foliation and stringers and clots of pegmatitic material. Dikes of pegmatite are common, many have diffuse contacts with the gneiss.

Folds are not clearly defined in this area, in part due to lack of strong foliation, but much of the pegmatitic material is folded complexly on a small scale, and may be migmatitic. Large scale foliation attitudes are well expressed by amphibolites. Minor west dipping faults with slickensides down dip occur, and may be due to gravity rather than tectonics.

Traverse 3-D. Stations 3-64 to 69. From mouth of Sassi creek across and up slope to northeast.

The majority of this traverse crossed till, with bedrock observed only in Sassi creek and along the edge of a prominent bedrock ridge north of Sassi creek. Bedrock in Sassi creek is Nh, predominantly schist> gneiss> amphibolite in lithologic layers 5 to 20 cm thick. Foliation in the creek strikes roughly north and is vertical. A conspicuous but rare component of the gravels in Sassi creek is composed of coarse grained pyroxenite.

Bedrock on the ridge north of Sassi creek is Ni, coarse grained biotite gneiss> schist> amphibolite. Foliation is well developed, but variably oriented. The entire ridge may be a landslide. Minor faults are common.

Traverse 3-E. Stations 3-70 to 3-82. Sassi village to north wall of Sumari canyon, return via mouth of Sumari canyon and Skardu road.

Bedrock at Sassi village is bio-muscovite schist> gneiss> amphibolite> marble, in lithologic bands 1.0 to 15.0 cm thick.

S1 foliation is well developed parallel to lithologic bands, and a strong S2 spaced fracture/ mylonitic shear foliation occurs sub parallel to S1. Crenulation lineations are well developed in micaceous rocks.

Bedrock on the north wall of Sumari canyon is Ni, biotite gneiss of

varying grain size and thickness of banding. Foliation is well developed, but inconsistent in orientation. The rock is deeply weathered and cut by numerous minor faults. The entire north wall of the Sumari canyon is probably part of the Sumari landslide.

Bedrock on the south wall of Sumari canyon is Ni, fine to medium grained biotite gneiss. The rock is fresh and has consistent foliation which strikes north and is near vertical. At the mouth of Sumari creek, bedrock is again Nh, bio-muscovite schist, gneiss with marble and amphibolite. Some of the rock is mylonitized.

South of the mouth of Sumari canyon, the bedrock planation and glacioflu-vial sediment cover noted near Sassi die out, but the sedimentary sequence is clearly tilted 20 to 30 degrees east.

Traverse 3-F. Stations 3-83 to 3-86. River bank exposures at Sassi village.

Bedrock along the east bank of the Indus at Sassi is Nh, bio schist> bio gneiss> amphibolite> marble. Most of the rock is mylonitized. Sl foliation is strong and parallel to lithologic layering, with marble layers occurring as intrafolial isoclinal folds and amphibolites occurring as boudins. The isocli-nal fold axes plunge steeply north, and are associated with a mineral linea-tion. Gentle open folds in foliation occur around the north plunging lineation and around a subhorizontal axis.

On the west bank of the Indus, the contact between Nh and Kh is vertical and marked by chaotic folding and boudinage (Fig. A-1c.)

Traverse 3-G. Stations 3-87 to 3-91. Skardu Road from Hanuchal village to Shuta village.

Bedrock at Hanuchal village is Kh, predominantly amphibolite with biotite gneiss cut by granodiorite and pegmatite dikes. Sl Foliation is strong and consistently oriented. From Hanuchal to Shuta, bedrock is Ks, medium grained equigranular gabbro with a weak foliation, and igneous banding parallel to the foliation. At Shuta, an inclusion of epidote biotite augen gneiss approximately 5 m by 30 m occurs in the gabbro.

Traverse 3-H. Stations 3- 92 to 3-97. Skardu road at Dassu creek to Dassu village.

Bedrock at Dassu creek bridge is Nh, described in Traverse 3-A. A distinct bedrock planation occurs on the divide between Dassu and Khaltar creeks, and is capped with a thick flat topped till deposit. No bedrock is exposed on the west bank of Dassu canyon for the length of the traverse. The east bank is a steep cliff of Nh or Ni, with numerous minor faults and north striking east dipping foliation. In one exposure, the foliation is steep near the base of the cliff and shallow near the surface. The entire slope may be toppled, or part of a large landslide. Bedrock at Dassu village is coarse grained bio-muscovite gneiss, with inconsistent foliation. The outcrops are generally fractured and deeply weathered.

Traverse 3-I. Stations 3-98 to 3-102. Dassu village to Iskere village along south wall of Iskere canyon.

Between Dassu village and the mouth of Iskere canyon, bedrock outcrops are rare, but are generally fractured coarse grained bio-muscovite gneiss, with inconsistent foliation attitudes. The south wall of Iskere canyon has limited exposure of coarse grained coarsely layered biotite gneiss with minor amounts of biotite schist and amphibolite, cut by tourmaline granite pegmatites. On the north wall, exposure is excellent, and although foliation in the gneiss is

indistinct, amphibolite layers clearly define a moderately tight upright antiform (f3) with a north plunging axis. Open parasitic mesofolds are common in the hinge of the fold, with moderately north plunging axes. From Iskere village, the ridge separating the Mani and Baskal glaciers well exposed, with foliated rock dipping consistently 40-60 east. The summit tower of Layla peak is composed of a light colored massive rock, possibly granite.

Traverse 3-J. Stations 3-103 to 3-108. Dassu village to Hanumal village and Jutial village.

From Dassu village to Hanumal village only till is exposed. At Hanumal complex glaciofluvial sediments and till occur, some of which may have experienced Quaternary faulting. Proceeding upstream of Hanumal in Dassu canyon, bedrock is exposed in the creek bed in a cascade 155 m high. Bedrock on the west bank is presumably Nh, but is fractured, weathered and poorly exposed. Bedrock on the east side is well exposed massively layered biotite gneiss of Ni.

Traverse 3-K. Stations 3-109 to 3-114. Skardu road from Shengus to Baroluma canyon.

S1 at Shengus is oriented nearly horizontal at river level, dips south on north bank of river, north on south bank of river. Large scale folds in amphibolite layers visible high on north bank. Bedrock is exposed along road just west of Baroluma canyon and is predominantly amphibolite and garnet amphibolite with thick discontinuous pegmatite dikes. S1 foliation is tightly and complexly folded around north plunging axes and faults are numerous, generally northeast trending and moderately west dipping. A major fault occurs in Baroluma canyon, separating the amphibolite from Ns gneisses to the east. The Ns gneisses are fine grained biotite, garnet and sillimanite bearing gneisses with amphibolites, and occur in lithologic bands 0.5 to 25 cm thick with considerable lateral continuity. S1 is parallel to lithologic layering, and strikes northeast with near vertical dip. High on the south bank of the Indus, a major tight recumbent fold (f1) occurs, just west of the Baroluma fault.

Traverse 3-L. Stations 3-115 to 3-138 and 3-183, 3-184. Along Skardu road from Sassi village to small west loop of Indus, with traverse up first major ravine south of Ishkapal canyon.

From Sassi to Ishkapal canyon, traverse nearly parallels strike in Nh, which is bio and muscovite schist and gneiss, with subordinate amphibolite, calc silicate and marble. Lithologic layering varies from .5 cm to over 1 m, and distinctive lithologies (marble) are clearly lens shaped bodies or rootless intrafolial folds. Most of the rock shows varying degrees of mylonitization, and the unit as a whole has a distinctive red brown weathering patina.

S1 is strong and parallel to lithologic layering and a sub-parallel mylonitic/shear S2 foliation occurs. Minor north trending faults are common, with or without gouge, and offset is consistently east side up. Tight to isoclinal intrafolial f1 folds occur around north plunging axes. Open undulations of S1 occur around a moderately north plunging axis, and a shallowly south plunging axis. A crenulation lineation is associated with both open fold axes.

Just south of Sumari canyon, a body of Kh, shattered amphibolite, diorite, gabbro with granitic dikes occurs. The body is overlain to the east by the tilted glacial sediments of TraverseD, and to the west, the contact between the Kh and Nh is obscured by till (Fig.A-2a).

The traverse up the gully south of Ishkapal canyon crosses S1 and lithologic layering in Nh at right angles. Nh is bio schist, leucogneiss, biotite

gneiss, marble and amphibolite, in lithologic layers 0.5 to 100 cm thick. Many lithologic layers are mylonite or cataclastite, and chloritic alteration is common. North trending east dipping faults are common, generally lined with gouge and sub parallel to S1. A vertical fault zone separates Nh from massive monotonous biotite gneiss to east (Ni). The fault zone is parallel to S1, and approximately 10 m wide, with numerous gouge zones.

At the northern end of the westward loop of the Indus, Nh is separated from Kh by a mylonite zone over 150 m thick, which is oriented 000, 90. The mylonite zone is visible to the north, on the west bank of the Indus, and clearly visible to the south, where it juxtaposes shallowly west dipping Kh with vertical Nh (Fig. A-2b). Nh adjacent to the mylonite zone is not exposed, Kh develops complex chaotic folds adjacent to the mylonite zone (Fig.A-3a, b).

Kh consists of amphibolite, biotite gneiss, marble and calcsilicate, epidote gneiss, basic intrusive and pegmatites. Lithologic layering varies from 1cm to 2 m thick, and is laterally continuous.

S1 foliation is parallel to lithologic layering, and is folded in tight and open folds around generally north plunging axes. Syntectonic pegmatites truncate the folds, but are themselves slightly folded.

Traverse 3-M. Stations 3-138 to 3-143 and 3-182. Around westward loop of Indus, south of Ishkapal canyon.

From the northern end of the loop to the southern end of the loop, bedrock is Kh. The dominant lithology is amphibolite and hornblende-epidote gneiss, with diorite, gabbro, calc silicate, marble and pegmatites. A distinctive unit of marble with fine amphibolite interlayers is at least 50 m thick.

S1 foliation is parallel to lithologic layering, and is folded in isoclinal to tight folds around generally northwest axes. The folds are locally complex to chaotic.

At the southern end of the loop, a broad fault/mylonite zone separates the Kh from Nh and Ni. Entering the fault zone from the west, minor faults in Kh become more common (Fig. A-3c), and the rocks become progressively mylonitized. The foliation becomes disrupted into phacoidal lenses, and steepens from 20 to 30 degrees west dip to vertical. A vertical mylonite and gouge zone separates Kh from Ni and Nh. The mylonite and gouge zone coincides with a steep gully on east of the Skardu road at the head of which Kh is separated from Ni,h by a wide grey gouge or mylonite zone. East of the mylonite/gouge zone, variably mylonitized Nh occurs with generally steep dips and north strike. A second major mylonite/gouge zone oriented 000, 60 E. East of this fault, minor faults and mylonitization become less common.

The fault zone is visible on the west bank of the Indus, occupying a steep gully separating Kh from Ni. Several discrete fault strands are clearly visible in polished exposures along the waterline.

Traverse 3-N. Stations 3-144 to 3-149. Lower Ishkapal canyon.

Bedrock at canyon mouth is Nh, finely banded bio schist, gneiss, amphibolite and marble. Overall, unit has distinctive red brown weathering patina. Lithologic layering is parallel to S1, which strikes north, with consistent steep W dip. Major faults occur, both parallel to S1, and dipping 60-70 E. One shows clear east side up offset of at least 30 m.

Nh is in contact with Ni along a shear zone parallel to S1, and S1 is parallel in both units. Nh is distinguished by an abrupt transition to massive and thickly layered monotonous grey biotite gneiss.

At least 7 major faults occur in Ni in a zone extending approximately 1.5

km east of the contact with Nh. The faults dip 50 to 60 east, and some clearly offset distinctive lithologic layers, east side up. The faults tend to dip most shallowly near the ridge crest, and are near vertical in the bottom of the canyon. The top 100 m of the ridgecrest is severely toppled, from approximately vertical to 30 E.

In the upper reaches of the canyon, the foliation strikes east.

Traverse 3-O. Stations 3-150 to 3-162. Skardu road from west loop of Indus to Khalola Canyon.

Bedrock along the road between the Raikot fault zone of Traverse 3-M to the mouth of Khalola canyon is Ni. The dominant lithology is biotite gneiss or augen gneiss with pegmatitic clots and stringers, and minor amounts of amphibolite, schist and rare calc silicate. The rocks are dominantly fine grained and in thick (0.5-2 m) discontinuous lithologic bands, although fine grain size and thin banding occur.

Sl foliation is generally strong and parallel to lithologic banding, but can be indistinct in some massive gneiss layers. Sl generally strikes north and dips steeply west. Minor faults occur, generally parallel to foliation.

In riverbed exposures along the Indus at Khalola canyon, the dominant lithology is coarse grained granite gneiss, with abundant pegmatitic clots and stringers, and rare thin discontinuous amphibolite interlayers. Foliation is weakly defined by discontinuous seg bands of biotite. Two types of migmatite occur, one in which pegmatitic stringers are abundant and chaotically folded, and another in which vaguely foliate gneiss is in sharp contact with equigranular gneiss, and biotite seg bands persist vaguely from the gneiss to the equigranular rock (Fig. A-4a, b, c).

South of Khalola canyon, the road traverses the foot of the Burumdoin landslide, along a shallowly west dipping gouge zone in coarse biotite gneiss up to 10 m thick. At the south end of the slide the bedrock is again thickly layered coarse augen gneiss, with Sl moderately west dipping.

Traverse 3-P. Stations 3-163 to 3-178. Along Skardu road from south end of Burumdoin slide to Shengus.

Entire traverse in Ni, as far as Shengus. Ni predominantly coarse grained biotite and muscovite gneiss, with smaller amounts of augen gneiss, biotite and muscovite schist, amphibolite, and rare calc silicates. Lithologic banding is variable but predominantly coarse, and laterally discontinuous. Hydrothermal alteration, gossan and sulfur and sulfosalt deposits are common along fractures and foliation planes.

Sl is strongly developed parallel to lithologic layering on outcrop scale, but can be indistinct in some massive gneiss layers. Sl strikes north and dips moderately to steeply west at the beginning of the traverse, and the strike shifts progressively through northwest to west approaching Shengus, while the dip becomes progressively shallower. Open undulations in sl do occur. The change in strike closely parallels the 90 degree bend to the east made by the Indus, and at the bend, the river follows a single foliation plane.

Minor faults occur throughout the traverse, generally north striking and east dipping.

A south dipping crenulation lineation is consistently developed, and a mineral lineation occurs less commonly.

On the west bank of the Indus opposite stations 3-160 to 3-165, a small basin occurs. A major fault contact between Kh or Ks and Ni trends south across the basin, and climbs towards the ridge crest to the south. It is marked by a wide zone of brightly colored hydrothermal alteration and a conspicuous linear

feature when viewed at low sun angle. Numerous east dipping faults are exposed in Ni adjacent to the major fault.

The south bank of the Indus opposite stations 3-170 to 3-173 offers a section perpendicular to S1, and reveals numerous rootless isoclinal intrafolial folds within thick uniformly west dipping lithologic layers.

Traverse 3-Q. Stations 3-179 to 3-181. Up minor gully between Sumari and Ishkapal canyon.

Traverse extends across strike of Nh, to contact between Nh and Ni. The contact is conformable to S1, and marked by a shear zone 25 cm wide. Minor foliation plane shears also occur in Nh.

South of the contact locale, Ni and Nh are cut by a major steep fault zone trending slightly northwest. The fault zone originates at the Kh body of Traverse 1, to the north, and to the south passes up and over the divide into Ishkapal canyon. The fault zone is poorly exposed, but contains mylonites, biotite schist, and amphibolite, garnet amphibolite and gabbro characteristic of Kh.

Traverse 3-R. Stations 3-190 to 3-197. Skardu road from Baroluma canyon to Juche canyon.

The entire traverse is in Ns, finely laminated fine grained pelitic gneiss, amphibolite, leucogneiss and calc silicate gneiss. Tourmaline granite and pegmatite dikes are common.

The axis of the Bulache antiform crosses the road just west of Juche canyon. Strong S1 parallel to lithologic layering has consistent northeast strike, and dips west on the west limb of the antiform, east on the east limb.

A body of coarsely banded ortho augen gneiss occurs just east of the hinge of the antiform.

Traverse 3-S. Stations 3-215 to 3-228. Sassi village to Khaltaro village.

The traverse crosses till from the Skardu road to the base of the divide between Khaltar and Dassu canyons. Bedrock at the base of the divide is Nh, biotite muscovite schist and gneiss with a red brown weathering patina. Proceeding west and up the canyon, the rock becomes variably mylonitized and sheared, and several major north trending east dipping faults occur. A single zone of mylonite and cataclastite approximately 100 m wide separates the sheared and mylonitized Nh from Kh, with abundant concordant granitic dikes. Further up the divide, the fault directly juxtaposes massive gabbro with minor marble and amphibolite inclusions against Nh.

Further up Khaltar canyon, the fault zone is visible along the ridgecrest as a zone of brightly colored hydrothermal alteration, and both walls of the canyon ore gabbro. At the furthest upstream extent of the traverse, the west wall of the canyon is still gabbro, the east bank is covered, but has abundant Ni float.

A major fault with east side up displacement is visible on the west wall of the canyon, further north. From a vantage point part way down from Khaltar village, at least two major east dipping faults are visible high on the slope between Sumari canyon and Ishkapal canyon.

Traverse 4-A. Stations 4-3 to 4-11. Up Sassi creek.

The traverse begins at the head of the vertical walled gorge of traverse 3-D, and for several hundred meters to the east, the creek flows directly along top surface of a gently west sloping bedrock plateau which is overlain by till. Bedrock exposed in creek bed along top of bedrock plateau is finely laminated

biotite schist and amphibolite of Nh. Sl consistently north trending and vertical. Numerous minor east side up faults occur parallel to Sl. Isoclinally folded pegmatitic dots are common in Sl.

To the east, the bedrock plateau steps up abruptly and the creek is incised in a deep vertical walled gorge. At least four vertical faults coincide with the step, all are north trending and vertical, parallel to Sl. the faults are 1-3 m wide, and all produce steps in the bedrock plateau surface. One clearly offsets the overlying till.

Traverse 4-B. Stations 4-12 to 4-16. Repeat visit to Raikot fault zone at 3-134, and traverse to Kh body just south of Sumari canyon.

Mylonitic lineations measured at Raikot mylonite zone, generally north plunging.

From a vantage point above 3-134, several features are noted to the north. The fault zone of station 3-180 is definitely continuous with the Kh body at Sumari canyon, and the western contact of the Kh is against till (Fig. A-3a).

On the cliff forming the west face of the Kh body, the contact between till and the overlying Kh is a horizontal thrust.

Traverse 4-C. Stations 4-17 to 4-23. Traverse to Sumari village via Hurban village.

The traverse crosses till from Sassi to Sumari, but excellent views to the north reveal several steep north trending bedrock faults directly on strike with prominent scarps in till (Fig. A-3a). Till clasts are deeply pitted, with quartz veins standing as much as 1.5 cm above rock surface.

From Hurban to Sumari, traverse crosses poorly exposed Ni, with numerous fracture zones, inconsistent foliation attitudes. Sumari village occupies a north trending graben floored with till. Bedrock along the west edge of the graben is a jumble of huge blocks with inconsistent foliation attitudes. Bedrock east of the graben is Ni, with good exposure and consistent foliation.

Traverse 4-D. Stations 4-24 to 4-31. Irrigation channel originating in Khaltar creek, and terminating on cliff west of the mouth of Khaltar canyon.

The Raikot fault mylonite zone crosses the Indus just west of the mouth of Khaltar canyon, and crosses the Skardu road under gravel cover. The mylonite zone forms prominent notches packed with till in the bedrock plateau on both banks of the Indus, and passes into Khaltar canyon to the north.

Bedrock at the origin of the irrigation canal is sheared, fractured and mylonitized Ni at least 75 m thick. The canal parallels the mylonite zone along the canyon, then swings west across the zone. the canal crosses the zone in the till filled notch in the bedrock plateau. Bedrock west of the mylonite zone is partially mylonitized biotite gneiss, biotite schist and leucogneiss, with a strong Sl and numerous small isoclinal folds around north plunging axes. The unit is not clearly either Nh or kh, and may be an allochthonous fault block.

Traverse 4-E. Stations 4-33 to 4-48. From Sassi village to Dassu village, Iskere village, and base of Haramosh, return via Barche village, Hanumal village and Bulladas village.

From Sassi to Dassu, the traverse crosses till. On the east wall of Dassu canyon, south of Dassu village, good exposure of toppled or openly folded Ni or Nh, with numerous foliation plane faults and connecting interfolial ramps (Fig. A-5 b). Also note several discontinuous Quaternary traces on same wall. Along till plateau at Dassu, note distinct Quaternary scarps at toes of fans.

From Iskere village to Kutwai lake at the base of Haramosh, the traverse

crosses till. Bedrock in north wall of Haramosh (Fig. A-6b), on divide between Mani and Baskal glaciers, and in south face of Phuparash (Fig. A-6a) is all Ni or Nh, uniformly foliated, with consistent northwest strike and moderate to steep east dip. A contact between Ni and Nh is suggested in all three exposures by a sharp change from massive and coarsely laminated monotonous grey rock to finely laminated variegated grey black and brown rock. The summit tower of Haramosh is intruded by numerous thick subhorizontal leucocratic dikes. In the course of crossing the Mani glacier, no clasts were seen that were not typical of Ni or Nh and the dominant clast was biotite gneiss.

No bedrock was encountered between Iskere village and Hanumal. The floor of Iskere canyon is covered in gently graded alluvium, between a major landslide or neoglacial moraine dam at Iskere village, and a Barche age terminal moraine at Barche.

Numerous fault like features occur in glaciofluvial sediments around Hanumal village, but may be ice contact features. A clear east dipping reverse fault cuts a glaciofluvial terrace at Hanumal, producing a north trending east side up scarp approximately 15 m high.

Traverse 4-F. Stations 4-49 to 4-54. Death march up irrigation canal along north bank of Rahmgat canyon.

Bedrock along the traverse is predominantly foliated Ks gabbro with numerous Kh metasedimentary inclusions. The rock is generally quite shattered and altered to clay, chlorite and epidote. Foliation is variable, but generally strikes east to northeast and dips steeply north. Closely spaced gouge lined faults occur in a wide variety of orientations breaking the rock into polyhedral volumes 10 to 100 m in diameter. No consistent sense of orientation was observed. Bedrock exposure and passable terrain end approximately 2 km west of an obvious trace of the Raikot fault. The fault is vertical, and juxtaposes gabbro with leucocratic dikes and/or marble inclusions against uniformly foliated Nanga Parbat group rocks. The trace of the fault is marked by hydrothermal alteration of bedrock and Quaternary deposits and by a distinct topographic step on the divide between Rahmgat and Bunji canyons. The fault truncates the hinge of a huge recumbent isoclinal f1 fold in the Nanga Parbat rocks.

Traverse 4-G. Stations 4-55 to 4-67. Up Bunji canyon, from Bunji village to Shinz village.

Bedrock in Bunji canyon is Kh, all the way east to the Raikot fault, which crosses the canyon at the confluence of Shinz creek. The Kh consists of biotite-epidote-hornblende schists and gneisses, with minor marble interlayers. Leucocratic intrusive rocks are common, ranging from slightly discordant and strongly foliated to sharply discordant and undeformed. Chloritic alteration, skarns and copper mineralization are associated with the contacts of the dikes.

S1 attitudes smoothly approaching the Raikot fault, from due east strike, through northwest to northeast strike, with steep north dips. Numerous north striking east dipping reverse faults occur approaching the fault zone (Fig. A-5 a) and are most common adjacent it.

The westernmost unit of the fault zone is a gouge zone within Kh, at least 35 m wide. West of this zone is a mylonite zone approximately 150 m thick, which separates the Kh from Ns to the east. Mylonitic foliation, the gouge zone, and S1 in both kh and Ns all strike 030, 90. Minor east dipping fractures are common in the mylonite zone, and a transition from Kh protolith to Ns protolith occurs within the zone.

Ns consists of fine grained finely laminated leucogneiss, garnet gneiss and pelitic gneiss. Lithologic layering is remarkably laterally continuous, and

the steep west dip persists for several km to the east.

From Shinz, the fault zone can be traced to the south over the Bunji-Rainigat divide as an abrupt topographic step and zone of hydrothermal alteration. The valley of Shinz creek is parallel to the fault zone, and the western wall is Kh, the eastern wall Ns.

Traverse 4-H. Stations 4-67 to 4-79. Slope east of Hanuchal village, and Skardu road between Hanuchal and confluence of Gilgit river.

North and east of Hanuchal village, a contact occurs between Kh and Ks. The contact is a zone of Ks dikes in Kh, grading to Kh inclusions is Ks, and is locally conformable with foliation in Kh. The contact crosses the Skardu road at Hanuchal village, and is visible on the south bank as a steep transition from foliate to massive rock.

The Kh is dominantly amphibolite with thick granitic orthogneiss layers. The Ks is dominantly equigranular gabbro which locally has primary igneous layering. Marginal facies of Ks are diorites and coarse hornblende pegmatites.

Along the Skardu road west of Hanuchal, numerous inclusions of Kh occur in Ks, one at least 250 m thick.

Traverse 4-I. Stations 4-80 to 4-85. Khalola canyon.

The bedrock exposed on the inaccessible north wall of the canyon for the entire traverse is Ni, thickly laminated biotite gneiss with laterally discontinuous lenses, and boudins of biotite schist, amphibolite and calc silicate. Discordant pegmatite dikes are common.

Sl strikes consistently north, and dips steeply west. Rootless intrafolial folds occur. Minor east side up faults occur parallel to Sl, and two in particular are directly on strike with the Burumdoin landslide. Bedrock along the contact of the landslide is extensively hydrothermally altered.

Traverse 4-J. Stations 4-86, 4-87-88. Detail, Raikot fault zone at station 3-143, and bedrock exposures along Indus at mouth of Khalola canyon.

Additional structural measurements made in Raikot fault zone include mylonitic lineations, which all plunge moderately to steeply north and slickensides which plunge north and south.

Bedrock at the mouth of Khalola canyon is massive biotite gneiss with amphibolite and calc silicate layers and abundant pegmatitic stringers. Sl is poorly defined in massive gneiss, but amphibolite and calc silicate layers define Sl and occur as boudins and rootless intrafolial fold hinges. Pegmatitic stringers and biotite laminae are chaotically folded, suggesting anatexis.(Fig. A-4 a, b, c).

Traverse 4-K. Stations 4-92 to 4-100. Up Shengus creek

Bedrock along entire traverse is Ns, fine grained finely laminated pelitic gneiss, biotite gneiss and amphibolite.

Sl generally strikes east, and dips south, with dip increasing to the north. Sl is gently folded around three axes; horizontal and east trending (f2), south plunging (f3) and southwest plunging (f1). A strong mineral lineation parallels the southwest axes, and a moderately developed crenulation lineation parallels the south plunging axis.

Traverse 4-L. Stations 4-101 to 4-109, and 4-117 to 4-128. Skardu road from 2 km east of Shengus village to Juche canyon. Bedrock west of Shengus is Ni, coarse grained massive biotite gneiss with amphibolite, schist and calc silicate.

S1 is variable but generally strikes west to northwest, dips moderately south. Large scale open folds occur around a south plunging axis (f3), and a large moderately tight intrafolial antiform is visible on the divide between Mushkin and Mayar canyons. Small scale open folds, a mineral lineation and a crenulation lineation all plunge moderately south, parallel to the f3 axes. Gentle open folds occur around a west trending horizontal axis (f2), and are refolded by f3 folds.

The contact between Ni and Ns occurs just west of Shengus and is transitional, and parallel to S1. Ns between Shengus village and Baroluma canyon is predominantly fine grained biotite and pelitic gneiss, with coarse grained amphibolite. S1 in this area strikes west, dips variably south, with a major west trending synclinal axis along the Indus. Open minor folds and a weak crenulation (f2) occur parallel to the west trending syncline. Rootless intrafolial folds (f1) and fold boudins occur with southwest plunging axes, and minor open folds and a strong mineral lineation parallel the axes. Open folds occur around a south plunging axis (f3) with a parallel crenulation lineation, and refold the horizontal axes (f2).

Adjacent to the Baroluma fault at Baroluma canyon, complex tight folding occurs around axes which tend to plunge steeply east.

Ns east of the Baroluma fault is fine grained finely laminated biotite-garnet-sillimanite-kyanite gneiss, para-amphibolite and calc silicate, with abundant discordant granite pegmatites.

The hinge of the Bulache antiform occurs just west of Juche canyon, and plunges moderately northeast. Large open parasitic folds occur in the hinge zone, along with a northeast plunging crenulation. S1 on the west limb of the antiform strikes northeast, dips steeply west at Baroluma canyon, and less steeply near Juche canyon. Foliation on the east limb strikes northeast and dips consistently east. Isoclinal intrafolial (f1) folds are common, around a variety of axes.

Traverse 4-M. Stations 4-110 to 4-116. Shengus village northeast to ridge above Baroluma canyon.

Ns bedrock is poorly exposed along most of the traverse, with S1 dipping variably south. Bedrock at the top of the west wall of Baroluma canyon is fractured and altered. Up Baroluma canyon, the Baroluma fault clearly juxtaposes the steeply east dipping east limb of the Iskere antiform with the steeply west dipping west limb of the Bulache antiform.

On the south bank of the Indus opposite Shengus, a large tight recumbent intrafolial fold occurs.

Traverse 4-N. Stations 4-129 to 4-133. Structural data, from Indus bank exposures at Sassi, and Kh on west bank of Indus south of Ishkapal canyon.

The dominant structure in the mylonitized Nh along the Indus at Sassi is a north trending steeply west dipping mylonitic foliation. A strong mineral lineation plunges consistently north in the mylonitic foliation. The foliation and the lineation are gently folded around a southwest plunging axis.

Two generations of folds occur in Kh, tight to isoclinal folds and fold boudins with northwest plunging axes (f1) and open to moderately tight folds around a variety of axes (f2). A mineral lineation parallels the f1 axes, and both are refolded around f 2 axes. A crenulation lineation occurs parallel to the f2 axes.

Table A-1. Field Data

Station	Sample	S1	S2	Folds	Fault; slick	Lineations
Traverse 3-A						
3-18	mylonite	336, 66E	343, 85E		338, 78E; 158, 42	
	or. tace		356, 76E		020, 85E; 330, 34	
	027, 20E		019, 70E		039, 88E; 039, 31	
3-19		343, 78E			358, 90	
3-20	A, mylonite	340, 85W			355, 84E; 345, 47	
	B, marble	318, 90				
3-21		348, 77W				m, 320, 54
3-22		357, 86E		fl A 000, 55		
		350, 90		AP 345, 65W		
				fl A 010, 45		
				AP 003, 75W		
				fl A 330, 70		
				AP 359, 65W		
				fl A 010, 45		
				AP 342, 84W		
3-23		340, 70W				
		358, 69W				
3-24	mylonite			A 199, 15		
				AP 075, 37E		
3-26	calc sil.	351, 79W		fl A 000, 60		
		350, 84W		AP in S1		
		358, 69W				
3-28	mylonite	354, 80W	000, 90		335, 42E	
3-29	schist	347, 77W			005, 37E; 305, 60	
3-30		345, 71W			010, 57E	
3-31		343, 77W			002, 77E	
3-32		undulates		A 310, 62		m 310, 67

Slickensides measured between 3-26 and 3-30, given as plane; pitch of slick

008, 86W; 25N	006, 83W; 35N	003, 87W; 30N	005, 87W; 42N
338, 87W; 33N	006, 81W; 35N	354, 87W; 28N	003, 79W; 23N
348, 90 ; 50N	356, 79E; 56N	325, 67W; 70N	351, 82W; 34N
359, 69E; 65N	340, 81W; 52N	352, 86W; 45N	345, 85W; 35N

Traverse 3-B						
3-33	A, myl or.	345, 75 E		fl A 355, 75		
	050, 54E			fl A 310, 62		
	B, calc.					
3-34				fl A 320, 58	340, 65E	
				AP 015, 62W		
3-35		353, 80W				
3-36		015, 60W	338, 65W	? A 325, 57		c 325, 57
		003 77W		fl A 015, 62		c 000, 15
3-38				fl A 037, 63		c 037, 63
				AP 015, 55W		
3-39		013, 60W				
3-40	bio gneiss	012, 67W				c 320, 52

Station	Sample	S1	S2	Folds	Fault; slick	Lineations
Traverse 3-B continued.						
3-42	chlorite				005, 61W; 310, 55	
					280, 74S; 085, 17	
					068, 37W; 100, 10	
3-43		325, 74E				
3-44	amph	040, 75W				
3-45		020, 62W				
3-46		000, 90		fl A 340, 80		
3-47	gneissic granite	015, 57W				
Traverse 3-C						
3-48	amph		343, 80E			
3-49			353, 85E			
3-50			353, 80E			
3-55			330, 45E			
3-56			014, 66E			
3-58			025, 58W		340, 80E	
3-59	amph				068, 50E; 193, 45	
3-61			042, 83W		345, 57W	
			040, 75W			
			295, 71E			
			085, 58W			
3-62	A, gneiss		040, 52W		052, 72E; 135, 5	
	B, granite		027, 60W		020, 55W	
Traverse 3-D						
3-67			350, 60E		335, 52E	
			320, 50E			
			350, 52E			
3-69	A, gneiss					
	B, pxite					
Traverse 3-E						
3-70			350, 85W			c, 315, 64
			350, 89W			c, 165, 9
3-73			340, 35E		015, 78N	
			330, 49E			
			334, 38E			
3-74			343, 55E		345, 30E	
			358, 65E			
3-75			325, 36E		289, 44N	
					319, 46E	
3-77			320, 49E			
3-78	bio gneiss		340, 90			
3-79	bio gneiss		350, 50E			
3-80			000?, 20-30E			
3-82	marble		349, 71W			

Station	Sample	Sl	Folds	Fault; slick	Lineations
Traverse 3-F					
3-84	A, amphibolite B, garnet gneiss C, myl., or. 345, 51 W	334, 72W	A 045, 52		m, 045, 52
Traverse 3-G					
3-87	A, amphibolite B, diorite	010, 25W			
3-89	gabbro	035, 37W			m, 110, 25
3-90		035, 45W		071, 81N	
3-91	A, gabbro B, augen gneiss	040, 44W			
Traverse 3-I					
3-98		027, 87W			
3-99		030, 70W			
3-101	granite		f3 A 007, 44 f3 A 000, 45	295, 74E;305, 34	
3-102	bio gneiss				
Traverse 3-J					
3-106		316, 28W		355, 65W	
3-107	Bio gneiss	017, 42W			
3-108		004, 61W			
Traverse 3-K					
3-111				045, 75W 040, 47W 050, 90; 060, 30 065, 43W	
3-113	pelitic gneiss	035, 90 030, 75W	f1 A 005, 40 f1 A 025, 07		
Traverse 3-L					
3-115		346, 90			c, 346, 61
3-116	mu-bio-garnet gneiss	350, 75W		018, 66E; 055, 54	c, 000, 42
3-117		348, 86W	A 185, 27 AP 080, 25S		
3-118	A ultramylonite B calc silicate	357, 85W	f1 A 000, 27 f1 A 000, 42 f1 A 185, 32		
3-119	A garnet amphibolite B amphibolite C diorite				
3-120	marble, or.	005, 90 050, 23W			
3-121		000, 80W			
3-122		347, 77W			c, 350, 62 c, 350, 30

Station	Sample	Sl	Folds	Fault; slick	Lineations
Traverse 3-L continued.					
3-123	A bio-mu gneiss B bio-garnet gneiss C bio-garnet gneiss D calc silicate	334, 82W	fl A 035, 66	080, 80S	
3-124		000, 75W			c, 333, 60 c, 352, 28 c, 190, 28
3-126		350, 80W			c, 320, 51 c, 175, 32
3-127	mylonite	004, 70W			m, 040, 50 c, 000, 29
3-128		017, 87W			
3-129		000, 80W		345, 80E	
3-130	mu-bio schist	000, 77W 350, 80W		020, 60E	
3-131		003, 72W 010, 72W		020, 90 025, 60E	
3-132				358, 80W	
3-133	A amphibolite B amphibolite C amphibolite D calc silicate	005, 35W 025, 15W		000, 90	

3-134; Detailed traverse of mylonite zone separating Nh, Kh. Samples numbered 184-X

Dist. m	Lithology	Sample	Other
0	marble		complex chaotic folds
0-.6	ultramylonite	184-A	fault, 4 cm thick at 0m
-4.5	mylonite	184-B	amphibolite protolith
-58	mylonite = amphibolite		
58	mylonite	184-C	
-66	mylonite		
66	augen gneiss mylonite	184-D	
-88	augen gneiss = mylonite		
-104	mylonite		bio gneiss protolith
104	ultramylonite	184-E	garnet-bio schist protolith
-125	bio gneiss, mylonite		
125	leucogneiss mylonite	184-F	oriented 000, 77W, Sl 000,77W
-152	cover		
-167	mylonite, gneiss, schist	184-G	
167	extensive cover		

3-135	hbl-epidote gneiss	015, 24W	fl A 300, 20 fl A 315, 5 AP 330, 14S	
3-136			fl A 285, 35 AP 315, 56W fl A 315, 25 AP 315, 90	

Station	Sample	S1	Folds	Fault; slick	Lineations
Traverse 3-L continued.					
3-183	para amphibolite				
3-184		335, 30W			
Traverse 3-M					
3-138			A 125, 35 AP 015, 35W A 325, 25 AP 325, 75E		
3-139	amphibolite	030, 35W			
3-140	A amphibolite B amphibolite	030, 25W			
3-141	marble	040, 20W			

3-143, 182 pace and compass traverse of fault zone, from east to west. Samples numbered as 143-X or 182-X.

Leg 1. 330, 60 m.
0-12, biotite gneiss and augen gneiss with pegmatitic stringers, S1 026, 72W.
12, fault parallel to S1, 35 cm wide.
12-35, fine grained biotite gneiss and schist with red-brown weathering.
35-36, augen gneiss progressively mylonitized towards the north.
36-39, laminated biotite gneiss, marble, calc silicate, amphibolite and pegmatite.
39, Fault, oriented 037, 75E. S1 east of fault; 022, 75W, west of fault; 019, 72W
39-60, fine grained biotite gneiss and schist.

Leg 2 258, 37 m.
0-3, biotite gneiss, amphibolite, marble
3, fault, 60 cm wide, oriented 025, 90.
3-24, biotite gneiss, amphibolite, marble
24, gouge lined fault 1.0 m thick, oriented 033, 70E.
24-34, finely laminated biotite gneiss and marble
34-37, laminated mylonite and marble

Leg 3. 270, 21m.
0-21, biotite gneiss, marble, biotite gneiss mylonite. S1 020, 74E.

Leg 4. 300, 62 m.
0-6, biotite gneiss, amphibolite, calc silicate.
6-28, biotite gneiss and augen gneiss.
28-33, fine grained biotite gneiss.
33-37, amphibolite.
37-62, augen gneiss, S1 007, 85E.

Leg 5. 336, 122 m.
0-2, augen gneiss.
2-13, fine grained biotite garnet gneiss.
13, fault 20 cm wide, lined with gouge, 009, 70E.
13-20, moderately sheared augen gneiss.

20, fault irregular, 5 cm wide, 340, 70E.
20-70, massive biotite augen gneiss with ultramylonite layers parallel to S1.
70, fault 70 cm wide, lined with augen gneiss gouge, 040, 60E.
70-73, biotite augen gneiss.
73, fault, 60 cm wide, gouge lined, 020, 50E. Samples, 143-A biotite garnet gneiss, 143-B augen gneiss.
73-122, finely laminated biotite muscovite schist. Extensive hydrothermal alteration, gossan, sulfosalts along S1 planes. S1 012, 75W.

All the faults in this leg coalesce in a single broad fault zone on the cliff to the east of the section. the fault zone is oriented 000, 60E.

Leg 6. 315, 114 m.
0-37, fine grained finely laminated biotite muscovite schist with minor marble and calc silicate. Sample 143-C of schist.
37-53, biotite schist cut by three faults each approximately 25 cm wide, lined with gouge and oriented 355, 50E. Up the cliff to east of section, the faults coalesce into a vertical foliation plane fault 2 m wide and lined with gouge.
53-87, fine grained finely laminated biotite garnet gneiss (possibly mylonite), S1 000, 72W.
87-114, fine grained finely laminated biotite gneiss (possibly mylonite) with augen gneiss and marble,

Leg 7. 307, 67m.
0-11, fine grained finely laminated biotite gneiss.
11, foliation plane fault, 70 cm wide, gouge lined.
11-32, fine grained finely laminated biotite gneiss with minor marble.
32-49, fine grained finely laminated marble, possibly mylonitic, sample 143-E, oriented 030, 37W. S1 358, 65E.
49, fault, oriented 025, 60E with 3 m of apparent reverse dip slip.
49-52, marble.
52-60, biotite gneiss, augen gneiss, biotite garnet gneiss and mylonite.
60-67, marble.

Leg 8, 295, 32 m.
0-32, marble, this body lenses out parallel to foliation within 100m in either direction.

Leg 9, 270, 62 m.
0-20, talus cover.
20-36, biotite schist, biotite gneiss and mylonite. Mylonite sample 182-F.
36, foliation plane fault, 0.5 m wide, gouge lined. Oriented 340, 64 W.
36-47, variably mylonitized biotite gneiss.
47, fault, 1 m wide, gouge lined, 350, 74E. Sample 3-182 E, mylonite.
47-57, biotite gneiss, augen gneiss and mylonite, S1 345, 80W.
57-60, fault, 2.5 m wide, gouge lined, 015, 85W.
60-62, hydrothermally altered cataclastite and mylonite.

Leg 10, 295, 45 m.
0-45, pervasively sheared mylonite and amphibolite. Extensive hydrothermal alteration, with gossan, sulfosalts. Sample 182-D.

Leg 11, 230, 53 m.
0-8.5, pervasively sheared mylonite, extensively hydrothermally altered. Shear

foliation oriented 000, 65W.
8.5, fault, .5 m wide, gouge lined,005, 70W.
8.5-45, foliated fine grained amphibolite and biotite gneiss, variably mylonitized. Cut by spaced shears, oriented 340, 80W, with steeply north plunging slickensides. Sample 182-C, mylonite.

Leg 12, 230, 122 m.
0-15, fine grained amphibolite and biotite gneiss, cut by several minor faults oriented 000, 70-80E. S1 325, 57W, variable.
15, fault, .2 to 1.0 m wide, gouge and breccia lined, 015, 90.
15-26, foliate fine grained amphibolite (mylonite) transitional to coarse grained mylonite from 25-26 m.
26-55, coarse grained moderately foliated amphibolite.
55, fault, 1-2 m wide, gouge lined, 020, 62W.
55-70, amphibolite, cut by four minor gouge lined faults sub parallel to foliation.
70, fault, 6-50 cm wide, gouge lined, sub parallel to S1. S1 010, 56W.
70-72, amphibolite
72, fault, 4-6 cm wide, gouge lined, sub parallel to S1, 010, 68W. Cut by second fault, 1 cm wide, 350, 54E, .75 m apparent reverse offset.
72-122, foliate fine grained amphibolite. S1 strikes north, west dip decreases to west. Foliation disrupted into phaccoidal packets. Fracture zones common.

Leg.13, 212, 76 m.
0-16, fine grained foliated amphibolite and marble.
16, fault, 1-2 cm wide, gouge lined, 000, 60W, slicks 335, 55.
16-27, steeply east dipping foliated amphibolite.
27, fault 2-5 cm wide, 090, 12W. This fault truncates against fault at 16 m.
27-74, fine grained foliated amphibolite dipping gently west. shears sub-parallel to foliation cut foliation into phaccoidal packets.
74, 2 small faults, 000, 70W with slicks 300, 58 and 020, 70E, with slicks 005, 42.
74-76, fine grained foliated amphibolite.

Leg 14, 225, 65 m.
0-49, fine grained foliated amphibolite. Foliation dips moderately west, undulates. In some areas, shears sub parallel to foliation truncate foliation, forming lens shaped packets.
49, fault, 350, 90, 15 cm wide at road, widens rapidly up cliff to 3 m. Packed with gouge and breccia. Drag on foliation adjacent to fault indicates east side up displacement.
49-65, foliated amphibolite, moderate undulating west dip.

Leg 15, 255, 46m.
0-31, foliated amphibolite, with undulating moderately west dip. Foliation becomes less well defined to west.
31-38, weakly foliated fine grained ortho-amphibolite with marble inclusions. S1 343, 40W. Sample 182-A, amphibolite.
38-46, transition from amphibolite with marble inclusions to laminated marble cut by amphibolite dikes. Primary intrusive relation.
46, coarse grained marble and medium grained amphibolite interlayered in beds 8-30 cm thick. Cut by dikes of ortho-amphibolite.

End of pace and compass traverse, station 3-143.

Station	Sample	Sl	Folds	Fault; slick	Lineations
Traverse 3-N					
3-144				000, 75E	
3-146		353, 84W		000, 60-70E	
3-149	suite				
Traverse 3-M					
3-150		017, 75W		043, 70W	
				000, 90	
Traverse 3-M continued.					
3-151	A biotite gneiss	000, 82W		040, 60W	
	B augen mylonite	030, 67W			
		020, 72W			
3-152		006, 79W			
3-154		008, 60W			
3-155		029, 62W			
3-156	A gneiss				
	B migmatite				
3-157					m, 357, 17
3-158				070, 24W; 295, 18	
3-159		348, 70W			
3-160		000, 42W			
3-161		357, 61W			
3-162		357, 43W			
Traverse 3-N					
3-163		353, 54W			
3-164		325, 40W			c, 195, 30
3-166		350, 35W			
3-167		328, 43W			
3-168		315, 30W			m, 190, 27
		342, 64W			c, 195, 25
					c, 185, 32
3-169		330, 40W		007, 80E	
3-170	calc silicate	315, 47W			c, 155, 25
3-171	A amphibolite	325, 45W			
	B biotite schist				
	C biotite gneiss				
3-172		348, 56W			c, 190, 30
3-173	biotite gneiss	072, 37S			c, 210, 34
3-174		274, 45S			
3-175		300, 58S			
3-176		310, 45W			c, 185, 35
3-177	A pelitic schist	071, 61E	fl A 260, 5		
	B biotite schist		AP 074, 60S		
3-178		080, 50S			
Traverse 3-Q					
3-179		352, 84		000, 60E	

Station	Sample	S1	Folds	Fault; slick	Lineations
Traverse 3-Q continued					
3-181	A mylonite	335, 86W			
	B biotite gneiss	350, 85W			
	C amphibolite	005, 63E			
	D garnet amphibolite				
	E anorthite pegmatite				
Traverse 3-R					
3-191	A pelitic gneiss	340, 60W			
	B tourmaline granite				
	C biotite gneiss				
3-192		010, 63W			
3-193		065, 40W			
Traverse 3-R continued.					
3-194		348, 45E			
3-195		013, 57E			
3-196	kyanite gneiss	021, 70E			m_y 200, 20
3-197	garnet gneiss	015, 40E			
Traverse 3-S					
3-216		358, 71W			
3-217				356, 44W	
3-226				344, 35E	
3-227	A mylonite, oriented 020, 81W				
	B mylonite, oriented 340, 30W				
3-228	marble mylonite oriented 318, 57W				
Traverse 4-A					
4-9		352, 90		352, 90	
4-10				008, 90	
Traverse 4-B					
4-12	A amphibolite	350, 80W			c_y 340, 20
	B biotite schist				c_y 338, 60
					c_y 180, 20
4-13	A oriented mylonite		f_2 A 180, 17		m_y 000, 45
	348, 84W		A_P 075, 20 E		m_y 225, 40
	B mylonite		f_2 A 155, 4		m_y 345, 32
	C mylonite		A_P 335, 22W		c_y 240, 40
	D oriented mylonite		f_1 A 263, 15		
	000, 85W		f_1 A 315, 30		
	E, para amphibolite				
Traverse 4-C					
4-22	A amphibolite	040, 57W			
	B biotite gneiss				

Station	Sample	Sl	Folds	Fault; slick	Lineations
Traverse 4-D					
4-25			fl A 340, 38 fl A 345, 67		
4-26		025, 68W			
4-27	A marble B schist C amphibolite	357, 72W		005, 60E	m_y 322, 54
4-28	A_y oriented mylonite 345, 70W B_y oriented mylonite 333, 67W		fl A 295, 45		m_y 035, 57
4-29	A mylonite B mylonite	017, 70W			
4-30		005, 64E			m_y 330, 56
Traverse 4-D continued.					
4-31	A leucogneiss B amphibolite C biotite garnet schist	024, 64W	fl A 315, 45		
4-32	pyroxenite				
Traverse 4-E					
4-36		043, 57W			
4-44	biotite gneiss				
4-45	amphibolite				
4-47		350, 52W			
Traverse 4-F					
4-50	A gabbro B amphibolite	300, 87W 082, 84E		010, 30W	
4-51		070, 65E		020, 67W; 030, 24	
4-52				350, 90	
4-53				070, 90	
Traverse 4-G					
4-56	A biotite schist B amphibolite C skarn	090, 75N			
4-57		090, 60N			
4-58		090, 60-70N			
4-59		330, 90			
4-60	A oriented mylonite 025, 85W B oriented mylonite 045, 90 C oriented mylonite 304, 50S D oriented mylonite 060, 34S	030, 85E 025, 85W 025, 90 040, 90		340, 65E	

Station	Sample	Sl	Folds	Fault; slick	Lineations
Traverse 4-G continued					
4-61	A leucogneiss				
	B garnet gneiss				
	C staurolite gneiss				
4-62		025, 90			
4-65	epidote gneiss				
Traverse 4-H					
4-67		285, 46N			
4-68		065, 47N			
4-69	A gneiss inclusion	030, 57S			
	B gneiss inclusion				
4-70	A gabbro	035, 45N			
	B gneiss inclusion				
4-71		000, 70W			
4-72	epidote gneiss	345, 60W			
4-73	A gabbro				
4-74		060, 20W			
Traverse 4-H continued.					
4-78	A marble inclusions				
4-79		007, 64W			
4-80		023, 64N			
Traverse 4-I					
4-82		000, 90			
4-84	A biotite gneiss				
	B biotite schist				
	C amphibolite				
4-85	A calc silicate				
	B calc silicate				
Traverse 4-J					
4-86	A oriented mylonite	002, 85W		090, 77S; 255, 65	m, 000, 35
	087, 67S	025, 45W			m, 350, 46
	B oriented mylonite			015, 65E; 135, 50	m, 310, 50
	235, 58W	000, 80W		342, 50E; 230, 42	m, 315, 65
				345, 62E; 040, 55	m, 325, 50
		000, 67W		000, 67W; 300, 65	m, 310, 70
4-87		025, 45W			m, 350, 46
4-88	A para amphibolite	010, 67W			m, 000, 27
	B biotite gneiss				m, 350, 10
Traverse 4-K					
4-92	sillimanite schist	065, 26S	f2 A 260, 12		c, 270, 4
					c, 225, 17
					m, 200, 35
4-94		090, 50S			m, 232, 31
4-95		090, 60S			m, 245, 34
4-96		295, 34S	f3 A 000, 55		

Station	Sample	S1	Folds	Fault; slick	Lineations
Traverse 4-K continued					
4-97		296, 45S			m_y 245, 40
4-99		283, 36S			m_y 236, 20
		293, 34S			m_y 242, 31
4-100		295, 35S	f1 A 245, 20		m_y 242, 24
Traverse 4-L					
4-101		090, 42S	f1 A 240, 40		m_y 220, 28
			f1 A 242, 34		m_y 195, 30
					c, 215, 22
4-102	amphibolite	310, 25W			
4-103		278, 34N	f1 A 247, 14		
4-104		277, 14N	f1 A 252, 30		
			f1 A 233, 18		
			f1 A 320, 42		
			f3 A 170, 54		
			f3 A 161, 28		
4-105		047, 60E			m_y 073, 15
4-106	A pelitic gneiss	030, 87W		053, 55W; 183, 61	c, 032, 9
	B calc silicate	023, 77E	A 030, 15	035, 65E	c, 203, 6
	C amphibolite	343, 55W	A 202, 15		c,
			A 015, 30		
			A 040, 16		
			A 043, 14		
4-107	mica schist	340, 50W			c, 225, 45
					m_y 200, 8
					m_y 320, 34
4-108		020, 70W			m_y 015, 10
					c, 220, 52
					c, 220, 52
4-117	calc silicate	315, 42S	f3 A 178, 44		c, 178, 44
			f2 A 075, 0		m_y 184, 30
4-118		300, 42S	f3 A 167, 29		c, 167, 29
			A 225, 26		c, 225, 26
4-119	amphibolite	080, 8S	f1 A 233, 18		m_y 232, 4
			f3 A 185, 65		m_y 210, 15
4-120	tourmaline gneiss	321, 20	f1 A 228, 34		m_y 184, 35
			f1 A 230, 20		m_y 192, 34
			f2 A 267, 8		c, 088, 6
			f2 A 088, 6		m_y 247, 25
		065, 30S			m_y 211, 30
					m_y 232, 8
4-121			f2 A 096, 5		c, 254, 2
			f2 A 080, 7		
		067, 35S	f1 A 070, 5		m_y 222, 10
			f3 A 200, 20		m_y 200, 20
			f3 A 180, 22		
		080, 19S	f2 A 250, 8		m_y 055, 3

Station	Sample	Sl	Folds	Fault; slick	Lineations
Traverse 4-I continued					
4-122	A layered gneiss	045, 70W	fl A 050, 85		c, 015, 52
	B garnet gneiss		fl A 230, 70		
4-123		029, 62W	fl A 005, 50		c, 225, 52
4-124		010, 70E	fl A 225, 3		c, 024, 20
			fl A 200, 14		
			fl A 040, 6		
			fl A 037, 4		
4-125		033, 58E	A 053, 15		c, 162, 25
		010, 25E			c, 165, 14
4-127		027, 58E			c, 000, 27
4-128		000, 16W	f3 A 032, 17		c, 038, 15
Traverse 4-H					
4-110		060, 68S	f2 A 090, 0		
			fl A 230, 40		m, 230, 40
4-111		009, 45E	A 035, 39		m, 215, 39
		035, 30E	A 232, 7		
4-112		310, 34S			m, 235, 34
		067, 69E			m, 237, 24
4-113		073, 47S			
4-114	calc silicate	038, 50W	fl A 253, 24		m, 250, 28
		258, 47E			m, 245, 32

Station	Sl	Fold Axis	Axial Plane	Lineations, m.	Lineations, c.
Traverse 4-N					
4-132		fl 245, 18	053, 70W	316, 14	240, 29
		fl 296, 34	032, 36W	315, 23	029, 3
		fl 298, 34	285, 38E	323, 44	232, 26
		fl 283, 24	303, 39W		240, 10
		fl 321, 22	350, 22W		183, 65
		f2 229, 18			
		f2 220, 7			
		f2 242, 26			
4-133	008, 64W	200, 40		330, 65	
	356, 74W	203, 32		336, 55	
	002, 60W	168, 20		319, 47	
	353, 50W			313, 42	
	342, 37W			290, 28	

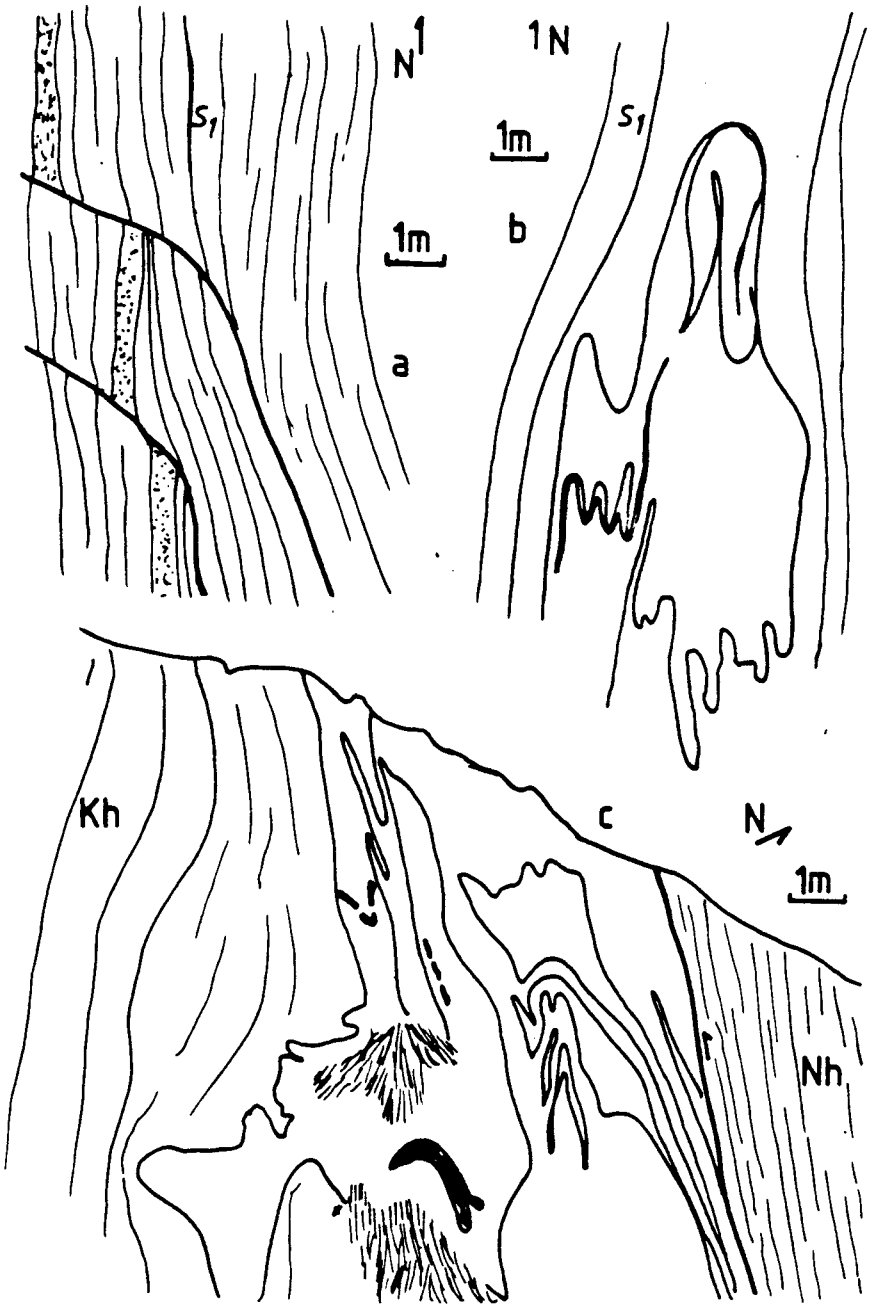

Figure A-1. Structural Details. a. Minor foliation plane faults in Nh with ramps across foliation. Note east-side-up offset. Station 3-26. b. F1 isoclinal intrafolial fold of calc-silicate and marble layers within biotite schist. Station 3-26. c. Complexly folded marble and amphibolite layers in Raikot mylonite zone opposite Sassi village. Station 3-84.

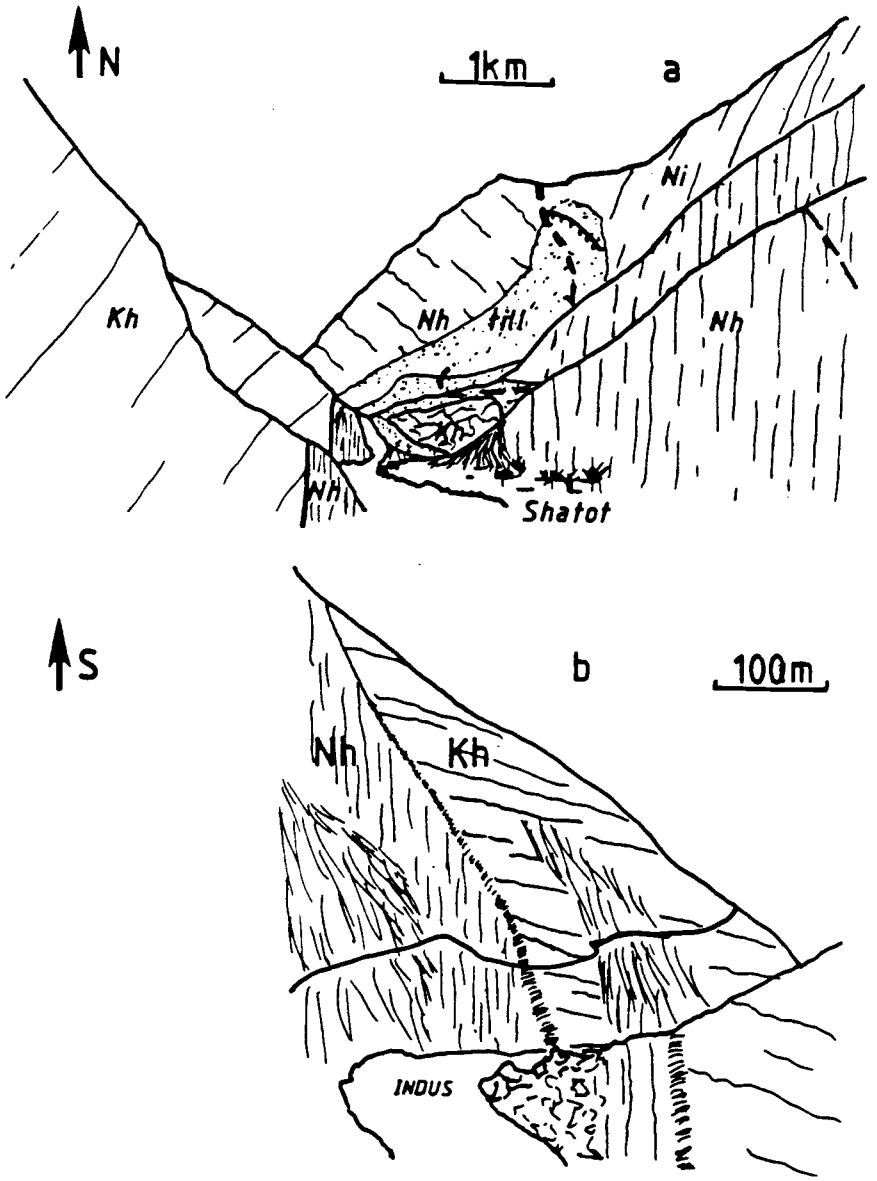

Figure A-2. Raikot fault details. a. View to the south of the east wall of the Indus gorge south of Shatot village. The Raikot mylonite zone separates vertical Nh from gently west dipping Kh. The mylonite zone crosses the Skardu road on the east bank, and is visible on the west bank as well. Station 3-137. **a.** View north showing Kh fault sliver on east bank of the Indus gorge north of Shatot village. The trace of the Sassi Dassu fault (heavy dashed line) passes across till and the ridge north of Sassi village. Note scarp in till at fault, and vertical Raikot mylonite zone on west bank of Indus. Station 4-13.

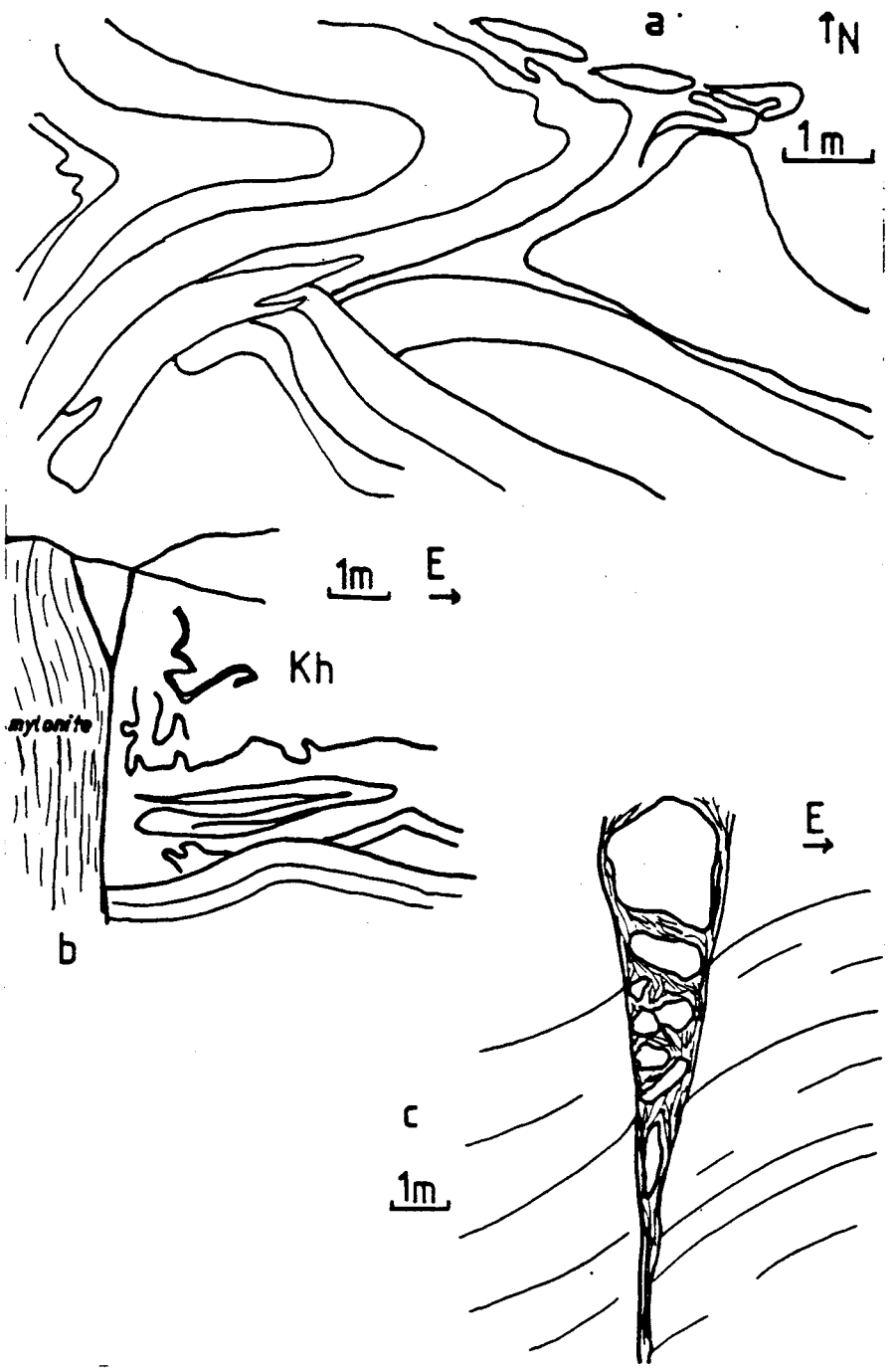

Figure A-3. Raikot fault drag. a. complex folding in Kh amphibolites adjacent to Raikot mylonite zone. Station 3-138. **b.** Folding in Kh amphibolite and marble adjacent to Raikot mylonite zone. 3-134. **c,** minor fault in Raikot fault zone, with east side up drag. Station 3-143.

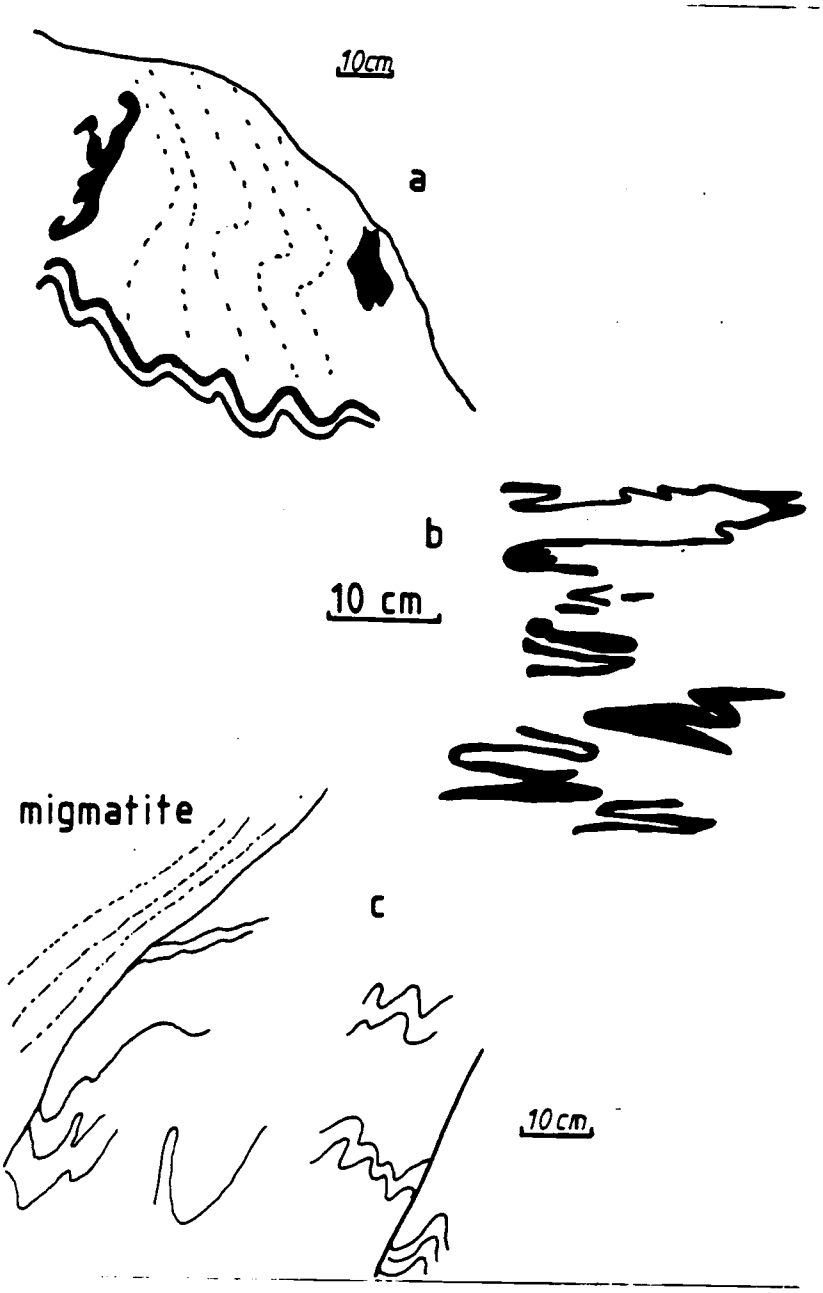

Figure A-4. Migmatites. **a.** Ni migmatitic gneiss, with folded pegmatitic stringers (solid black) and biotite laminae (dashed line). Station 4-88. **b.** Complexly folded pegmatitic stringers in Ni biotite gneiss/migmatite. 4-88. **c,** diffuse contact between biotite gneiss with tightly folded biotite folia, and equigranular gneiss/migmatite with diffuse biotite laminae/schlieren. Station 3-156.

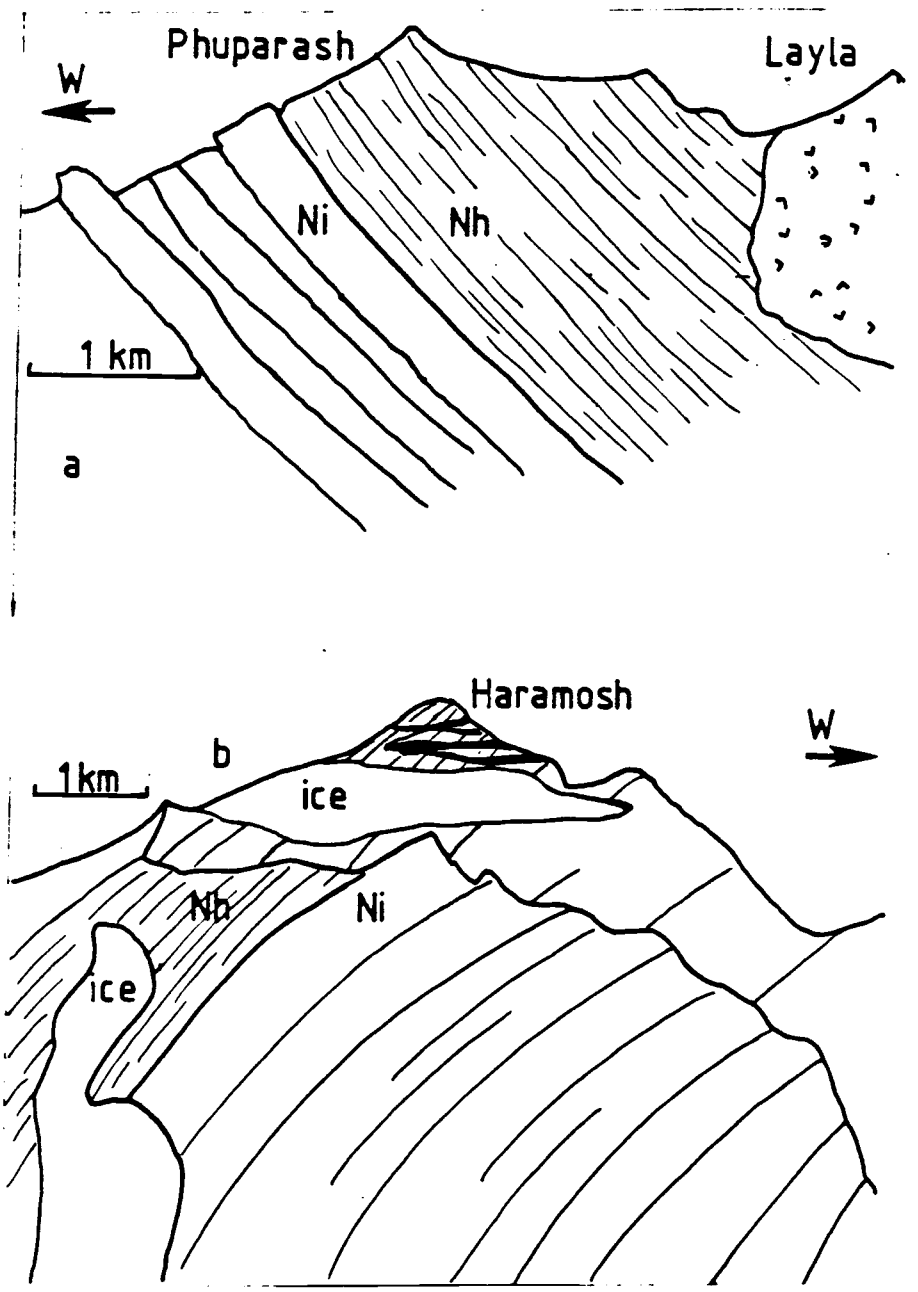

Figure A-5. Structure in the upper Iskere Canyon. a. View to the north of the south face of Phuparash/Layla. Consistently east dipping foliation with possible contact between thinly laminated Nh and thickly laminated Ni. Note intrusive rock at summit of Layla. Station 4-42. b. View south of the North face of Haramosh, with consistently east dipping foliation and possible contact between Nh and Ni. Note abundant pegmatites in summit tower. Station 4-43.

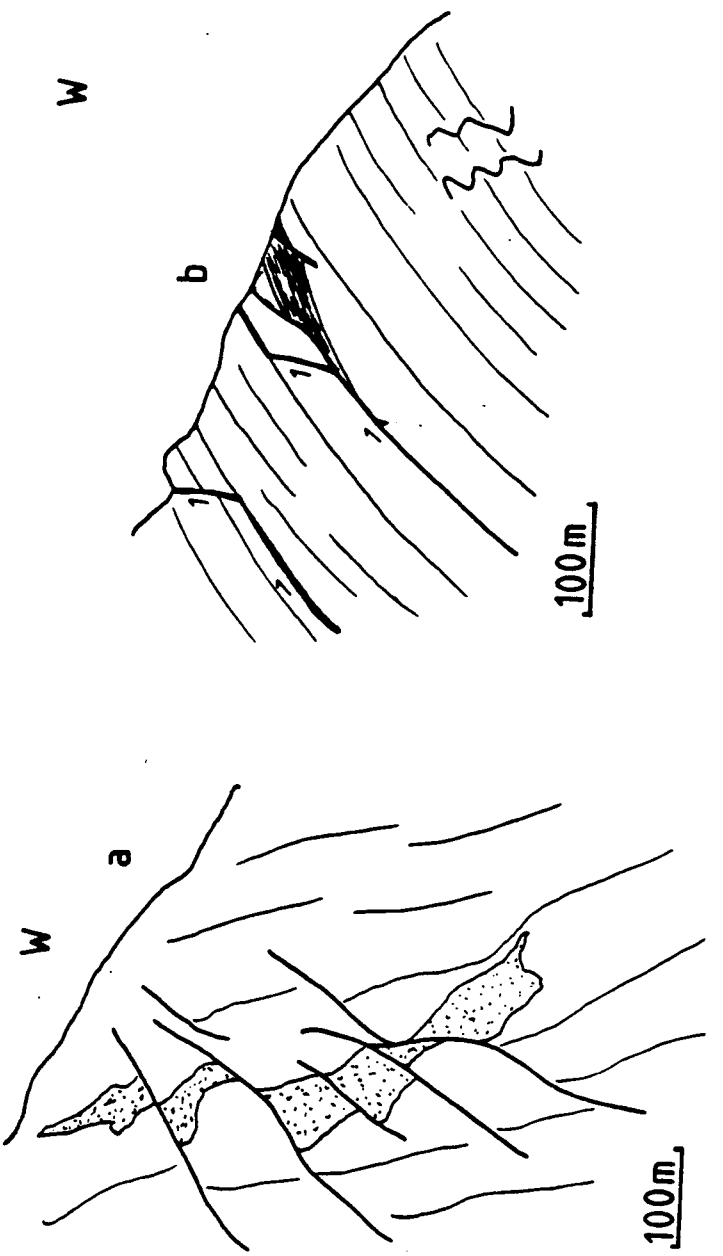

Figure A-6. Minor faults. a. View of south wall of Bunji canyon, approximately 1.5 km west of Raikot fault. Numerous east dipping east side up faults offset a concordant pegmatite. Station 4-62. b. North facing cliff on the north bank of Dassu canyon between Dassu and Sassi village. Foliation plane faults ramp across foliation. Station 4-46.

Appendix 2

Lithologic and petrographic descriptions.

A general lithologic description is provided for each major unit, followed by detailed petrographic descriptions of rocks studied in thin section.

Key to abbreviations.

Mineral phases; An = andesine, Ab = albite, Al = almandine, Ap = apatite Au = augite, Bi = biotite, Cc = calcite, Ch = chlorite, Cz = clinozoisite, Di = diopside, Do = dolomite Fo = forsterite, Gp = graphite, Gr = grossular, Hb = hornblende, Id = idocrase, Kf = potassium feldspar Ky = kyanite, La = labradorite, Ma = margarite, Mi = microcline, Mu = muscovite, Ol = oligoclase, Py = pyrite, Qz = Quartz, Ru = rutile, Sc = scapolite, Se = sericite, Si = sillimanite, Sp = sphene, To = tourmaline, Wo = wollastonite, Zi = zircon, Zo = zoisite

Textural terms; SPO = shape preferred orientation, MT = mortar texture, PG = polygonized or polygonization, UE = undulatory extinction, SG = sub grains or sub grain formation, NM = neomineralization or crystallization, ER = embayed and/or replaced, SR = static recrystallization, PE = polygonal-equigranular or mosaic, GB = grain boundaries, FX = broken or fractured, BX = bent, SF = surface formed, SD = surface deformed, XB = xenoblastic, SB = sub idio blastic, IB = idioblastic, PB = porphyroblastic or porphyroblast, PC = prophyroclast, gr = grained, twx = twins.

Kohistan Sequence

Hanuchal amphibolite (Kh)

Kh consists of medium to coarse grained hornblende, biotite and epidote gneisses and amphibolite, interlayered with metamorphosed leucocratic dikes and sills, and subordinate calc silicates and marbles. The various lithologies occur in layers which vary from a few cm to several m thick, and which are parallel to a strong S1 foliation. The lithologic layers are laterally continuous, and in at least one outcrop a primary structure (basalt? dikes in marble) is observed. Metamorphosed leucocratic intrusive rocks generally occur as concordant or weakly discordant bodies, strongly foliated parallel to S1. Kh is recognized in the field by its relatively monotonous gray-green color and strong layering and foliation. The unit is in the albite epidote amphibolite facies, and the common occurence of epidote distinguishes it from the rocks of the Nanga Parbat group.

Skarns, metasomatic asbestos deposits and chlorite schists are all associated with young Kg dikes in Kh. Locally, chyrsocolla occurs on foliation planes in Kh.

Petrographic Descriptions

Sample Number 3040-B

Rock Name Garnet bearing biotite muscovite semi-schist **Facies** Albite-epidote amphibolite **Protolith** Psammite **Distance from Raikot Fault** 0.5 km **Stained Billet** yes **Photo** no

General Petrofabric Strong S1 defined by mica segregation bands, quartz ribbons and SPO of mica. Coarse garnet and albite augen, wrapped by and flattened in S1. Moderate S2 developed as discrete zones of strong BX and PG.

Mineralogy

Phase	%	Character
Ab	Major	XB, fine gr, no twx, moderate SPO. Cuspate to serrate GB. Also as coarse PB, with UE and SG.
Qz	Major	XB, fine gr, moderate SPO, cuspate to serrate GB. UE, SG, PG common. Also as coarse ribbons.
Mu	Minor	IB, coarse gr, with strong SPO. BX, FX, PG common.
Bi	Minor	SB, fine gr, and IB medium gr intergrowths with mu. BX, FX, PG common.
Al	Minor	SB, coarse PB with moderate SPO. Minor alteration to chlorite along fractures.
Ep, Ap	Trace	

Metamorphic/Deformational/Crystallization History

Metamorphism							Deformation		
		Ab	Qz	Mu	Bi	Al	S1	S2	
	M1	NM	NM	NM	NM	NM	SF		D1
	M1	NM	NM		NM		SF		D1
		UE	UE	BX	BX		SD	SF	D2
		SG	SG	PG	PG				D2
			PG						D2

Summary Psammitic sediment strongly deformed and metamorphosed in albite epidote amphibolite conditions. Subsequent strong deformation produced strain in all phases, and S2 incipient mylonitic foliation.

Sample Number 3-087A

Rock Name garnet and biotite bearing amphibolite **Facies** albite epidote amphibolite **Protolith** basic igneous rock**Distance from Raikot Fault** 4 km **Stained Billet** no **Photo** no

General Petrofabric Moderate S1 defined by discontinuous pl seg bands and weak to moderate SPO of hb, bi. Predominantly coarse gr hb with interstitial pl.

Mineralogy

Phase	%	Character
Hb	Major	Coarse elongate SB with moderate SPO, and fine gr SB. ER by qz and pl. Some FX.
Pl	Major	XB, equant, albite, pericline and deformation twx common. Some zoned. An % 40.
Qz	Minor	XB, fine gr, with moderate SPO, some UE and SG.
Op	Trace	Irregular masses and thin plates on bi.
Al	Trace	SB, equant.
Bi	Trace	IB, fine gr, on hb GB and cleavage. Altered to ch.
Ap	Trace	XB, coarse gr.
Zi, Cz	Trace	

Metamorphic/Deformational/Crystallization History

Metamorphism						Deformation	
	Hb cs	Hb fn	Pl	Al	Bi	Sl	
Igneous	NM		NM				
Ml	ER	NM	NM?	NM	NM	SF	Dl

Summary Albite epidote amphibolite or amphibolite grade ortho amphibolite. Experienced weak metamorphic/deformation event, followed by minor retrograde alteration to chlorite. Possibly an early dike of Ks.
Note Spectacular deformation twx in pl.

Sample Number 3-091B

Rock Name Epidote Albite augen gneiss **Facies** albite epidote amphibolite **Protolith** psammitic sediment **Distance from Raikot Fault** 7.5 km **Stained Billet** no **Photo** no

General Petrofabric Coarse gr gneiss with Sl defined by discontinuous bi and qz/pl seg bands and by SPO of qz, pl ep and bi.

Mineralogy

Phase	%	Character
Ab	Major	SB, fine gr in matrix with SPO and contact inhibition against bi. Also as PB with SPO. Peri cline and albite twx common. An % 5.
Qz	Major	XB, fine gr, with SPO. SG, UE and serrate GB common.
Bi	Minor	IB, fine gr, with SPO.
Ep	Minor	IB, elongate grains show SPO.
Mu	Trace	IB, random orientation.
Ap, Zi	Trace	

Metamorphic/Deformational/Crystallization History

Metamorphism						Deformation	
	Ab	Qz	Bi	Ep	Mu	Sl	
Ml	NM		NM			SF	Dl
Ml	NM	NM	NM	NM		SF	Dl
M2?					NM		

Summary Albite epidote amphibolite facies meta psammite, metamorphosed syntectonically to produce Sl. Late muscovite possibly due to intrusion of Ks.
Note Sample collected from Kh inclusion in Ks.

Sample Number 3-133D

Rock Name garnet epidote gneiss. **Facies** albite epidote amphibolite **Protolith** calcareous sediment **Distance from Raikot Fault** 1.0 km **Stained Billet** no **Photo** yes

General Petrofabric Fine grained equigranular gneiss with Sl defined by weak segregation bands and weak to moderate SPO of epidote. Dominant texture is sub PE.

Mineralogy

Phase	%	Character
Qz	Major	XB, with weak SPO, minor UE and SG. PE texture.
Ep	Major	2 populations, fine IB with moderate SPO, and cse SB with ER.
Gr	Minor	Fine gr SB, equant.
Sp	Trace	
Zi	Trace	IB, equant.

Metamorphic/Deformational/Crystallization History

Metamorphism						Deformation	
	Ep 1	Ep 2	Qz	Gr	Sl		
Ml	NM		NM		SF	Dl	
Ml	ER	NM	NM	NM	SR		

Summary Albite epidote amphiboite facies meta calcareous sediment. The deformation which produced Sl may have been followed by a static metamorphism which crystallized garnet, the second population of epidote and produced the overall PE texture.

Sample Number 3-135

Rock Name Quartz and sphene bearing amphibolite **Facies** albite epidote amphibolite **Protolith** basic sediment or igneous rock **Distance from Raikot Fault** 0.2 km **Stained Billet** no **Photo** no

General Petrofabric Strong Sl defined by segregation bands and moderate SPO in hb. Mostly cse hb with interstitial qz and pl.

Mineralogy

Phase	%	Character
Hb	Major	IB, coarse gr, moderately elongate, moderate SPO. Rational GB, and general PE texture with pl.
Pl	Major	XB, equant, with PE texture. Albite and pericline twx common. An % 70.
Qz	Minor	XB, equant, with PE texture.
Sp	Minor	2 populations, fine rounded IB, and coarse rounded IB, with moderate SPO.
Cz	Minor	IB.
Bi	Trace	Ib, no SPO, cuts all other phases.
Ap, Zi	Trace	
op	Trace	

Metamorphic/Deformational/Crystallization History

Metamorphism							Deformation	
	Hb	Pl	Qz	Sp	Bi	Sl		
Ml	NM	NM	NM	NM		SF	Dl	
Ml	NM	NM	NM	NM	NM	SR		

Summary Albite epidote amphibolite facies amphibolite derived from basic/calcareaous sediment or basic igneous rock. Initial metamorphism was accompanied by deformation to form Sl, but was followed by static metamorphism to produce PE texture.

Note Unusually coarse sphene and unusually high total sphene content (ca. 2 %).

Sample Number 3-141

Rock Name Calc silicate marble **Facies** green schist or albite epidote amphibolite **Protolith** impure limestone **Distance from Raikot Fault** 0.25 km **Stained Billet** yes **Photo** yes

General Petrofabric Predominantly coarse gr Cc, with PE texture modified along GB. Minor amounts of calc silicate mineral with no SPO. S1 defined by an amphibolite segregation band with moderate SPO of tr and bi.

Mineralogy

Phase	%	Character
Cc	Major	XB, coarse gr, equant with PE texture. GB are serrate. Deformation twx common. Some MT.
Mu	Minor	IB, BX, FX, some replacement by qz.
Qz	Trace	XB, UE.
Pl	Trace	SB, albite and pericline twx common, some ER, An % 40?
Mi	Trace	Xb, UE
Ep	Major	SB, In amphibolite segregation band
Tr	Major	IB, In amphibolite segregation band
Py	Trace	XB, with hematite rims
Sc	Trace	XB, reaction relation with pl?
Id	Trace	IB, ER by pl
Sp, Zo	Trace	
Ma, Bi	Trace	

Metamorphic/Deformational/Crystallization History

Metamorphism					Deformation	
		Cc	Mu	Qz	S1	
	M1	NM	NM	NM	SF	D1
	M1	PE	NM	NM	SR	
		MT	BX	UE	SD	D2

Summary Albite epidote amphibolite facies marble derived from an impure limestone. The main metamorphism and S1 forming deformation were followed by a static metamorphism, producing PE texture. Subsequently D2 strains most phases slightly, but does not produce new surface.
NoteGood example of mortar texture in Cc.

Sample Number 3-182A

Rock Name amphibolite **Protolith** basic dike **Facies** Albite epidote amphibolite **Distance from Raikot Fault** 0.1 km **Stained Billet** no **Photo** no

General Petrofabric Predominantly hb with interstitial ep, to, pl and qz. Strong S1 defined by SPO of hb and ep, moderate SPO of bi. Strong lineation defined by SPO of hb, in S1. S2 at high angle to S1 defined by closely spaced fractures, generally lined with ch.

Mineralogy

Phase	%	Character
Hb	Major	IB, ER by pl and overgrown by ep. FX common, and alteration to ch.
To	Major	XB, ragged zoned clear to blue grains, intergrown with fine bi and ch.
Pl	Minor	XB, equant, albite and deformation twx common. An % 45. Altered

		to sericite.
Qz	Minor	XB, equant.
Ep	Minor	2 populations, irreg XB with to, bi and IB prisms with strong SPO.
Bi	Minor	2 populations, medium gr SB, with moderate SPO, and fine gr ragged SB, with no SPO.
Ch	Minor	In radial clumps, veins, along S2, as alteration of hb, bi, and with to and fine gr bi.
Ap, Zi	Trace	

Metamorphic/Deformational/Crystallization History

Metamorphism								Deformation		
	Hb	Pl	Qz	Ep 1 Bi 1	Ep 2 Bi 2	To	Ch	S1	S2	
M1	NM	NM		NM				SF		D1
M2			NM		NM	NM	NM	SD	SF	D2

Summary Albite epidote amphibolite facies meta intrusive rock. Syn metamorphic deformation produced S1. S2 fracture associated with late deformation, and hydrothermal alteration or retrograde metamorphism.
Note Field relations indicate that protolith was basic dike intrusive into limestone country rock.

Sample Number 4-013E

Rock Name biotite bearing quartz amphibolite. **Facies** Albite epidote amphibolite **Protolith** basic calcareous sediment **Distance from Raikot Fault** 0.1km **Stained Billet** yes **Photo** yes

General Petrofabric Strong S1 defined by segregation bands and SPO of all phases. S2 defined by spaced shear bands, S3 defined by closely spaced fractures perpendicular to S1.

Mineralogy

Phase	%	Character
Hb	Major	IB, elongate coarse gr, somewhat ER by qz, pl. Some FX, BX.
Pl	Major	XB, deformations twx common.Original PE texture modified by SG, MT.
Qz	Major	XB, elongate, with extensive UE, SG, PG.
Ep	Minor	IB, elongate, some ER by qz, pl.
Bi	Minor	IB, on hb cleavage and GB. FX, BX, PG common.
Cc, Sp	Trace	

Metamorphic/Deformational/Crystallization History

Metamorphism								Deformation	
	Hb	PL	Qz	Bi	Ep	S1	S2	S3	
M1	NM	NM	NM		NM	SF			D1
M1				NM					
M2 ?	ER	SG	UE	BX	ER	SD	SF		D2
	BX	MT	SG	PG			SF		D2
	FX		PG	FX			SD	SF	D2

Summary Albite epidote amphibolite facies meta calc-basic sediment. Initial metamorphism accompanied S1 forming deformation, possibly followed by static

metamorphism. Late dynamic metamorphism associated with formation of S2, S3. **Note** Sample is from amphibolite interlayered with marble (3-141).

Sample Number 4-056A

Rock Name garnet bearing biotite epidote gneiss **Facies** albite epidote amphibolite **Protolith** psammitic sediment.**Distance from Raikot Fault** 1.0 km **Stained Billet** yes **Photo** no

General Petrofabric Strong S1 defined by segregation bands and SPO of bi and ep. Qz-pl have PE texture.

Mineralogy

Phase	%	Character
Qz	Major	XB, equant, or slightly elongate due to contact inhibition by bi.
Pl	Major	XB, equant, or slightly elongate due to contact inhibition by bi. alteration ot sericite.
Bi	Minor	SB, greenish yellow, BX common, and minor alteration to ch.
Cz	Minor	IB, ER by qz and pl, minor alteration to ch.
Al	Minor	SB, flattened, ER by pl.
Ep	Trace	"pistachite" alteration of cz, with ch.
Ap	Trace	Fine IB.
Ru, Op	Trace	

Metamorphic/Deformational/Crystallization History

Metamorphism								Deformation
	Qz	Pl	Bi	Cz	Al	Ch	Sl	
M1					NM			
M1	NM	NM	NM	NM			SF	D1
M2	UE		BX	ER	ER	NM		D2
	SG							D2

Summary Albite epidote amphibolite facies meta psammite. Initial metamorphism and S1 forming deformation followed by a static metamorphism. Late retrograde metamorphism accompanies weak dynamic metamorphism.

Sample Number 4-056B

Rock Name quartz epidote biotite amphibolite **Facies** albite epidote amphibolite **Protolith** basic-psammitic sediment **Distance from Raikot Fault** 1.0 km **Stained Billet** yes **Photo** yes

General Petrofabric Strong S1 defined by segregation bands and SPO of hb, bi and ep. Overall texture is PE. S2 surface defined by fine parallel fractures.

Mineralogy

Phase	%	Character
Hb	Major	IB, coarse gr, with PE texture, some ER by qz, pl.
Pl	Major	XB, equant or slightly elongate due to contact inhibition with bi. Deformation twx and UE common.
Qz	Major	XB, weakly elongate. Serrate GB, SG, UE common.
Bi	Minor	SB, coarse gr and ER in hb rich bands, fine gr in hb poor bands. BX.

Ep	Minor	IB, some ER with qz and pl.
Ch	Trace	alteration of bi.
Ap, Mu	Trace	

Metamorphic/Deformational/Crystallization History

Metamorphism						Deformation		
	Hb	PL	Qz	Bi	Ep	Sl	S2	
M1	NM	NM	NM	NM	NM	SF		D1
M2?	ER			ER	ER			
			SG	BX		SD	SF	

Summary Albite epidote amphibolite facies meta basic psammite. Initial metamorphism and S1 forming deformation were followed by static metamorphism, and subsequent weak retrograde and dynamic metamorphism.

Sample Number 4-065

Rock Name biotite epidote amphibolite **Facies** albite epidote amphibolite **Protolith** basic igneous rock **Distance from Raikot Fault** 0.2km **Stained Billet** no **Photo** no

General Petrofabric Strong S1 defined by segregation bands and strong SPO of bi, moderate SPO of hb, ep. S2 defined by closely spaced fractures at high angle to S1.

Mineralogy

Phase	%	Character
Hb	Major	SB, with ER by qz, pl. Extensive alteration to ch, FX.
Pl	Major	XB, extensive alteration to se, common albite twx and FX.
Ep	Minor	IB, crosscut and poikiloblastically enclose hb. FX.
Bi	Minor	IB, extensively altered to ch.
Ch	Minor	Along fractures, and after bi and hb.
Mu	Minor	IB.
Ap, Zi	Trace	
Op	Trace	

Metamorphic/Deformational/Crystallization History

Metamorphism						Deformation		
	Hb	Pl	Ep	Bi	Ch	Sl	S2	
M1	NM	NM		NM		SF		D1
M1? M2?			NM					
M2	FX	FX	FX		NM	SD	SF	D2

Summary Albite epidote amphibolite facies meta igneous rock. Initial metamorphism and S1 forming deformation followed by retrograde and dynamic metamorphism, possibly accompanied by hydrothermal alteration.

Sample Number 4-070A

Rock Name biotite epidote gneiss/hornfels **Facies** albite epidote amphibolite **Protolith** psammittic sediment **Distance from Raikot Fault** 5.0 km **Stained Billet** no **Photo** yes

General Petrofabric S1 defined by segregation bands is tightly folded, and wraps ep PB. Micas show weak SPO parallel to S1, but are mostly random. Overall

qz/pl/ep fabric is PE.

Mineralogy

Phase	%	Character
Pl	Major	XB, with strong PE texture modified by weakly serrate GB.
Qz	Major	As above.
Bi	Major	IB, green, random orientation.
Ep	Minor	SB, some allanite cores.
Cc	Minor	XB, PE.
Sp	Minor	
Ap	Minor	Unusually coarse SB.

Metamorphic/Deformational/Crystallization History

Metamorphism							Deformation	
		Pl	Qz	Bi	Ep	Cc	Sl	
	Ml	NM	NM	NM	NM	NM	SF	Dl
Intrusion							SD	
	M2		NM	NM		NM		

Summary Albite epidote amphibolite facies meta psammite. Initial metamorphism and Sl forming deformation followed by folding, followed by static recrystallization as an inclusion in Ks.
Note Sample from Kh inclusion in Ks. Companion sample of surrounding intrusive rock is 4-070B.

Shuta Gabbro Ks

Ks is a group of diorite, gabbro and norite plutons intruded into Kh. The rocks are generally medium grained equigranular rocks with weak Sl parallel to Sl in surrounding country rock. Primary igneous layering is commonly observed in both outcrop and thin section. Kh inclusions are common in the gabbro, ranging from a few cm to several hundred m across. Contacts between the Ks and Kh are generally broad zones of diking and inclusions, and are generally parallel to Sl. The unit is distinguished in the field by its dark grey to grey green color, and massive character.

Petrographic Descriptions

Sample Number 3-042

Rock Name Epidote diorite **Distance from Raikot Fault** 1.2 km **Stained Billet** no **Photo** no

General Petrofabric Medium gr equigranular rock with weak Sl defined by slightly flattened hb grains. Overall rock has a moderately strong PE texture.

Mineralogy

Phase	%	Character
Hb	50	Subhedral, slightly elongate. Simple twx common. Minor alteration to ch.
Pl	40	Anhedral, equant, albite and pericline twx common. An % 55.
Ep	5	Euhedral, cut bi, hb, pl. Some ER by qz and pl.
Bi	2	Euhedral, random orientation, some BX, ER.
Sp	<1	Rounded sphenoids

Qz	<1	
Cc	Trace	Irregular masses
Ap	Trace	Fine subhedral gr.
Zi	Trace	Euhedral

Summary Intrusive diorite, overprinted by weak metamorphism and deformation resulting in tendency to PE texture, and weak S1 foliation.

Sample Number 3-089

Rock Name Norite **Distance from Raikot Fault** 5.0 km **Stained Billet** no **Photo** yes

General Petrofabric Medium gr equigranular rock with weak S1 defined by elongate pyroxene grains.

Mineralogy

Phase	%	Character
Pl	48	Elongate rounded subhedra, with myrmekite and Kf rims. Albite twx common. An % 50.
Cpx	25	Slightly elongate subhedral gr. Cores of opx common, and rims of hb, bi.
Opx	10	Pink/green subhedra, commonly with cpx rims.
Bi	9	Coarse ragged poikilitic gr, and fine euhedral flakes on cleavage in cpx, opx.
Kf	9	Interstitial grains, and reaction rims on pl, commonly myrmekitic.
Op	3	Rounded subhedral grains.

Summary Intrusive norite, with sequential crystallization of opx, cpx, hb. Late crystallization of significant Kf and fine bi may be due to contamination from Kh country rock. Weak deformation produced S1, possibly intrusive auto deformation.

Note Excellent examples of Kf reaction rims on pl.

Sample Number 4-070A

Rock Name Norite **Distance from Raikot Fault** 5 km **Stained Billet** no **Photo** yes

General Petrofabric Medium gr equigranular rock with pronounced planar fabric defined by primary igneous layering.

Mineralogy

Phase	%	Character
Pl	45	Elongate subhedral gr, with strong SPO and LPO due to settling. Albite twx common. Marginal overgrowths of Kf common.
Px	25	Euhedral grains of cpx, commonly cored by opx, both extensively ER by pl, qz, ep, op. Commonly with rims of hb and bi. Some twx and exsolution lamellae.
Hb	10	Exclusively as fine grained marginal overgrowths on px.
Bi	10	As fine euhedral plates on px, and as coarse randomly oriented subhedral grains with opaques. Some ER by pl or kf.

Kf	6	Coarse poikilitic grains and rims on pl, commonly myrmekitic.
Op	2	
Ap, Qz	Trace	

Summary Intrusive norite. Sequential crystallization of of opx, cpx, hb and bi. Late crystallization of significant Kf and fine bi may be due to contamination from Kh country rock. Crystal settling of tabular pl crystals results in strong SPO and lattice preffered orientation.
Note Excellent example of primary settling texture.

Sample Number 4-073A

Rock Name Diorite **Distance from Raikot Fault** 2.25 km **Stained Billet** no **Photo** no
General Petrofabric Equigranular medium gr rock. Interlocking hb crystals with interstitial pl.

Mineralogy

Phase	%	Character
Hb	70	2 populations, euhedral to subhedral equant, and coarse gr poikilitic.
Pl	30	Equant, anhedral, albite, pericline and deformation twx common.
Bi	<1	Euhedral, crosscuts hb, pl. Commonly altered to ch, some BX and FX.
Ep	Trace	
Ch	Trace	Alteration of bio.
Zi, Op	Trace	

Summary Intrusive diorite, possibly overprinted by weak metamorphism responsible for poikilitic hb and epidote. Weak deformation, insufficient to produce a fabric, possibly intrusive auto deformation.

Sample Number 4-134A

General Petrofabric Equigranular medium to coarse gr rock with weak S1 defined by vaguely elongate felsic and mafic clots. S2 defined by spaced microfractures.

Mineralogy

Phase	%	Character
Hb	35	2 populations, early coarse euhedral gr with ER by pl, and later fine subhedral overgrowth.
Pl	50	Anhedral, with albite, pericline and deformation twx and zoning. An % 45
Ep	9	Euhedral, crosscuts early hb, includes late hb. Some ER by qz, pl.
Bi	8	Euhedral, random orientation. Crosscuts early hb.
Sp, Ap	Trace	
Ru, Zi	Trace	

Summary Intrusive diorite, possibly overprinted by weak metamorphism producing second generation hb and epidote. Weak deformation has produced vague S1,

possibly intrusive autodeformation.

Kohistan Granites (Kg)

Kg are a series of leucocratic dikes which cut both Kh and Ks. The dikes range in size up to 20 m thick, and locally comprise up to 20 % of an outcrop. Two ages of two mica granodiorite occur, the older exhibits considerable deformation. Both are cut by younger granitic pegmatites.

Sample Number 4-134B

Rock Name Biotite and muscovite bearing granodiorite **Distance from Raikot Fault** 9.25 km **Stained Billet** yes **Photo** yes

General Petrofabric Coarse pl and kf phenocrysts in a matrix of finer gr pl, qz, kf.

Mineralogy

Phase	%	Character
Ab	55	Phenocrysts with zoning and albite twx, and fine anhedral matrix grains. Commonly contain rounded blebs of qz. UE. Also pl/qz myrmekite.
Qz	25	Anhedral fine matrix grains. UE, SG.
Mi	20	Phenocrysts and fine matrix grains.
Mu	Trace	Euhedral, randomly oriented.
Bi	Trace	Euhedral, randomly oriented.
Ep	Trace	

Summary Intrusive granite, possibly overprinted by weak metamorphism to produce qz blebs in pl and mi and ep. Weak strain indicated by qz, pl.

Sample Number 4-134C

Rock Name Biotite and muscovite bearing granodiorite **Distance from Raikot Fault** 9.25 km **Stained Billet** yes **Photo** yes

General Petrofabric Equigranular rock with weak Sl defined by flattened qz, pl, kf and weak SPO of mica.

Mineralogy

Phase	%	Character
Pl	40	Anhedral and slightly flattened. Zoning and albite, pericline and deformation twx common. Serrate GB, some UE.
Qz	35	Anhedral and slightly flattened. UE, SG, serrate GB.
Kf	19	Anhedral. UE, serrate GB.
Bi	4	Fine gr subhedra, moderate SPO.
Ep	<1	Euhedral
Mu, Zi	Trace	
Ru, Sp	Trace	

Summary Intrusive rock with no clear metamorphic overprint. Weak deformation, predominantly of qz, produces weak Sl.

NANGA PARBAT GROUP

Nanga Parbat Granites (Ng)

Nanga Parbat group granites occur as undeformed dikes of granite, tourmaline granite and pegmatite, both concordant and discordant with foliation in country rock. Dikes range up to 10 m thick, and on small pluton was observed telescopically in the summit tower of Layla peak. Tormaline granites commonly occur as selvages to pegmatites, which are locally mined for green tourmaline, aquamarine and topaz.

Sample Number 3-101

Rock Name 2 mica tourmaline bearing granite **Stained Billet** yes **Photo** yes **General Petrofabric** Coarse grained equigranular rock, no evidence of significant deformation.

Mineralogy

Phase	%	Character
Kf	36	Coarse equant anhedra of perthite or microcline. Graphic exsolution textures and myrmekite.
Pl	33	Equant anhedra with zoning and albite and pericline twx. Some UE, reaction rims against kf.
Qz	30	Coarse irregular anhedra. SG common.
Bi	trace	Equant random euhedra altered to ch.
Mu	trace	Equant euhedra with bi, and fine anhedra on pl.
To	trace	Coarse zoned phenocrysts, with some ER by qz, pl and bi.
Zi	trace	Medium to fine grained euhedra.

Summary Equigranular biotite muscovite tourmaline granite. No significant deformation.

Sample Number 3-191B

Rock Name 2 mica tourmaline granite **Stained Billet** yes **Photo** yes **General Petrofabric** Coarse grained equigranular rock with sub PE fabric.

Mineralogy

Phase	%	Character
Kf	30	Coarse equant anhedra of perthite or microcline. Exsolution, myrmekite and pl inclusions.
Pl	30	Coarse equant anhedra with zoning and albite and pericline twx. Some UE, reaction rims against kf. Commonly altered to se.
Qz	38	Coarse irregular anhedra. SG, UE and serrate GB common.
Bi	trace	Equant random euhedra altered to ch. Some BX.
Mu	trace	Equant euhedra with bi, and fine anhedra on pl. Some ER.
To	trace	Coarse irregular zoned phenocrysts.

Summary Biotite muscovite tourmaline granite. Nearly PE texture indicates some static post crystallization metamorphism. Weak late deformation.

Haramosh schist (Nh)

The Haramosh schist is a unit of interlayered biotite and muscovite schist and gneiss with marble, calc silicate gneiss and amphibolite. The various lithologies occur in laterally discontinuous lithologic layers which range from a few cm to several m thick, and average 0.5 to 1.0 m thick. A strong S1 foliation occurs parallel to the lithologic layering. Primary structures have been completely transposed by the S1 forming deformation. The unit is distinguished in the field by its lithologic variety, thin lithologic bands, abundance of marble and schist, and characteristic red brown weathering color.

Petrographic Descriptions

Sample Number 3-026A

Rock Name Diopside tremolite calc silicate gneiss **Facies** amphibolite **Protolith** impure marble or calcareous psammite **Distance from Raikot Fault** 0.2 km **Stained Billet** no **Photo** yes

General Petrofabric Dominant fabric is PE, with weak S1 defined by SPO of tr. Also contains pods of quartz surrounded by poikiloblastic di and tr.

Mineralogy

Phase	%	Character
Di	Major	IB, PE texture.
Tr	Major	SB, moderately elongate, some ER or inclusion of cc, qz.
Cc	Minor	XB, poikiloblastic.
Qz	Minor	Xb, in pods. UE.
Bi	Minor	IB.
Ap	Minor	SB, PE.

Metamorphic/Deformational/Crystallization History

Metamorphism						Deformation	
	Di	Tr	Cc	Qz	S1		
M1	NM	NM	NM	NM	SF	D1	
M1	NM	NM	NM	NM	SR		
				UE		D2	

Summary Amphibolite facies gneiss derived from a calcareous sediment. Initial metamorphism and S1 forming deformation were followed by a static metamorphism. Late dynamic metamorphism is weak.
Note Excellent PE texture of di, tr.

Sample Number 3-029

Rock Name Biotite muscovite schist **Facies** amphibolite **Protolith** psammitic sediment **Distance from Raikot Fault** 0.5 km **Stained Billet** yes **Photo** yes

General Petrofabric Strong S1 defined by segregation bands and strong SPO of mica and quartz ribbons. S1 contains annealed isoclinal fold hinges, and annealed wraps around pl PB. S2 defined by spaced mylonitic shears and fractures sub parallel to S1.

Mineralogy

Phase	%	Character
Mu	Major	SB, coarse gr, BX, FX, PG, annealed folds.
Pl	Major	XB, cloudy, some Albite twx. Also as early PB.
Qz	Major	XB, fine gr, and in ribbons and elongate domains. UE, SG, PG.
Bi	Major	SB, coarse gr, FX, BX, PG.
Sp, CC	Trace	

Metamorphic/Deformational/Crystallization History

Metamorphism						Deformation	
	Mu	Bi	Pl	Qz	S1	S2	
M1	NM	NM	NM	NM	SF		D1
M1	FOLDING		WRAP	RIBBON	SD		D1?
M1	NM	NM	NM	NM	SR		
	PG	PG		PG	SD	SF	D2

Summary Amphibolite grade meta psammite. Initial metamorphism and S1 forming deformation involved or were followed by isoclinal folding event. During folding event, S0 was transposed, S1 wrapped around PB. Subsequent SR annealed folded and wrapped micas, quartz ribbons. Late dynamic metamorphism involves all phases but pl, produces S2.
Note Excellent example of annealed isoclinal fold hinges.

Sample Number 3-082

Rock Name Proto mylonitic calc silicate bearing marble **Facies** amphibolite **Protolith** impure limestone **Distance from Raikot Fault** 0.5 m **Stained Billet** no **Photo**

General Petrofabric Moderately strong S1 defined by segregation bands. Dominant fabric is polygonized cc, with porphyroclasts of calc silicate minerals.

Mineralogy

Phase	%	Character
Cc	Major	XB, flattened, with bent twin lamellae, SG, PG, serrate GB, MT.
Pl	Minor	Albite and deformation twx, UE common. Occurs as reaction rims between zo and cc. An % 70?
Qz	Minor	elongate XB, with UE, SG.
Zo	Minor	IB prisms, commonly with pl rims. FX.
Sc	Minor	
Di	Minor	IB, deformation twx, BX.
Hb,Zi	Trace	
Gr,Sp	Trace	
Bi,Mu	Trace	

Metamorphic/Deformational/Crystallization History

Metamorphism						Deformation	
	Cc	Zo	Pl	Qz	S1		
M1?	NM	NM		NM	SF		D1
M1?			NM				
	PG	FX	UE	SG	SD		D2

Summary Amphibolite grade impure marble. Main metamorphism produced wide range of calc silicate minerals, maximum prograde conditions indicated by reaction of zo and cc to form pl. Subsequent dynamic metamorphism has strongly deformed cc

fabric.
Note good mortar texture in cc, deformation twx in di, reaction rims on zo.

Sample Number 3-130

Rock Name garnet and kyanite bearing biotite muscovite gneiss **Facies** amphibolite **Protolith** psammitic sediment **Distance from Raikot Fault** 0.25 km **Stained Billet** yes **Photo** no

General Petrofabric Strong S1 defined by segregation bands and elongate PB qz ribbons and strong SPO of mica. S1 wraps PB, but the wraps are annealed. S2 defined by spaced mylonitic shears, sub parallel to S1.

Mineralogy

Phase	%	Character
Pl	Major	XB, moderately elongate by contact inhibition with mica. UE, SG, serrate GB, albite and peri cline twx common. Also as PB, with PE texture.
Kf	Major	XB, elongate by contact inhibition, some SG.
Qz	Major	Early unstrained ribbons modified by extensive UE, SG, PG.
Mu, Bi	Minor	SB, in coarse aggregates coarsely recrystallized from early BX grains. BX, PG along S2.
Ky,Al	Trace	SB needles, BX, FX.
Op,Ap	Trace	
Zi	Trace	
Ch	Trace	alteration of bi.

Metamorphic/Deformational/Crystallization History

Metamorphism								Deformation	
	Pl	Kf	Qz	Mu	Bi	Al	S1	S2	
M1	NM			NM	NM	NM	SF		D1
M1	NM	NM	NM	NM	NM	WRAP	SD		D1
M1	NM	NM	NM	NM	NM		SR		
	SG	SG	PG	PG	PG		SD	SF	D2

Summary Amphibolite grade meta psammite. Deformation associated with or subsequent to initial metamorphism wrapped S1 around PB, and generated qz ribbons. Subsequnet SR annealed ribbons, bent mica, PB. Final dynamic metamorphism deforms all phases, generates S2.

Sample Number 4-012A

Rock Name biotite bearing quartz diopside amphibolite **Facies** amphibolite **Protolith** calcareous sediment **Distance from Raikot Fault** 0.3 km **Stained Billet** no **Photo** no

General Petrofabric Weak S1 defined by elongate felsic blebs, moderate SPO of hb.

Mineralogy

Phase	%	Character
Hb	Major	IB, coarse gr, poikiloblastic. Decussate texture with pl.
Pl	Major	XB, equant, albite, pericline and deformation twx common. Diffuse zoning, somewhat serrate GB, and sericitic alteration common.

Qz	Minor	XB ribbons modified by SG, UE, PG.
Di	Minor	IB, ER by pl. Some inclusins or overgrowths of hb, red brown alteration along cleavage.
Bi	Minor	IB-SB, Randomly oriented, weak BX.
Cc	Minor	
Sp,Ap	Trace	
Op	Trace	

Metamorphic/Deformational/Crystallization History

Metamorphism							Deformation	
		Hb	Pl	Qz	Bi	Di	Sl	
	M1	NM	NM	NM	NM	NM	SF	D1
	M1					ER		
			UE	PG	BX		SD	D2

Summary Amphibolite grade meta calcareous sediment. Initial metamorphism and S1 forming deformation possibly followed by SR, to generate decussate texture. Subsequent dymnamic metamorphism affects most phases, but does not develop a fabric.
Note sample collected from a rootless isoclinal intrafolial fold hinge in biotite schist.

Sample Number 4-027A

Rock Name Calc silicate bearing marble **Facies** amphibolite **Protolith** impure limestone **Distance from Raikot Fault** 0.1 km **Stained Billet** yes **Photo** yes

General Petrofabric PC of cc and calc silicates in fine gr matrix of polygonized cc. S1 weakly defined by segregation bands.

Mineralogy

Phase	%	Character
Cc	Major	Mostly PC in PG matrix, with some MT in less strained bands.
Do	Major	As above, distinguished by stain.
Fo	Minor	Rounded IB?, some alteration to serpentine.
Mu	Minor	IB, BX, kinked, intergrown with ma.
Ma	Minor	IB, BX, kinked, intergrown with mu.
Di	Minor	IB to SB, deformation twx, some BX.
Ap	Minor	SB.

Metamorphic/Deformational/Crystallization History

Metamorphism								Deformation	
		Cc	Do	Mu	Ma	Fo	Di	Sl	
	M1?	NM	NM	NM	NM	NM	NM	SF	D1?
		PG	PG	BX	BX		BX	SD	D2

Summary Amphibolite grade meta limestone. Initial metamorphic and deformation history largely obscured by late dynamic metamorphism.
Note Excellent examples of kinked mica, intergrowths of mu and ma.

Sample Number 4-027B

Rock Name biotite muscovite schist protomylonite **Facies** amphibolite **Proto-**

lith psammitic sediment **Distance from Raikot Fault** 0.1 km **Stained Billet** no **Photo** no

General Petrofabric Dominant fabric is PC in matrix of PG qz, pl and mica. Strong S1 defined by segregation bands and SPO of mica. S1 undulates around PC, and is cut by S2, spaced mylonitic shears.

Mineralogy

Phase	%	Character
Pl	Major	PC
Kf	Major	PC
Qz	Major	UE, MT, SG, PG.
Mu	Minor	BX, PG.
Bi	Minor	BX, PG.
Al,Zo	Trace	
Ap,Op	Trace	
Zi	Trace	

Metamorphic/Deformational/Crystallization History

Metamorphism			Deformation		
		All phases	S1	S2	
	M1?	NM	SF		D1
		PG, SG, BX	SD	SF	D2

Summary Protomylonite derived from amphibolite grade meta psammite. Significantly more deformed than 4-027C, immediately adjacent amphibolite.

Sample Number 4-027C

Rock Name biotite bearing quartz garnet amphibolite **Facies** amphibolite **Protolith** calc-basic sediment **Distance from Raikot Fault** 0.1 km **Stained Billet** no **Photo** yes

General Petrofabric Strong S1 defined by segregation bands, SPO of hb and bi, and qz ribbons. S1 undulates around PB, and is cut by S2, spaced conjugate mylonitic shears. A weak S3 is defined by closely spaced microfractures.

Mineralogy

Phase	%	Character
Hb	Major	SB, coarse gr. With some SG, common BX, and replacement by bi.
Pl	Major	XB, eguant or elongate in S1. Diffuse zoning and albite twx common. Has UE, BX, and SG.
Qz	Minor	Ribbons and elongate gr, with UE, SG, PG.
Al	Minor	Equant SB, ER by pl, qz.
Bi	Minor	SB, medium gr, strongly BX, PG.
Op	Minor	Elongate XB gr, and trains of fine gr in S1.
Ap	Minor	XB, with SPO in S1.
Zi, Sp	Trace	
Cz	Trace	

Metamorphic/Deformational/Crystallization History

Metamorphism			Deformation			
		All phases	S1	S2	S3	
	M1?	NM	SF			D1?
		PG, SG, BX	SD	SF	SF	D2

Summary Amphibolite grade meta calcareous sediment. Initial metamorphic and deformation history largely obscured by late dynamic metamorphism.
Note Sample interlayered with rocks of 4-027A and 4-027B.

Sample Number 4-033B

Rock Name diopside zoisite calc silicate gneiss **Facies** amphibolite **Protolith** calcareous sediment **Distance from Raikot Fault** 0.5 km **Stained Billet** yes **Photo** no

General Petrofabric S1 defined by segregation bands, and weak SPO of hb, di. Significant deformation of all phases, but no S2.

Mineralogy

Phase	%	Character
Qz	Major	XB, with strong UE, SG, PG, MT.
Pl	Major	XB, with strong UE, some SG and marginal PG. Deformation twx and deformation lamellae common.
Mi	Major	As above.
Di	Minor	SB prisms, with ER by qz, pl and overgrowth of hb.
Hb	Minor	IB, overgrowth on di.
Zo	Minor	IB prisms, some alteration to cz, pl. FX.
Sp	Minor	IB, with SPO in S1.
Ap, Op	Trace	
Cc	Trace	

Metamorphic/Deformational/Crystallization History

Metamorphism								Deformation
	Pl	Mi	Qz	Di	Hb	Zo	S1	
M1	NM	NM	NM	NM		NM	SF	D1
M2				ER	NM	ER		
	PG	PG	PG			FX	SD	D2

Summary Amphibolite grade meta calcareous sediment. Initial metamorphism and S1 forming deformation followed by a retrograde metamorphism to produce hb and cz on di and zo. Strong late dynamic metamorphism.

Iskere gneiss (Ni)

The Iskere gneiss is a unit of coarse grained thickly layered biotite gneiss, with subordinate amounts of biotite schist, amphibolite and calc silicate gneiss. Lithologic layers in Ni are laterally discontinuous, and are 0.25 to 5 m thick, with an average thickness of approxiamtely 2 m. S1 foliation defined by segregation bands and SPO of micas is parallel to lithologic layering, but is commonly diffuse because of the small content of mica in much of the unit. Blebs and stringers of pegmatitic material occur commonly in the massive biotie gneiss,a nd are locally chaotically folded. Amphibolite and calc silicate occur commonly as discontinuous lenses, rootless intrafolial fold hinges and fold boudins. The unit is distinguished in the field by its lack of lithologic variety, thick lithologic layering, abundance of pegmatitic stringers and massive grey outcrop appearance.

Sample Number 3-059

Rock Name quartz biotite amphibolite **Facies** amphibolite **Protolith** basic sediment **Distance from Raikot Fault** 3km **Stained Billet** no **Photo** no

General Petrofabric Strong Sl defined by segregation bands and moderate SPO of hb, bi, pl. Mostly equigranular, with some composite pl PB.

Mineralogy

Phase	%	Character
Hb	Major	SB, with rational GB. Weakly ER by qz, pl.
Qz	Major	XB, elongate parallel to Sl. UE and SG common.
Pl	Minor	SB to XB, with diffuse albite twx common. Straight GB. PB are PE composites. An % 60?
Bi	Minor	SB, weak SPO in Sl. ER by qz, pl and altered to ch.
Mu	Trace	SB gr, and radial aggregates in pl.
Cc	Trace	XB.
Ap	Trace	IB.
Op	Trace	
Zi	Trace	Rounded IB.

Metamorphic/Deformational/Crystallization History

Metamorphism							Deformation	
		Hb	Pl	Qz	Bi	Mu	Sl	
	Ml	NM	NM	NM	NM		SF	Dl
	Ml?	SR	SR	SR			SR	
	M2?	ER			ER	NM		
				SG				D2

Summary Amphibolite grade meta basic sediment. Initial metamorphism and Sl forming deformation followed by a weak static metamorphism, then by a weak retrograde metamorphism and deformation.

Sample Number 3-097

Rock Name biotite gneiss. **Facies** amphibolite **Protolith** psammitic sediment or felsic igneous rock **Distance from Raikot Fault** 3.0 km **Stained Billet** yes **Photo** no

General Petrofabric Coarse equigranular kf/qz/pl fabric with discontinuous mica segregation bands and coarse pl PB.

Mineralogy

Phase	%	Character
Pl	Major	XB, equant, with irregular GB. Albite twx common. Minor alteration to se. An % 35 ?
Qz	Major	XB, equant, with irregular GB. UE, SG common.
Kf	Minor	XB, equant, poikiloblastic, some myrmekite.
Bi	Minor	SB, weak SPO, minor alteration to ch.
Mu	Minor	IB, random orientation, crosscuts other phases.
Zi, Zo	Trace	
Ap	Trace	
Ch, Se	Trace	Alteration of bi, pl.

Metamorphic/Deformational/Crystallization History

Metamorphism								Deformation	
	Pl	Kf	Qz	Bi	Mu	Ch	Se	Sl	
M1	NM	NM	NM	NM				SF	D1
M1				SR				SR	
M2	MOBILE GB				NM	NM	NM		
			SG						D2

Summary Amphibolite facies meta psammite or meta granite. Initial metamorphism and S1 forming deformation followed by static metamorphism, then by weak retrograde metamorphism. Late weak deformation.

Sample Number 3-102

Rock Name biotite gneiss **Facies** amphibolite **Protolith** psammitic sediment or granite **Distance from Raikot Fault** 5.0 km **Stained Billet** yes **Photo** no

General Petrofabric Eguigranular equant pl/qz rock with poikiloblastic kf augen and discontinuous mica segregation bands. S1 crudely defined by segregation bands and alignment of augen.

Mineralogy

Phase	%	Character
Kf	Major	IB to SB, coarse poikiloblasts, and finer equant gr.
Qz	Major	XB, equant, with UE and some SG.
Pl	Major	XB, equant with common albite twx and myrmekitic quartz inclusions/replacements. An % 20?
Bi	Minor	SB, randomly oriented.
Mu	Trace	IB, randomly oriented, overgrowth on bi.
Al	Trace	Equant IB and flattened SB.
Ap, Zi	Trace	

Metamorphic/Deformational/Crystallization History

Metamorphism								Deformation	
	Pl	Kf	Qz	Bi	Mu	Al	Sl		
M1	NM		NM	NM		NM	SF		D1
M1		NM			NM		SF		D1
M1							SR		
			SG						D2

Summary Amphibolite facies meta granite or meta psammite. Initial metamorphism and S1 forming deformation followed by weak static metamorphism. Late weak deformation.

Sample Number 3-170

Rock Name diopside biotite calc silicate gneiss. **Facies** amphibolite **Protolith** calcareous sediment **Distance from Raikot Fault** 4.0 km **Stained Billet** no **Photo** no

General Petrofabric PE intergrowth of di, pl qz, with vague S1 defined by folded wispy bio bands.

Mineralogy

Phase	%	Character
Di	Major	IB, equant, PE.
Pl	Major	XB, equant, PE.
Qz	Minor	XB, equant, PE, minor UE, SG.
Bi	Minor	SB, minor BX.
Cc	Minor	XB.
Mi	Minor	Poikiloblastically includes pl.
Zi, Ap	Trace	
Se	Trace	Alteration of pl.

Metamorphic/Deformational/Crystallization History

Metamorphism								Deformation
		Di	Pl	Qz	Bi	Mi	Cc	Sl	
	Ml	NM	NM	NM	NM		NM	SF	Dl
	Ml			FOLDING				SD	Dl
	Ml					NM		SR	
				SG	BX				D2

Summary Amphibolite facies meta calcareous sediment. Initial metamorphism and Sl forming deformation included folding of Sl, and was followed by extensive static metamorphism. Weak late deformation.

Sample Number 3-171B

Rock Name biotite gneiss **Facies** amphibolite **Protolith** psammitic sediment or meta granite **Distance from Raikot Fault** 5.25 km **Stained Billet** yes **Photo** no

General Petrofabric Sl defined by discontinuous segregation bands, qz ribbons and moderate SPO of pl.

Mineralogy

Phase	%	Character
Qz	Major	XB, fine equant gr and ribbons. UE common.
Bi	Major	IB to SB, semi randomly oriented gr, coarsely recrystallized from earlier PG grains.
Pl	Major	XB, elongate gr, with common albite, pericline and deformation twx.
Kf	Trace	Marginal on pl.
To, Mu	Trace	
Op	Trace	

Metamorphic/Deformational/Crystallization History

Metamorphism						Deformation
		Qz	Pl	Bi	Sl	
	Ml	NM	NM	NM	SF	Dl
	Ml	SR	SR	SR	SR	
		UE				D2

Summary Amphibolite facies meta psammite. Initial metamorphism and Sl forming deformation involved folding or strong bending of Ml micas, subsequently recrystallized during a post Dl static metamorphism. Weak late deformation.

Sample Number 4-022B

Rock Name quartz biotite schist **Facies** amphibolite **Protolith** psammitic sediment **Distance from Raikot Fault** 2.5 km **Stained Billet** no **Photo** yes

General Petrofabric Generally equigranular with weak S1 defined by thin discontinuous segregation bands and weak SPO of bi. Vague hints of isoclinal folding of S1.

Mineralogy

Phase	%	Character
Bi	Major	IB, semi random orientation. Coarsely recrystallized after earlier polygonized mica.
Qz	Major	XB, coarse equant gr, some elongation by contact inhibition by bi. UE and SG common.
Pl	Minor	XB, equant with albite twx. Minor alteration ot se. An % 30?
Ap	Minor	
Zo, Zi	Trace	IB.
Ru	Trace	

Metamorphic/Deformational/Crystallization History

Metamorphism					Deformation	
		Qz	Pl	Bi	S1	
	M1	NM	NM	NM	SF	D1
	M1		FOLDED		SD	D1
	M1	SR	SR	SR	SR	
		UE				D2

Summary Amphibolite facies metapsammite. Initial metamorphism and S1 forming deformation included isoclinal folding of M1 phases, which was subsequently annealed in a static metamorpism. Late weak deformation.

Sample Number 4-045

Rock Name quartz biotite amphibolite **Facies** amphibolite **Protolith** basic sediment **Distance from Raikot Fault** 4.0km **Stained Billet** yes **Photo** no

General Petrofabric Generally PE texture with S1 defined by discontinuous segregation bands and weak SPO of hb and bi.

Mineralogy

Phase	%	Character
Hb	Major	SB, with rational GB, weak ER by qz, pl, weak UE.
Qz	Major	XB, equant, PE fabric modified by serrate GB. UE and SG common.
Pl	Minor	XB, equant, with albite and pericline twx. Kf? common as graphic exsolution blebs, and rounded quartz inclusions common. An % 65?
Bi	Minor	IB, coarse grained, semi random orientation. Minor alteration to ch and mi
Cc	Minor	XB.
Ch	Trace	Alteration of bi.
Mu	Trace	Radial aggregates after pl.
Ru, Ap	Trace	
Op, Sp	Trace	
Zi	Trace	

Metamorphic/Deformational/Crystallization History

Metamorphism								Deformation	
	Hb	Qz	Pl	Bi	Ch		Sl		
M1	NM	NM	NM	NM			SF		D1
M1	SR	SR	SR	SR			SR		
M2	ER		EX		NM				
		UE							D2

Summary Amphibolite facies meta basic/calcareous sediment. Initial metamorphism and S1 forming deformation followed by a static metamorphism and SR. Late retrograde metamorphism causes ER of hb, EX in pl, ch after bio. Weak late deformation.

Sample Number 4-088A

Rock Name biotite quartz amphibolite. **Facies** amphibolite **Protolith** basic sediment or igneous rock **Distance from Raikot Fault** 2.5 km **Stained Billet** no **Photo** yes

General Petrofabric Strong S1 defined by elongate mineral clots, discontinuous segregation bands and moderate SPO of hb, bi. S1 isoclinally folded, and folded grains completely recrystallized into semi randomly oriented aggregates.

Mineralogy

Phase	%	Character
Hb	Major	IB, moderate SPO, some simple twx, weak ER by qz, pl. In coarsely recrystallized aggregates after earlier polygonized grains.
Bi	Minor	IB, moderate SPO. In coarsely recrystallized aggregates after earlier polygonized grains.
Qz	Minor	XB, elongate by contact inhibition and in elongate folded pods, Weak UE, some SG.
Pl	Minor	XB, elongate by contact inhibition. Albite and pericline twx common.
Zo	Minor	SB.
Zi	Tr	SB.
Ep	Tr	After hb.
Ch	Tr	After bi.
Se	Tr	After pl.

Metamorphic/Deformational/Crystallization History

Metamorphism									Deformation	
	Hb	Bi	Qz	Pl	Se	Ch	Ep	Sl		
M1	NM	NM	NM	NM				SF		D1
M1		FOLDING						SD		D1
M1	SR	SR	SR	SR				SR		
M2	ER		UE		NM	NM	NM			D2

Summary Amphibolite faces meta basic sediment. Initial metamorphism and S1 forming deformation included isoclinal folding of M1 phases, which was subsequently annealed in a static metamorpism. Late weak retrograde metamorphism and deformation.

NoteExcellent example of annealed folds. Metasedimentary inclusion in massive biotite gneiss (4-088B).

Sample Number 4-088B

Rock Name biotite gneiss **Facies** amphibolite **Protolith** granite or psammitic sediment **Distance from Raikot Fault** 2.5 km **Stained Billet** yes **Photo** yes

General Petrofabric Coarse equigranular texture with vague S1 defined by thin discontinuous mica segregation bands. Some mica bands are coarsely recrystallized from early micas polygonized in a folding event. Composite augen of pl, and poikiloblastic augen of kf.

Mineralogy

Phase	%	Character
Pl	Major	XB, equant, albite, pericline and deformation twx common. An % 35?
Kf	Major	XB, equant, both mi and perthite. UE common, also as poikiloblastic augen.
Qz	Major	XB, equant, irregular GB. UE and SG common.
Bi	Minor	IB, somewhat ER by qz, pl. Coarsely recrystallized aggregates after earlier polygonized grains.
Mu, Zo	Trace	IB.
Ap, Op	Trace	
Ru	Trace	

Metamorphic/Deformational/Crystallization History

Metamorphism						Deformation	
		Pl	Qz	Kf	Bi	S1	
	M1	NM	NM	NM	NM	SF	D1
	M1		FOLDING			SD	D1
	M1	SR	SR	SR	SR	SR	
	M2		MOBILE GB				D2

Summary Amphibolite grade meta granite or psammite. Initial metamorphism and S1 forming deformation included isoclinal folding of M1 phases, which was subsequently annealed in a static metamorpism. Late weak retrograde metamorphism possibly produced irregular qz, pl, kf GB. Late weak deformation.
Note Good examples of recrystallized fold hinges.

Sample Number 4-102

Rock Name quartz biotite garnet amphibolite **Facies** amphibolite **Protolith** basic igneous rock or sediment **Distance from Raikot Fault** 5.0km **Stained Billet** yes **Photo** yes

General Petrofabric Generally equigranular rock with weak S1 defined by elongate qz and pl clots.

Mineralogy

Phase	%	Character
Hb	Major	SB, weak SPO, ER by qz, pl.
Pl	Major	Xb, equant, with albite, pericline and deformation twx. Graphic and myrmekitic EX of kf? and qz common.
Qz	Minor	XB, equant with serrate GB, UE and SG.
Bi	Minor	SB, random orientation. weak ER by qz, pl.
Al	Minor	Originally equant IB, now extensively ER by pl.
Sp	Minor	Rounded IB.

Zo	Trace	SB
Ap	Trace	
Kf	Trace	EX in pl.
Ch, Se	Trace	After bi, pl.

Metamorphic/Deformational/Crystallization History

Metamorphism									Deformation
	Hb	Pl	Qz	Bi	Al	Ch	Se	Sl	
M1	NM	NM	NM	NM	NM			SF	D1
M1	SR	SR	SR	SR				SR	
M2	ER	EX		ER	ER	NM	NM		
			SG						D2

Summary Amphibolite facies meta basic sediment or igneous rock. Initial metamorphism and S1 forming deformation was followed by SR in a static metamorpism. Late retrograde metamorphism produced ER of hb, bi, al and EX in pl. Late weak deformation.
Note Excellent exsolution textures in pl, excellent replaced garnets.

Sample Number 4-114

Rock Name zoisite grossular calc silicate gneiss **Facies** amphibolite **Protolith** marly sediment **Distance from Raikot Fault** 5.0 km **Stained Billet** yes **Photo** yes

General Petrofabric Initial S1 defined by seg bands of hb, zo and sp overgrown by coarse randomly oriented pl and gr.

Mineralogy

Phase	%	Character
Pl	Major	IB, coarse randomly oriented poikiloblastic laths. Albite, pericline and deformation twx common. Some FX. Some myrmekitic intergrowth with zo. An % 70.
Hb	Major	IB, equant PE texture. Minor alteration to ch.
Gr	Minor	SB, equant poikiloblastic gr.
Zo	Minor	Xb, as inclusions in pl and gr. Some relict prisms with hb, sp show SPO in initial Sl.
Sp	Minor	SB, in PE segregation bands.
Cc	Minor	
Zi	Trace	

Metamorphic/Deformational/Crystallization History

Metamorphism							Deformation
	Pl	Gr	Hb	Zo	Sp	Sl	
M1			NM	NM	NM	SF	D1
M1	NM	NM				SR	

Summary Amphibolite facies meta marl. Initial metamorphism and S1 forming deformation produced a segregation banded PE textured hb/zo/sp rock. Subsequent static metamorphism, crystallized randomly oriented pl and gr poikiloblasts.
Note Excellent example of overgrowth texture, unique example of PE texture in sp.

Sample Number 4-117

Rock Name garnet diopside calc silicate gneiss **Facies** amphibolite **Protolith** calcareous sediment **Distance from Raikot Fault** 3.75 km **Stained Billet** yes **Photo** yes

General Petrofabric Coarse irregular equant pl PB overgrow initial pl/di fabric which included Sl defined by segregation bands and SPO of hb and di.

Mineralogy

Phase	%	Character
Pl	Major	XB, coarse equant gr with irregular GB. Poikilitically enclose di, qz, sp and gr. Albite and pericline twx common.
Di	Minor	Coarse gr, extensively ER by pl. Some overgrowth by hb.
Hb	Minor	SB, ER by pl.
Gr	Minor	SB, fine equant gr.
Qz	Minor	XB, equant irregular gr, and rounded blebs in pl.
Wo	Minor	SB prisms parallel to Sl, ER by pl.
Sp	Trace	IB, coarse gr, ER by pl.
Zi, Ap	Trace	

Metamorphic/Deformational/Crystallization History

Metamorphism								Deformation
	Pl	Di	Hb	Qz	Gr	Wo	Sl	
M1	NM	NM		NM		NM	SF	Dl
M2	NM	ER	NM	NM	NM	ER		

Summary Amphibolite facies meta calcareous sediment. Initial metamorphism and Sl forming deformation produced a segregation banded pl/di/qz rock. Subsequent static retrograde metamorphism, replaced di an original pl with randomly oriented pl and gr. **Note** Excellent ER texture of di.

Shengus gneiss (Ns)

The Shengus gneiss is a unit of thinly laminated fine grained pelitic schist and gneiss with subordinate amounts of amphibolite and calc silicate gneiss. Lithologic layering is laterally continuous although there is abundant evidence of isoclinal folding. Lithologic layers range from 1 cm to 1m thick, and average 5 to 50 cm. A strong Sl foliation occurs parallel to the lithologic layering, defined by segregation bands and shape preferred orientation of mica and hornblende. Porphyroblasts of potassium feldspar, tourmaline and garnet are common, ranging in size up to 20 cm in diameter. Minor amounts of kyanite and sillimanite are common in the gneiss, and place the rocks in the amphibolite facies. The unit is recognized in the field by fine grain size, thin continuous lithologic layering and lithologic variety.

Sample Number 3-113

Rock Name garnet bearing biotite gneiss **Facies** amphibolite **Protolith** pelitic sediment **Distance from Raikot Fault** 6.5 km **Stained Billet** yes **Photo** yes

General Petrofabric Predominantly fine grained PE fabric of kf, pl and qz, with asymmetric composite PB of kf or bi and al. Thin films of qz or feldspar occur along PE grain boundaries, particularly in PB, suggesting anatexis. Moderate Sl defined by segregation bands and weak SPO of bi. Sl wraps PB, but is annealed.

Mineralogy

Phase	%	Character
Kf	major	XB, fine gr, equant or slightly elongate by contact inhibition with bi. PB are PE composite of medium gr.
Pl	major	As above, but no PB.
Qz	major	As above.
Bi	minor	IB, fine gr in matrix, coarse gr and randomly oriented in PB.
Al	minor	Irregular SB, wrapped by Sl.
Ky	trace	SB, ER in bi, al PB.
Si	trace	IB needles with ky.
Mu	trace	IB.
Ap	trace	

Metamorphic/Deformational/Crystallization History

Metamorphism								Deformation	
		Kf	Pl	Qz	Al	Bi	Ky	Si	Sl	
	Ml	NM	NM	NM	NM	NM	NM		SF	Dl
	Ml	SR	SR	SR				NM		

Summary Amphibolite facies meta pelite. Initial metamorphism and Sl forming deformation may have been preceeded by dynamic metamorphism to account for fine grain size. Initial metamorphism followed by static metamorphism to produce PE texture. Isoclinal folding event during initial deformation suggested by asymmetry of PB.
Note Excellent example of asymmetric PB, si and ky coexistence, and possible anatectic films on PE GB.

Sample Number 3-177A

Rock Name muscovite and biotite bearing gneiss **Facies** amphibolite **Protolith** pelitic sediment **Distance from Raikot Fault** 5.0 km **Stained Billet** yes **Photo** yes

General Petrofabric Predominantly fine grained PE fabric of kf, pl and qz, with mica PB. Thin films of qz or feldspar occur along PE grain boundaries, suggesting anatexis. Moderate Sl defined by segregation bands and weak SPO of bi. Sl wraps PB, but is annealed.

Mineralogy

Phase	%	Character
Kf	major	XB, fine gr, PE, equant or slightly elongate by contact inhibition with bi.
Pl	minor	As above.
Qz	minor	As above, with UE.
Bi	minor	IB, fine gr, weak SPO, weak BX, some alteration to ch. Occurs in equant pre to syn kinematic PB with si, possibly psuedomorph after garnet.
Mu	minor	Coarse SB, ER by qz, kf, pl and si.
Si	minor	Fibrolite, randomly oriented, associated with bi and mu.
To, Ap	trace	
Op, Zi	trace	
Ch, Se	trace	Alteration of bi, pl respectively.

Metamorphic/Deformational/Crystallization History

Metamorphism								Deformation	
	Kf	Pl	Qz	Al?	Bi	Mu	Si	Sl	
Ml	NM	NM	NM	NM	NM	NM		SF	Dl
Ml	SR	SR	SR	ER	SR	ER	NM		
			UE		BX				D2

Summary Amphibolite facies meta pelite. The initial metamorphism was followed by static metamorphism to produce PE texture and possibly culminated in anatexis. Weak late deformation.
Note Good example of randomly oriented fibrolite with bi and breakdown of mu to si and kf.

Sample Number 3-196

Rock Name kyanite sillimanite garnet schist **Facies** amphibolite **Protolith** pelitic sediment **Distance from Raikot Fault** >15 km **Stained Billet** no **Photo** yes

General Petrofabric Very fine grained qz, pl, bi matrix with composite ky, al, bi and kf PB. Strong Sl defined by segregation bands and moderate SPO of bi. Sl wraps PB.

Mineralogy

Phase	%	Character
Qz	major	XB, elongate gr with SG and UE. Some in PE intergrowths with kf and pl.
Pl	minor	XB, fine gr, equant in sub PE intergrowth with kf, qz. Rare pericline, albite and deformaton twx. Minor alteration to sericite.
Kf	minor	XB, equant with some UE, in sub PE intergrowths. Also as PB.
Bi	minor	Ragged fine gr SB, ER and intergrown with mu. Also randomly oriented IB with ky in PB. Some BX.
Mu	minor	SB to XB, very fine gr, ragged, weak SPO, some association with si. Probably late retrograde.
Ky	minor	Ragged SB prisms, with weak SPO, and composite PB with bi.Some UE, BX, and association with si.
Si	minor	IB needles, randomly oriented.
Al	minor	SB, equant to elongate, extensively ER by qz, pl, bi. Minor alteration to ch.
To	trace	SB, equant, ER.
Gp	trace	Equant irregular masses.
Zi	trace	
Ch	trace	Alteration of bi, al.
Se	trace	Alteration of pl.

Metamorphic/Deformational/Crystallization History

Metamorphism									Deformation	
	Qz	Pl	Kf	Bi	Mu	Ky	Si	Al	Sl	
Ml	NM	NM	NM	NM		NM		NM	SF	Dl
Ml	SR	SR	SR	SR			NM		SR	
M2				ER	NM			ER		
	SG		UE	BX		UE				D2

Summary Amphibolite grade meta pelite. Initial metamorphism and S1 forming deformation followed by static metamorphism, which crystallized randomly oriented si, and caused SR of other phases. Subsequent retrograde metamorphism grew widespread fine mu, and caused ER in al, bi, to. Weak late deformation. **Note** Good random sillimanite needles, and interesting random composite ky augen.

Sample Number 4-061A

Rock Name Garnet and kyanite bearing gneiss **Facies** amphibolite **Protolith** pelitic sediment **Distance from Raikot Fault** 0.2 km **Stained Billet** yes **Photo** yes

General Petrofabric Very fine grained PE matrix of qz, pl, kf with S1 defined by segregation bands, elongate composite kf PB and SPO of sparse fine bi and ky.

Mineralogy

Phase	%	Character
Kf	major	XB, fine gr equant in PE intergrowth with qz, pl. Minor UE. Also as elongate composite PB of medium gr mi, with PE texture, and thin films of qz or feldspar along grain boundaries.
Pl	major	Same as kf, but no PB.
Qz	major	Same as pl.
Bi	trace	IB, very fine gr, some alteration to ch.
Ky	trace	IB, stubby prisms with strong SPO, some BX.
Al	trace	SB, equant to elongate, fine gr. Inclusions of SB ky, qz, bi common.
Mu	trace	With bi.
Ap	trace	Fine gr needles.
Si	trace	IB needles in radial groups, extremely fine gr.

Metamorphic/Deformational/Crystallization History

Metamorphism									Deformation	
		Kf	Qz	Pl	Bi	Ky	Al	Si	S1	
	M1	NM	NM	NM	NM	NM			SF	D1
	M1	SR	SR	SR			NM	NM		
		UE	UE	UE		BX				

Summary Amphibolite grade meta pelite. Initial metamorphism and S1 forming deformation followed by static metamorphism, which crystallized randomly oriented si, helicitic al and caused SR of other phases. Weak late deformation. **Note** Excellent example of PE composite augen.

Sample Number 4-061B

Rock Name Kyanite biotite garnet gneiss **Facies** amphibolite **Protolith** pelitic sediment **Distance from Raikot Fault** 0.2 km **Stained Billet** yes **Photo** no

General Petrofabric Predominantly fine grained pl and qz in PE fabric with PB of kf, al and kf segregation bands. S1 defined by seg bands and moderate SPO of most phases. S1 wraps PB, with strain preserved in S1 forming phases. Weak mylonitic S2.

Mineralogy

Phase	%	Character
Qz	major	XB, equant or elongate due to contact inhibition by bi. UE, SB,

		PG common, and MT near PB.
Pl	major	XB, equant or elongate due to contact inhibition by bi. Some albite twx, UE and PG. Commonly altered to se.
Kf	minor	XB, as pl and qz. Also as composite PE PB of mi, with fine qz or feldspar films on GB. Also sub graphic exsolution texture in PB.
Bi	minor	SB, ragged, BX.
Ky	minor	SB prisms, BX.
Al	minor	SB, elongate extensive ER by qz, pl, bi. Some FX.
Zi	trace	IB.
Op	trace	Elongate, SPO.
Ap	trace	SB.
Ru	trace	

Metamorphic/Deformational/Crystallization History

Metamorphism								Deformation	
	Qz	Pl	Kf	Al	Ky	Bi	Sl	S2	
M1	NM	NM	NM	NM	NM	NM	SF		D1
M1	SR	SR	SR				SR		
M2			EX						
	PG	SG	SG	FX	BX	BX	SD	SF	D2

Summary Amphibolite facies meta pelite. The initial metamorphism was followed by static metamorphism to produce PE texture and possibly culminated in anatexis. Retrograde metamorphism caused EX in mi, and ch and se after pl and bi. Strong late deformation and incipient formation of mylonitic S2.
Note Good examples of exsolution texture in kf PB.

Sample Number 4-061C

Rock Name Diopside staurolite garnet gneiss **Facies** amphibolite **Protolith** marl-pelitic sediment **Distance from Raikot Fault** 0.2 km **Stained Billet** no **Photo** yes

General Petrofabric Fabric is fine grained equigranular with a weak S1 defined by thin discontinuous felsic bands and moderate SPO of st. Incipient S2 occurs as spaced bands of polygonization. S3 occurs as spaced fractures.

Mineralogy

Phase	%	Character
Al	major	Slightly flattened IB, ER by qz and pl. Helicitic trains of qz, pl, zi.
Qz	major	XB, strongly elongate and PG along S2. UE and SG common.
St	minor	SB, embayed prisms with moderate SPO, UE common.
Pl	minor	XB, with Albite twx, SG and UE common.
Di	minor	SB, ER by qz, pl. Greenish.
Bi	minor	SB, some shreddy, with weak SPO. Some BX. Associated with st.
Sp	minor	Rounded SB.
Op, Zi	trace	

Metamorphic/Deformational/Crystallization History

Metamorphism									Deformation	
Al		Qz	St	Di	Bi	Pl	Sl	S2	S3	
M1	NM	NM	NM	NM	NM	NM	SF			D1
M2	ER		ER	ER	ER					
		PG	UE		BX	SG	SD	SF	SF	D2

Summary Amphibolite facies meta marl. Initial metamorphism and S1 forming deformation were followed by a retrograde metamorphism which caused ER in most phases. Late stage deformation involves formation of incipient mylonitic foliation, fracturing.

Sample Number 4-092

Rock Name Biotite muscovite sillimanite gneiss **Facies** amphibolite **Protolith** pelitic sediment **Distance from Raikot Fault** 7.5 km **Stained Billet** yes **Photo** no

General Petrofabric Fine grained, sub PE fabric, with strong S1 defined by segregation bands and weak to moderate SPO of qz, pl, kf, much of which is due to contact inhibition against bi with moderate SPO. Composite PB of si, mu and qz occur. Thin films of qz or feldspar occur along PE grain boundaries, suggesting anatexis. Moderate S1 defined by segregation bands and weak SPO of bi. S1 wraps PB, but is annealed.

Mineralogy

Phase	%	Character
Qz	major	XB, equant grains elongate by contact inhibition, PE fabric modified by cuspate to serrate Gb. UE, SG common.
Pl	major	As qz, with Albite and pericline twx and alteration to se common.
Kf	major	As qz, and as poikiloblasts and myrmekite.
Bi	minor	IB, with moderate SPO, minor alteration to ch.
Mu	minor	SB, ER by qz, kf, si and in intergrowths with si. Moderate to strong SPO.
Si	minor	Randomly oriented fibrolite clots and fine prisms with weak to moderate SPO. Commonly with mu and in composite PB.
Al	trace	Sb, flattened and ER by qz, pl.
Ch	trace	Alteration of bi.
Se	trace	Alteration of pl.
Ap	trace	SB, SPO.
Op	trace	With si, mu.
Ru	trace	

Metamorphic/Deformational/Crystallization History

Metamorphism								Deformation	
	Qz	Pl	Kf	Mu	Bi	Si	Al	S1	
M1	NM	NM	NM	NM	NM		NM	SF	D1
M1	SR	SR	NM	ER	SR	NM		SR	
M2							ER		

Summary Amphibolite facies meta pelite. Initial metamorphism and S1 forming deformation followed by static metamorphism which produced random sillimanite annealed deformed S1 and culminated with mu breakdown and possible anatexis. Weak retrograde metamorphism causes ER of garnets, alteration of pl and bi to se and ch.

Sample Number **4-106B**

Rock Name **Diopside scapolite marble** Facies **amphibolite** Protolith **impure limestone** Distance from Raikot Fault **6.0 km** Stained Billet **no** Photo **yes**

General Petrofabric **Coarse equigranular PE fabric, with weak S1 defined by discontinuous segregation bands of di and sc, weak SPO of di and sc.**

Mineralogy

Phase	%	Character
Cc	major	XB, PE with straight GB, weak bending of twin lamellae.
Di	minor	IB, ER by sc and cc, some overgrowth of hb.
Sc	minor	SB, PE.
Pl	minor	SB, with albite twx, some oddly diffuse. In PE growths with cc.
Qz	minor	Rounded XB, with UE and SG.
Sp	minor	Coarse IB, ER, with strong pink/clear pleochroism.
Zi	trace	IB.
Op	trace	XB.
Hb	trace	On di.

Metamorphic/Deformational/Crystallization History

Metamorphism								Deformation
		Cc	Di	Sc	Pl	Qz	Sp	Sl	
	Ml	NM	NM		NM	NM	NM	SF	Dl
	Ml	SR	ER	NM		SR	ER	SR	

Summary Amphibolite facies meta limestone. Initial metamorphism and Sl forming deformation followed by static metamorphism, resulting in PE texture. No significant subsequent metamorphism ofr deformation.
Note Excellent example of PE texture.

Sample Number 4-119

Rock Name Biotite amphibolite Facies amphibolite Protolith calcareous sediment Distance from Raikot Fault 4.5 km Stained Billet no Photo yes

General Petrofabric Very fine grained PE fabric of hb and pl. No Sl, bi randomly oriented.

Mineralogy

Phase	%	Character
Hb	major	IB, PE.
Pl	major	XB, albite twx and diffuse zoning common.
Bi	minor	IB, random orientation, unusual marginal ER by pl leaves "shadows" around remnants of bi.
Op	minor	XB, elongate, with vague SPO. Also irregular equant grains.
Al	trace	XB, fine grained, irregular, ER.
Ch	trace	Alteration of bi.
Ap, Zi	trace	Rounded SB.

Metamorphic/Deformational/Crystallization History

Metamorphism							Deformation	
		Hb	Pl	Bi	Al	Sl		
	Ml	NM	NM	NM	NM	SF?	Dl?	
	Ml?	SR	SR	ER	ER	SR?		

Summary Amphibolite facies meta calcareous basic sediment. Initial metamorphism and Sl forming deformation followed by static metamorphism to produce PE fabric, or initial metamorphism was static. No significant subsequent deformation or metamorphism.
Note Excellent PE fabric, unusual fine grain size, unusual "shadow" replacement of bi by pl.

Sample Number 4-120

Rock Name Biotite muscovite tourmaline gneiss **Facies** amphibolite **Protolith** psammittic or pelitic sediment **Distance from Raikot Fault** 4.5 km **Stained Billet** yes **Photo** yes

General Petrofabric Sl defined by segregation bands and SPO of bi, mu and to PB. Fabric qz-pl-kf fabric in segregation bands is PE. Sl wraps PB, but is annealed.

Mineralogy

Phase	%	Character
Qz	major	XB, in fine equant grains PE with pl and kf, and in elongate ribbons, annealed into equant unstrained domains. UE and minor SG common.
Pl	major	Fine XB, equant and PE with qz and kf, except where elongate in Sl by contact inhibition with bi, mu. Albite and pericline twx common. Commonly altered to se.
Kf	major	As pl, but no twx.
Bi	minor	IB to SB, moderate SPO, minor alteration to ch. Annealed to semi randomly oriented coarsely recrystallized aggregates where deformed around PB.
Mu	minor	IB, as bi.
To	minor	SB PB with moderate SPO. ER by qz, pl. Dark green to yellow green pleochroism.
Si	trace	Fibrolite, with mu.
Zo, Ap	trace	SB.
Op, Zi	trace	Irregular, rounded.
Ru	trace	SB.
Ch, Se	trace	Alteration of bi, pl.

Metamorphic/Deformational/Crystallization History

Metamorphism								Deformation	
	Pl	Qz	Kf	Bi	Mu	Si	To	Sl	
M1	NM	NM	NM	NM	NM		NM	SF	D1
M1		PG		BX	BX			SD	D1
M1	SR	SR	SR	SR	SR	NM	ER?	SR	

Summary Amphibolite facies meta psammite or pelite. Initial metamorphism and Sl forming deformation included deformation of Sl around PB. Subsequent static metamorphism caused extensive SR to produce essentially PE fabric. No significant subsequent metamorphism or deformation.

Note Excellent example of to PB, and annealing of micas wrapped around PB. Good example of SR of quartz ribbons.

Sample Number 4-122A

Rock Name Meta sedimentary banded gneiss **Facies** amphibolite **Protolith** calcareous, basic and psammitic sediment **Distance from Raikot Fault** 7.0 km **Stained Billet** no **Photo** no

General Petrofabric Strong Sl defined by segregation bands and lithologic bands. Within 1 thin section, bands of psammitic gneiss, amphibolite and calc silicate gneiss occur. Sl also defined by moderate SPO of bi, hb, and weak

elongation of pl, qz, kf by contact inhibition with bi. Within segregation bands fabric is generally PE, with PB of al. PE fabric unusual, with curved GB, and numerous rounded inclusions of pl, qz, kf. Also unusual rims of feldspar on feldspar, and sub graphic textures in feldspar. Sl wraps PB but is annealed.

Mineralogy

Phase	%	Character
Pl	major	XB, equant and generally PE. Albite and pericline twx common. Qz or feldspar inclusions common, as are rims of untwinned pl on twinned pl. Some myrmekite, some poikilitic crystals overgrow PE fabric. Pl in calc silicate bands is La. Andesine in psammitic bands.
Kf	major	XB, equant and PE, with some elongation due to contact inhibition.
Qz	major	XB, PE, UE common.
Hb	minor	SB, ER by pl, qz, weak SPO.
Al	minor	SB, ER by pl, qz.
Bi	minor	SB with ragged ends. Moderate SPO, alteration to ch.
To	minor	SB, equant, ER by pl, qz. Associated with al, hb.
Cc	minor	XB, PE.
Di	minor	SB, ER by cc, sc. Minor alteration to hb.
Sc	minor	SB, PE.
Sp	minor	IB.
Zi	trace	IB.
Ap, Op	trace	
Ch, Se	trace	Alteration of bi, pl.

Metamorphic/Deformational/Crystallization History

Metamorphism								Deformation		
	Qz-PL-Kf	Bi	Hb	Al	To	Cc	Di	Sc	Sl	
M1	NM	NM	NM	NM	NM	NM	NM		SF	D1
M1	SR	SR			ER?	SR	ER	NM	SR	
M2?	NM		ER	ER	ER?					

Summary Amphibolite facies gneiss derived from variety of sedimentary protoliths. Initial metamorphism and Sl forming deformation followed by static metamorphism to produse PE fabric. Possible subsequent (retrograde ?) metamorphism results in ER of to, hb, al and overgrowths, myrmekite and graphic growths in feldspars.
Note Excellent example of fine scale lithologic banding.

Sample Number 4-122B

Rock Name Biotite garnet sillimanite kyanite gneiss. **Facies** Amphibolite **Protolith** pelitic sediment **Distance from Raikot Fault** 7.0 km **Stained Billet** yes **Photo** yes

General Petrofabric Moderate Sl defined by segregation bands and moderate SPO of mica, weak SPO of qz/pl/kf due to contact inhibition. PB of pl, kf, al, to, ky and si. Sl wraps PB, but is annealed.

Mineralogy

Phase	%	Character
Pl	major	XB, sub PE, weak SPO due to contact inhibition. Albite and pericline twx common. Some serrate GB, some alteration to se. Also as composite PE PB.
Kf	major	XB, sub PE, some UE.
Qz	major	XB, sub PE SG and UE common.
Bi	minor	SB, strong SPO, but all orientations occur.
Al	minor	SB, equant to elongate PB. Inclusions of to, bi, and helicitic trains of op. ER by qz and pl.
Ky	minor	Coarse SB PB. ER. Moderate SPO, BX and SG.
Si	minor	IB, fine prisms with weak SPO. BX and FX. Rare association with ky.
To	minor	IB to SB, with moderate SPO. Some zoned, some with op inclusions in cores.
Mu	trace	SB, ER. Associated with si.
Gp	trace	Elongate with SPO, and as equant irregular masses.
Ap	trace	IB, ER.
Zi	trace	IB, dark brown and clear.
Ch	trace	Alteration of bi.
Se	trace	Alteration of pl.

Metamorphic/Deformational/Crystallization History

Metamorphism									Deformation	
	Pl	Qz	Kf	Bi	Al	To	Ky	Si	Sl	
Ml	NM	NM	NM	NM	NM	NM	NM		SF	Dl
Ml	SR	SR	SR	SR				NM	SR	
M2					ER	ER	ER			
		SG	UE				BX	BX		D2

Summary Amphibolite facies meta pelite. Initial metamorphism and Sl forming deformation followed by static metamorphism which produced PE fabric, grew si. Weak late retrograde metamorphism caused ER in al, to, ky and alteration of bi and pl. Moderate late deformation.
Note Good examples of PE composite PB.

Mylonites

Sample Number 3-020C

Rock Name marble mylonite **Protolith** Nh marble? **Distance from Raikot Fault** 0.2 km **Stained Billet** no **Photo** yes

General Petrofabric Very fine grained mylonitic matrix of cc, pl and qz, with diffuse chaotically folded banding. PC of qz, pl, sc and biotite gneiss mylonite.

Ratio of matrix to PC. 9:1
Matrix Mineralogy Cc, pl, qz and mica?

Porphyroclast Mineralogy

Phase	Character
Pl	Some albite twx, alteration to se. Marginal PG common.
Qz	Rounded, marginal PG common, some grains entirely PG.

Bi Strongly BX.
Sc Rounded.

Summary Mylonite or ultramylonite derived from impure marble. Some complex mylonitic flow suggested by inclusion of gneiss mylonite, chaotic folding. **Note** Surrounding gneisses only slightly mylonitized. Excellent photos of PG PC, chaotic folds and biotite gneiss PC.

Sample Number 3-184A

Rock Name amphibolite mylonite **Protolith** amphibolite from Kh. **Distance from Raikot Fault** 0.0 km. **Oriented Photo** yes

General Petrofabric Fine dark matrix with strong mylonitic foliation (S1) and seg bands of qz, pl, hb. Foliation folded in isoclinal folds, with inconsistent vergence. Hb PC indicate sense of shear by FX, rotation. Fine neo mineralized mica forms S2 oblique to S1. Numerous microfaults with inconsistent offsets.

Ratio of matric to PC. 9:1
Matrix Mineralogy Hb, pl, qz, mica.

Porphyroclast Mineralogy

Phase	Character
Hb	FX, commonly flattened by formation of transverse microfaults and rotation. Possibly overgrown by postkinematic hb.
Pl	Rounded, PG.
Qz	Ribbons.

Summary Mylonite or ultramylonite derived from amphibolite. Possible post kinematic metamorphism indicated by transverse mica fabric and hb ovegrowths. **Note** Excellent photos of microfaults, folds. good example of late mica fabric, FX and rotated hb.

Sample Number 3-184E and 4-13A

Rock Name Ultramylonite **Protolith** biotie garnet gneiss **Distance from Raikot Fault** 0.0 km **Oriented** yes, 4-13A **Photo** Yes

General Petrofabric Strong S1 mylonitic foliation, with seg bands of qz or pl. S1 foliation has asymmetric folds which have inconsistent vergence. S-surfaces defined by mica PC. S2 fabric defined by fine grained neomineralized mica oblique to S1 and S-surfaces. Late spaced S3 shear bands also occur. Dextral slip indicated by S-C intersections; offset PC; asymmetric microfolds around rotated PC; inclination of fine grained PG qz or pl in seg bands.

Ratio of matric to PC. 9.5:1
Matrix Mineralogy Mica, pl? qz?

Porphyroclast Mineralogy

Phase	Character
Mu	In coarse SB, BX, and aligned in C surfaces. Probably postdates S1.
Pl	FX and rotated, some PG.
Al	FX, in comminuted trains.
Zi	Undeformed.

Summary Ultramylonite derived from biotite garnet gneiss. Initial mylonitization may have been followed by two periods of static recrystallization, the first produced coarse mu PC, which were subsequently deformed in formation of C-surfaces, the second produced the fine mica S2. Late deformation produced spaced shear bands. Consistently dextral shear sense.
Note All around excellent examples of many mylonitic features.

Sample Number 4-13C

Rock Name amphibolite ultramylonite **Protolith** Kh amphibolite? **Distance from Raikot Fault** 0.0 km **Oriented** yes **Photo** yes

General Petrofabric Strong mylonitic foliation, with fine to very fine grained PC in an almost aphanitic matrix. Seg bands of very fine grained PE qz or pl. Consistently dextral sense of shear indicated by inclined qz pl fabric in seg bands; asymmetric pressure shadows on hb PC; asymmetric microfolds around rotated PC.

Ratio of matrix to PC. >9.5:1
Matrix Mineralogy Pl? qz and fine green amphibole needles.

Porphyroclast Mineralogy

Phase	**Character**
Hb	Fine unstrained fragments
Pl	Rounded.

Summary Ultramylonite derived from amphibolite. Dextral shear sense, no evidence of static metamorphism.
Note Excellent example of inclined polygonal qz or pl fabric in seg bands.

Sample Number 4-28 A

Rock Name biotite gneiss mylonite **Protolith** Nh biotite gneiss **Distance from Raikot Fault** 0.1 m **Oriented** yes **Photo** yes

General Petrofabric Subequal amounts of polygonized matrix and coarse equant PC. Strong foliation defined by bands in rock, either original S1 or a mylonitic foliation. S1 undulates due to wrapping around PC. S2 defined by spaced conjugate shear bands, discontinuous due to interference by coarse PC. Sense of shear consistently dextral, indicated by asymmetrcally folded bi with trains of PG bi; grains offset by rotating PC and asymmetry of bent fractures in rotated PC.

Ratio of matrix to PC. 1:1
Matrix Mineralogy Qz, Pl and bi.

Porphyroclast Mineralogy

Phase	**Character**
Pl	Coarse equant PC, sub angular, with UE, SG some marginal PG.
Kf	As above
Bi	Asymmetrically folded, BX, PG along S2 bands.

Summary Protomylonite derived from biotite ortho or para gneiss. Consistent dextral shear sense, but S2 surfaces imply late stage plane flattening.

Sample Number 4-060 A

Rock Name kyanite garnet gneiss protomylonite **Protolith** Ns kyanite garnet gneiss **Distance from Raikot Fault** 0.0 km **Oriented** yes **Photo** yes

General Petrofabric Strong original or mylonitic S1 defined by seg bands and SPO of most phases. Bands of strong PG occur parallel to S1. Spaced bands of PG inclined to S1 may be C surfaces or shear bands. Dextral shear sense indicated by sense of offset on spaced microfaults on flattened and rotated garnets and by asymmetric microfolds around rotated garnet PC.

Ratio of matrix to PC. 1:9
Matrix Mineralogy Pl, qz, bi.

Porphyroclast Mineralogy
Phase Character
Al Flattened by rotation accomodated along spaced microfractures.
Pl SG, some PG.
Qz BX ribbons, with UE, SG, some MT.
Ky BX.

Summary Protomylonite (or possibly blastomylonite) derived from kyanite garnet gneiss. Dextral shear indicated by garnets.
Note Excellent example of garnets flattened by roatation of segments bounded by spaced microfaults.

Sample Number 4-86A

Rock Name amphibolite mylonite **Protolith** amphibolite **Distance from Raikot Fault** 0.0 km **Oriented** yes **Photo** no

General Petrofabric Matrix of finely PG material with strong mylonitic S1. S2 defined by spaced bands of strong PG oblique to S1. Sense of shear dextral, from asymmetric microfolds around rotated PC, and from asymmetric trains of PG material off PC.

Ratio of matrix to PC. 6:4
Matrix Mineralogy Pl, qz, bi.

Porphyroclast Mineralogy
Phase Character
Hb Equant, FX.
Pl Rounded, with SG.
Qz Ribbons with strong PG, MT.
Bi BX, strongly PG against S1 and S2 surfaces.

Summary Protomylonite derived from amphibolite or hb bearing biotite gneiss. Dextral shear sense.